*8th Mar 2018*

Dear GMD Editor & Reviewers,

**Re. Revision of gmd-2017-257: A General Lake Model (GLM)**

We thank you for the opportunity for our paper to be considered for publication in GMD, and are very grateful for the comments received during the discussion phase of the paper. We have found the comments very detailed and insightful and they have guided us to significantly improve this version of the manuscript.

We have already provided specific replies back to each of the reviewer comments in the discussion forum explaining our approach to the revision. A summary of the main issues identified were:

1. Numerous issues associated with mistakes in the notation and units of several equations, plus the ambiguous use of some symbols;
2. Lack of context/justification for the adoption of some of approaches/equations in the model description sub-sections (eg. surface mixing and inflows);
3. A long and potentially hard to navigate structure;
4. Issues with figure readability and axis labels;
5. Numerous typographical and minor editorial issues, plus some errors with reference citations and the formatting consistency in the reference list;
6. Requirement for a DOI to be included for the code-base.

The obvious issues with mistakes in the notation and units initially noted by R1 led to the development of a "preliminary revision" that was uploaded to the discussion forum (dated 8$^{th}$ Jan). This revision included significant changes to Section 2 of the paper and primarily addresses Item 1 above, and many of the issues relevant to Items 2-5 were resolved in this upload.

Here we upload a fully revised paper that further builds on these changes to address all the comments, where possible. The major change relates to a re-worked introduction to better introduce the need for the model and explain the structure of the paper. Further remaining notation/equation issues have also been resolved and improved descriptions of selected algorithms has been added. Additional improvements to several of the conceptual figures and simulation results have also been undertaken. Please refer to the individual responses for specific details. A tracked-changes version is at the back of this document.

The comments have also led to significant code adjustments, and so the model version associated with this version of the manuscript is updated on GitHub and is now v3.0. A DOI for the code is to be added if the paper is accepted for publication.

We thank you again for the significant time and effort that have gone into the discussion and look forward to your decision.

Kind Regards

Matthew Hipsey, on behalf of all co-authors.

**Anonymous Referee #1**

General comments

This article describes the scientific basis of a 1-dimensional hydrodynamic lake model that can be coupled to ecosystem models. The model has already been applied to many systems in the scientific community, and I think it is useful publish the model description in a scientific paper that can be referred to for future applications of the model. That said, I stopped reviewing after equation 16, because there were simply too many errors in the equations. I therefore propose to reject the current version of the manuscript and that the authors carefully check all equations before resubmitting the manuscript to this or another journal, depending on the decision of the editors.

REPLY: Thank you for taking the time to review the discussion paper and identify the errors - we sincerely apologise that simple issues related to units and notation were not more thoroughly checked prior to upload. Please note this revision does have some substantial changes to the paper including the notation, text and (some) figures. We very much look forward to your comments and suggestions on this version.

Errors in equations up to eq. 16:

eq. 2 and 3: I think something is wrong with the indices. $h_z$ is located between $h_{b-1}$ and $h_b$. $\alpha_b$ and $\beta_b$ describe the interpolation between $h_b$ and $h_{b+1}$. Thus, the indices in eq. 2 should be $\alpha_{b-1}$ and $\beta_{b-1}$.

REPLY: You are correct; the code was looping from one step behind so we had incorrectly omitted the -1 in the equation. It is now updated

eq 6: I think this equation is wrong. The right hand side is the total heat flux to the surface layer in W $m^{-2}$. This should be divided by $z_{msl}$ to get W $m^{-3}$. Then, it should be divided by the water density $\rho$ in kg $m^{-3}$ to get W/kg, and finally by $c_p$ to get °C/s for $dT_s/dt$. Therefore, the multiplication term on the left hand side should be $z_{msl}\ c_p\ \rho$, rather than $c_p/(A_S\ z_{msl})$.

REPLY: You are correct; it is now updated and in fact this section is now significantly revised. Table 1 now also includes all the notation and relevant units.

eq 9b / Fig. 3: I could not reproduce the maximum of the Briegleb function at 80 degrees zenith angle. Using equation 9c yielded a monotonically increasing function between 20 and 90 degrees (with a minimum at about 20 degrees). Also the equation in the legend is wrong, it should be SZA = $\Theta_{Zen}$*180/2π.

REPLY: You are correct; This was an error in creating the plot rather than the model itself, and Figure 3 has been re-created and caption updated.

eq. 12: I think $\phi_{SWS}$ (i.e. the shortwave radiation absorbed in the surface layer) should be replaced by $\phi_{SW}$ (z=0) in the nominator. Otherwise, the euphotic depth increases with increasing radiation absorbed in the surface layer, which does not make sense. Same in caption to Fig 4.

REPLY: The notation has been improved to prevent confusion; $\phi_{SWS}$ is what is absorbed and $\phi_{SW0}$ is what arrives at the top of the surface layer; The euphotic depth computation is now based on the fraction of incoming light.

eq. 16: I think in equations 16c and 16d $T_a$ should be replaced by absolute temperature (i.e., 273.15 °C should be added to $T_a$).

REPLY: You are correct; notation updated to have K and C unit options for temperature

Also units should always be provided, especially for empirical equations (e.g. $e_a$ in eq. 16, and $U_x$, RH, and diffusive radiation in eq. 9c).

REPLY: Units have been thoroughly checked and updated in the revised upload, plus the updated Table 1 summarises units for all variables/symbols to avoid confusion.

Besides that, a few other points I noticed up to page 11 (Page xx, Line yy is abbreviated as xx/yy)

In general, the paper is well written and easy to read, but there are quite a few long and complicated sentences which I think should be simplified to facilitate reading (first two examples: 2/24-29 , 3/12- 17).

REPLY: These examples have been re-written and the revised version has also been check for these issues as best as we could identify.

3/10: This list of references seems to be somewhat inconsistent. Some of the references refer to model development, some to model applications. It would be more logical to cite only model development references.

REPLY: Point noted, these papers were reflecting the diversity of 1D models we are aware of, but agree these should more specifically refer to development refs; introduction is updated.

4/30: The text seems to imply that the requirement for site-specific calibration in other models is due to numerical diffusion caused by the fixed grids. If that is the intention, this should be explained. If not, the sentence should be modified.

REPLY: Sentence modified.

5/7: Incomplete sentence

REPLY: Section has been revised and reworded.

Figure 1: Shouldn't the local runoff, and the submerged inflows and groundwater seepage be written in blue?

REPLY: Local runoff is computed by GLM (Eq 7 in updates manuscript). Submerged inflows and seepage however has been updated to be blue in Figure 1 as they are specified.

eq. 1: From the text (layer volumes are determined ...), I would have expected an equation for the individual layer volumes here, but this is the integrated volume from the bottom of the lake to the top of each layer. This should be clarified in the text.

REPLY: Section has been revised and reworded to hopefully introduce the layer structure and notation more clearly. The layer volume balance is not presented here due to the complexity of options and it is not appropriate at this early stage of the paper; however, edits later on have aimed to make this more clear. Notation now is V for cumulative volume to a point, and delV for layer volume.

6/3: technically, it is the same, but I think it would be clearer to write $2 \leq b \leq N_{BSN}$.

REPLY: Updated.

6/4: how are these finer depth increments determined?

REPLY: Now summarised in symbol table (Table 1).

6/9: Since the Unesco (1981) equation has been replaced by TEOS-10, I think it would make sense to use the latter rather than the former in a new model. I also think it should be mentioned that the density effect

of salinity in these seawater equations is quite different from that in most lakes where carbonates are usually the dominant species rather than NaCl.

REPLY: Thank-you for this suggestion. The revised code now has the TEOS option included, accessible via the setting density_model =1. The UNESCO option is also included, and facility for users to add a custom option.

6/24: heat balance **of** the surface layer 7/2-3: why is only rain but not snow multiplied with $f_R$? Also, even though this should be clear to the reader, it should probably be mentioned that S is in water equivalents.

REPLY: Updated.

eq 5: to be precise, this equation should be limited to a minimum of zero, as otherwise it will become negative if the rainfall is too weak.

REPLY: Updated - this was the case in the code, but not properly summarised in the Eq.

Fig 2: Add some space between the 10 and the exponent in the y-axes labels of panels c and d. Do all these time series start on 1 January of a year?

REPLY: Lakes do have variable start times (for various reasons) which is why we didn't use exact date in the x-axis. The individual lake simulations are documented on our GitHub site with explanations and we didn't want to make it too confusing here with too many details.

eq. 9a: instead of subtracting $\pi/2$ within the sine functions, it would be easier to use -cos.

REPLY: Apologies, there was a "-" sign wrong in this Eq so both should not have been - $\pi/2$. In the new manuscript (Eq 12a) we have the addition or subtraction of $\pi/2$ is listed properly in order to allow us to differentiate Sth vs Nth hemisphere sites.

eq. 9b: where does the factor 1.1 in the nominator of the first term come from? Maybe I overlooked something, but I could not find it in Briegleb et al. (1989).

REPLY: Thankyou for noticing this detail - this inclusion of 1.1 has been picked up from the implementation by Li et al (2006), who compared models and have this coefficient included.

However, for consistency, we have removed this from the Eq in the paper, and the code-base going forward. We note however, that the change made only a modest difference to the function.

Li, J., Scinocca, J., Lazare, M., McFarlane, N., Von Salzen, K. and Solheim, L., 2006. Ocean surface albedo and its impact on radiation balance in climate models. *Journal of climate*, *19*(24), pp.6314-6333.

eq. 9c: I was not able to check this equation, as the source is in Japanese, but I did not get anything similar to what is shown in Fig. 3 trying different values for RH, U and the diffusive radiation. Please check whether the equation is correct, and specify the values used to produce Fig. 3. Furthermore, Yajima and Yamamoto is dated 2014 here but 2015 in the reference list.

REPLY: Thankyou again for checking this - the equation implemented is based on the Equation 1c of this publication, whereby y is cos(solar angle), the a and b coefficients were set by multi-variate regression, and x1 is RH(%), x2 is wind speed (m/s) and x3 (-) is a parameter referring to the amount of atmospheric diffuse radiation.

We initially received the coefficients from the author (Yajima pers comm.) for our implementation, and following your comment we have now updated the Figure 3, the citation date, and the equation. The caption also now states the values of x, x2, x3 used in the graph. For your reference, R code for the algorithm is below:

```
angled = 1:89
angle = angled * pi/180
dr = 6
ux = 4
rh = 80
yalbedo = max( 0.02, 0.001 * rh * (1-cos(angle))^0.33 - (0.001 * ux * (1-cos(angle))^(-0.57)) - (0.001 * dr * (1-cos(angle))^(0.829)) )
```

Fig 4: y-axis of panel b is not depth, but elevation, y-axis of panel c is not labeled.

REPLY: You are correct; the y-axis should be height not depth. As part of the revised manuscript we have uploaded we have undertaken a major review of notation used throughout so that depth (z), height (h) and elevation (H) are used consistently.

All figures have been re-created and revised in the revision, to resolve these issues.

Also it seems that $A_{BEN}$ is calculated on a different time scale than the radiation in (c). Many low radiation events are clearly visible in (b) but do not show up in (c). This probably makes sense, but the time scale should be mentioned somewhere.

REPLY: Please note that in fact the ABEN is now being computed based on a percentage of light reduction (I/I0), rather than a specific light intensity.

The step changes in the panel (c) time-series are not due to time-scale of calculation, but rather to do with changes in the layer thickness and structure.

11/11: It does not look like the equations were copied from Henderson-Sellers (1986), but rather from either the original sources or from Flerchinger (2009)?

REPLY: The placing of the citation to Henderson-Sellers incorrectly gave the impression this is where the full expression was from. You are correct that that we have just chosen 4 based on original sources to implement within the model. We have now cited Henderson-Sellers and Flerchinger as sources for further description and information, rather than as a source for the algorithm set.

**Anonymous Referee #2**

General comments

1. This paper presents the formulation of a one-dimensional model of thermodynamics, mixing, and evaporative and momentum fluxes from lake surfaces, which conceptually should be applicable to a wide variety of lake morphologies. However, the manuscript achieves the paradox of simultaneously containing too much information and not enough information. It goes into great detail with many equations. However, in order to present this level of detail without losing the reader requires more care and at least some additional details.

REPLY: We greatly appreciate the authors comments and insights. We acknowledge the paper is heavy with information, and chose the journal Geoscientific Model Development for this submission as it does support papers focusing on model description. Given the nature of the model it is our desire to have a comprehensive description of the numerous sub-models and options that is peer-reviewed and citable, and, as a result, it has led to a long paper compared to a traditional manuscript. As outlined in the below comments, in this revised version we have endeavoured to improve the narrative and flow of the paper.

I have a few broad suggestions that I think might help.

2a. Before anything, you need to have a clear idea of who is in your audience. You could even have an explicit statement of this very near the beginning, and direct users with a lower level of expertise toward a simpler users' guide.

REPLY: The paper is intended as a description of the model rather than a research paper. Whilst there have been some unpublished manuals and incomplete documentation for the model during its initial development, we felt this is unsatisfactory for a model that has had increasing uptake by lake scientists. In our initial submission, we had stated the aim as:

"Given that individual applications of the model are not able to describe the full array of features and details of the model structure, the aim of this paper is to present a complete description of GLM, including the scientific background (Section 2), model code organization (Section 3), approach to coupling with biogeochemical models (Section 4), and to overview use of the model within the context of GLEON specific requirements for model analysis, integration and education (Section 5-6)."

Our audience is therefore to advanced users looking to understand the mechanics of the model, and/or users publishing applications that need to cite the model methods and approaches adopted in their individual simulations. We acknowledge some users will not dig into the detail and can following the "user" material we have provided on the model website. We note that we have not provided many details about how to run the model, but rather it was our intention for readers to be able to understand the science basis and model structure.

The updated introduction, will hopefully make this intent more clear.

2b. This reviewer has a back- ground explicitly in meteorology, but significant exposure to lake dynamics as well, albeit mostly regarding very large lakes. Depending on your intended audience, you might have readers who will have difficulty with terms such as aliquot and even the intended understanding of "scalar concentrations" as used on p. 27, lines 2-3.

REPLY: Thank-you for pointing these out. We have attempted to improve both these descriptions to improve the clarity of this terminology.

3. To reduce the length of a single paper, one option is to break it into multiple papers. Another is to move more of the detail to appendices. Since it is an online journal, there is probably not a large problem with

overall page length. Things as detailed as conversion of area as a function of depth to volume in a layer (eq. 1) seem like they could be skipped in the main text and relegated to an appendix.

REPLY: We appreciate the comment and agree with the general desire for shorter papers, and feel that in a model description paper such an argument could be made for several of the sub-model descriptions. However, a key purpose of our paper was to describe the model from start to finish (as is done through Section 2), and the layer structure and depth-area-volume relationship is key to the model approach. Aspects such as solar radiation and atmospheric stability computation are optional modules in the code-base and not directly related to what happens within the lake model, and so are included as appendices. Nonetheless, in the preliminary revision we have made some changes to Section 2.1 (referred to specifically in this comment) and feel the new wording of this section has a stronger narrative that hopefully connects it with the subsequent sections.

4. It would be useful to have a brief introduction to each sub-section. This should start out by stating the goal of that sub-section, i.e. what will be the final equation (or set of equations) derived in the section. Then state what elements will combine to get that final equation(s). One particularly glaring issue is that sub-section 2.5.2 ends with eq. 45, defining the variable f, but nowhere does it say how f relates to any other part of the model. It seems to be something that one would multiply by the difference in temperature (or another scalar) between layers) to get the exchange of that scalar between the two layers in a single time step. Whether this is exactly correct or not, the statement is missing from the manuscript.

REPLY: The revised version has attempted to address this general comment by strengthening the narrative in the sections from 2.1-2.7 (the main sub-model description sections). In reference to the comment about the "f" function, the use of the term scalar (and symbol C) is now better introduced, placing this Eq in context. We note that the f computed in this equation is required in the equation where concentrations are updated based on the magnitude of diffusivity between layers (Eq 54 in the revision, and Eq 44 in the original version).

5. A simple overall schematic would be good to have early on (Fig. 15 with less detail). This would make it less abrupt when "water quality model AED2" is mentioned on p. 27 (I may have missed it, but I don't think it was mentioned before.

REPLY: In light of other comments (#8 of the general comments and #42 of the specific comments), we re-drafted Figure 16 and improved clarity in the Fig 1 schematic, but in the ned chose not to make another schematic figure early in the paper. Hopefully the improved text flow in Section 2 will make this more clear.

6. Even if only for your own reference as author, Table 1 needs to be expanded to include every variable used in every equation! And in this expanded table, include every variant of each variable based on the use of different subscripts, prime, and circumflex ("hat"). With this many equations, it is rather inevitable that you also end up using the same symbol for different things (I noticed N in particular). Then, for each variant of each variable, put additional columns for: description, units, spatial type (defined at surface only, spatially continuous, or at discrete layers), and which equations it is used in. The reader needs to have all of these carefully defined.

REPLY: The revision includes a fully updated Table 1, and addresses the issue of confusion of notation by having a more consistent nomenclature scheme.

7. My high school chemistry teacher is the one who taught me how to use units in equations, and the importance of doing so, hence the need for them in the big table above. Some examples of problems with units in the equations that may indicate that the equation is simply wrong: In eq. 52, Q seems like it should have units of m cubed per s, and h units of m, so the right-hand side does not have units of velocity.

REPLY: We apologise for this mistake - this equation (now Eq 62) has been corrected (and the code was checked for consistency). The updated Table 1 now also has consistent units throughout, included for each variable.

8. I approached this manuscript with the immediate question of what makes this model better and more useful than the many others that are available. The introduction does a pretty good job of answering this, but it may be good to give some examples of uses that are not satisfied by other models. This could be introduced with a schematic of its components, options, and functions, at a lower level of detail than in Figs. 15 and 16.

REPLY: Thanks for this suggestion. We do not feel in this paper we have the scope to do a full meta-analysis of the features of all the other lake models and where they are inadequate relative to this effort. Given the number of sub-modules and options, and very wide array of application contexts, it becomes difficult to make judgments about what model options are required for specific lake types and we defer to users to use the model in an appropriate way. We note that Figure 1 does currently aim to be a schematic for the different model components, and functions, but agree this is currently not linked to applications or specific lake types. However, we were worried about adding another Figure and hope the improved introduction may help resolve this issue.

9. Anything that can be done to bring the reader's intuition into play when introducing equations will improve comprehension of the manuscript. Eq. 27 isn't the most problematic one, but I'll use it as an example. You might introduce it by saying something like: "Shortwave radiation is absorbed and attenuates with different e-folding depths for snow, white ice, and blue ice, and these also depend on the light's wavelength. The overall effect is..."

REPLY: Thanks for this suggestion. Wording has been extensively updated across sections 2.1-2.6 to try to improve the flow of the text and clarity of the descriptions.

10. Eq. 47 has me very mystified about how a standard definition of Richardson's number translates into this equation in terms of the angles of inflow geometry (part of the problem may be that I don't feel like I understand the meaning of the angle labeled alpha in Fig. 10; the illustration isn't helping me). It also has me asking "Richardson number at what location?" At the interface of the river water and ambient lake water?

REPLY: We have cited the original source (Fischer et al 1979) of this equation and approach in the original paper, however to improve the interpretability of this we have extended the sentence linking it to the figure.

11. Several of the figures have characters that are so small as to be illegible.

REPLY: We have redrafted the schematic figures with larger symbol fonts.

12. What about modularity of the model? Can other schemes for pieces of the model be plugged in? The details of how may be an appendix or even another paper or guide.

REPLY: The model is not written in an object-oriented fashion, however, custom schemes can be linked to for key sub-module components (e.g do_mixing, do_deep_mixing etc) with some code-adjustments. A comment on this will be added to the code structure section (Section 3).

Some particular examples of the general problems above are among the specific comments below.

Specific comments:

1. In nearly every review that I do, I refer to the rules of hyphens found at http://www.grammarbook.com/punctuation/hyphens.asp particularly Rule 1 on that page. Your manuscript is actually better than most, but here are the problems that I found: P. 2, line 23 should have "system scale" (no hyphen). "Time-scale" is sort of borderline; I tend to use it without a hyphen when it doesn't modify another noun. P. 4, line 15 and some figure captions: "time series". P. 13, lines 22 and 24: "Wind sheltering". P. 24, line 3: "user-specified".

REPLY: Thankyou for this link and advice. These are updated now in the revision.

2. P. 2, line 33: Change "spatial" to "vertical", to contrast with horizontal from earlier in the sentence.

REPLY: This is updated in the revision

3. P. 3, line 10: Stepanenko is misspelled.

REPLY: This is updated in the revision

4. P. 3, lines 17-18: Do you have any comment on use in small vs. large lakes? Both in terms of area and depth? There might also be considerations in terms of morphological complexity.

REPLY: We have now mentioned size when describing 1D models.

5. P. 3, lines 30-31 specifically mention temperature, salinity, and density. Later on, there is mention of the broader category of "scalars". Are you unnecessarily limiting yourself here? I am thinking of such things as dissolved oxygen (mentioned later) and concentrations of nutrients and contaminants.

REPLY: The reference to scalars is now updated in the preliminary revision (now page 5 line 30) to be more clear, and the option of coupling to a water quality model is mentioned (page 6 line 1)

6. P. 3, line 32: I think many readers will object to the use of "hydrodynamic" here, since it does not explicitly represent advection of water. Continuity equations say that dynamics requires at least two dimensions.

REPLY: We would argue that term hydrodynamic refers to the motion of water in general, rather than specifically need to resolve advection in two dimensions. In addition to vertical mixing and transport of water and its constituents, the model does parametrise horizontal advection of inflow water (Eq 62 in the revision). Therefore, whilst the model is not resolving the Navier-Stokes equations, the model approach is intended to capture the movement of water within the lake domain as it is filling, drying, and subject to inflows and withdrawals.

7. P. 4, lines 31-32: "user-defined" and "set by the user" are redundant.

REPLY: Section 2.1 has been significantly revised in the revision upload and this problem is removed.

8. P. 5, line 8: This model doesn't include it, but in reality, vertical advection of heat can be important along with vertical mixing. Again this may depend on the size of the lake, but this factor should be acknowledged here.

REPLY: Aside from mixing, the model captures to some degree the advection of heat and constituents in the water as brought about by inflow or outflow dynamics. For example, new inflowing water would add a layer and lift up layers above its insertion depth, which could be considered as vertical advection. Short term advection associated with internal waves, or perhaps upwelling in large lakes, however is not included.

9. Eq. 4 has issues with sign conventions, units, and possible missing terms depending on how one understands it. It is E multiplied by lake area should be considered a volume flux. For practical purposes these can be considered equivalent, but there would be another term for water density to convert between mass flux and volume flux. Are the evaporation, snowfall, and rainfall defined as being specifically over the area of the lake itself, or over the drainage basin? If over the lake, how is the Q term for runoff optional? I have a hard time imagining many cases of lakes in which it is not a major term in the water balance. If these variables are defined over the whole basin, is there an issue with agreement in timing between P – E and runoff?

REPLY: Eq 4 and this section is now corrected in the revision, with units clarified in Table 1. The heat flux conversion to volume is clarified in this version, accounting for density. The P, E and S terms are computed over the active lake surface. The inflows from the drainage basin into the lake are set by the user as an "inflow" (section 2.7). The local runoff term is not referring to runoff from the wider drainage basin where the lake sits, but the local land within the lake area (Amax-As) that is not inundated with water. This could be important in reservoirs where the volume is drawn down significantly from the maximum level set by the user, or for ephemeral wetlands; in both these cases this area would generally not be considered as part of the inflows from the wider drainage basin, and so Eq 7 (in the preliminary revision) allows for this "dry lake-bed area" to contribute to the water balance.

10. P. 7, line 21: "However" is an interjection, not a conjunction. Here, it stands between two independent clauses, so preceded with either a semicolon or period. Also p. 33, line 10 and p. 35, line 11.

REPLY: This is updated in the revision

11. Eq. 7 is a place where I started to distinctly feel the problem of definition of variables. I had to really think through what had happened to the subscript S from eq. 6 and why the "hats" were there in eq. 7.

REPLY: This is updated in the revision; both the updated notation in Section 2 and Table 1 should prevent this confusion.

12. Eq. 9a has a strange step function in space. Can you justify this not being a smooth function, but rather one value for all of the northern hemisphere, another for the equator (an infinitesimal amount of space), and another for the southern hemisphere?

REPLY: This function has been previously used by many authors for albedo and so is included - we acknowledge this option is simple and hence Option 2 and 3 are provided in the model (Eq 12 in the revision), with specific resolution of the solar angle.

13. P. 9, line 6: What makes the different formulas oceanic and lacustrine? Is there anything to help the reader's intuition for why these formulas should be different?

REPLY: We looked into this, and I think they are just different empirical approaches based on the indivdual researchers choice.

14. Audience issue: P. 10, line 14 departs from the main conceptual theme to give a specific file name. Detailed mathematical formulation and detailed user information don't mix very well.

REPLY: We agree with this observation and have remove the user detail in Section 2.

15. Eq. 14: Are you using a different temperature at the skin (interfacial layer) or bulk temperature a little deeper? Specify how deep.

REPLY: The surface temperature used in the long-wave computation is from the upper-most model layer. This is homogeneous over the depth of the surface layer (surface layer has a sub-script denoted "s"),

however we cannot specify the exact depth, as the model computes the surface layer thickness dynamically, based on the density gradient, mixing intensity and layer limits.

16. P. 11, line 10: Air temperature at how high above the surface? Standard is 2 m, but there may be adjustment needed if measurements are at a different height than that intended in the formulation.

REPLY: The air temperature used throughout the paper is now standardised to 10m and this is defined specifically in Table 1. For users with data from a different height, that may use the f_U parameter to scale the data appropriately.

17. Eq. 163: "Brutsaert" is misspelled.

REPLY: Updated in the revision

18. P. 11, line 13: The range of octals should be 0 to 8.

REPLY: Updated in the revision

19. P. 12, line 11: This should specify molecular weight of dry air, and it might be better to say mass rather than weight.

REPLY: Updated in the revision

20. P. 13, lines 5 and 9: I think these should reference eqs. 17-18 rather than 16-17.

REPLY: Updated in the revision

21. Eq. 23: The Latin v and Greek nu are somewhat difficult to distinguish here, and are even more difficult to distinguish in the text following.

REPLY: Updated in the revision; the notation has been standardised, thereby removing this issue.

22. P. 13, lines 16-18: Thanks for explicitly using units here. Am I correct in understanding that molecular heat conductivity is molecular heat diffusivity multiplied by heat capacity? I think it would be better not to use heat conductivity, but use diffusivity and capacity.

REPLY: Note that units in the revision are updated in the text where appropriate, and Table 1 now includes all units for all variables. You are correct that conductivity is related to diffusivity and heat capacity. The notation adopted (now Eq 28) is based on the original description in TVA (1972)

23. P. 13, line 22: "may be" should be two words.

REPLY: Updated in the revision

24. P. 15, line 13: This use of "conductive heat flux from the ice or snow cover to the atmosphere" particularly triggers my thought bias as a meteorologist. That bias prompts me to assume that this means flux through the atmosphere's interfacial layer, where molecular diffusion dominates. But I also wonder whether it means heat conduction through the ice. These are not equal in general, and need to be distinguished from each other.

REPLY: It does mean the upward conduction through the upper ice layer. For clarity this is depicted in the schematic in Rogers et al (1995) that we had mentioned in the text, on which the model is heavily based (Figure 5 in this source). As such, we chose not to reproduce the energy flux schematic in this manuscript, and have updated the text, but can consider a sub-plot if deemed necessary.

25. Eq. 26: Why isn't shortwave radiation here?

REPLY: This is the way the approach was reported in Rogers et al (1995) (Eq 7 in their paper) and we have followed that; in this case at the surface interface it is assuming the non-pentrative heat flux is in balance with the conduction of heat up to the surface. The conduction of heat up is based on the amount of light that has penetrated (as computed in Eq 31 in the revised upload). We updated the text here to prevent confusion and be more explicit that the net is referring to the non-penetrative component.

26. P. 16, lines 11 and 12: These are very wide ranges of albedo. Please describe the conditions under which different parts of this range manifest.

REPLY: The variation is discussed in the Vavrus et al (1996) paper that we cited; we have added a brief explanation about the variability to this sentence in the revision.

27. P. 18, line 10: The idea of energy required for mixing needs to be introduced more carefully. If you think of the water column as continuous in space, mixing is also a continuum. But the concept here is based on discrete layers, and this indicates how much energy is required to outright include a model layer in the mixed layer.

REPLY: The approach to bulk mixed layer models is well established and as such we provided suggested references for readers interested to gain a deeper understanding of the background: Kraus & Turner (1967) and Kim (1976) and Imberger & Patterson (1981). The model approach we have adopted also has been the subject of numerous prior publications that have thoroughly validated that the layer discretisation can accurately capture the mixing continuum in monomictic and polymictic lakes.

28. Eq. 31: C sub T seems completely undefined.

REPLY: Updated in the revision via Table 1

29. P. 20, line 14: This cannot be reproduced unless your definition of "epilimnion" and "hypolimnion" are precisely stated.

REPLY: Updated in the revision (now Eq 42.)

30. P. 20, line 20: Is K sub epsilon eddy diffusivity.

REPLY: Thankyou for noting this; the revision now includes an update to specify this.

31. Since the vertical axis in Fig. 8 has zero at the bottom, it appears to be height above the bottom, not depth. It might be worth explaining that the varying top height of the color fill is due to varying overall depth (assuming that this is correct).

REPLY: You are correct; in the revision we have been more careful in use and notation associated with depth, height and elevation, and have updated the figures as suggested to use height instead of depth.

32. P. 22, line 13 and eq. 43: This seems to say that sigma should have units of inverse seconds squared, which implies that the square-bracketed part of eq. 43 has units of (m/s) squared, but exponential operations can only be performed on unitless numbers.

REPLY: Thankyou again for noting this inconsistency. Both the top and bottom of the fraction in this equation (Eq 53 in the revision) are in the units of m^2, so the fraction for the exponential is dimensionless. Text has been updated.

33. P. 24, line 5: Slope is usually defined as a ratio of rise divide by run, not an angle. I would say that the slop is the tangent of the angle.

REPLY: You are correct, this sentence is updated.

34. The inset in Fig. 10 does not help me understand the meaning of the angle alpha, and it could use larger lettering.

REPLY: We have made a modification to this figure to improve readability and detail.

35. Equation 52 seems messed up. Units-wise, it seems to make more sense if h squared is in the denominator instead, but I also wonder why there is no dependence on width of inflow.

REPLY: We apologise for this error and it has been corrected in the revision (now Eq 62). The scheme does not account for the width of the inflow explicitly, but it is approximated based on the water height and channel angle (as depicted in the inset of Fig 10).

36. P. 26, line 16: In standard usage, dz represents an infinitesimal difference in z in continuous space, but here it is used to indicate a finite distance in discretely sectioned space.

REPLY: This expression and associated notation has been revised (now Eq 69). The symbol delta is now uniformly used to refer to a length-scale, as is the intent here.

37. P. 26, lines 16-17: It is difficult to understand the distinction between “height of withdrawal” and “edge of the withdrawal layer”.

REPLY: This description has been further developed in the revision (now Page 30), to explicitly define how the withdrawal thickness and the relevant layer edge is determined.

38. P. 26, line 19: Why say “fluid” rather than “water”?

REPLY: You are correct that water is more specific – we have replaced the use of fluid with water in the revision.

39. A formatting problem put some labels that belong to Fig. 12 on p. 27, while the rest of the figure is on p. 28.

REPLY: This has now been rectified

40. P. 28, lines 10-11: Removing no more than half of a layer’s mass per time step seems like a reasonable way to ensure numerical stability, but it would be good to re- mind the reader here of the layer merging scheme that is likely to kick in. This merging and disaggregation scheme, also mentioned on p. 34, is never really described well.

REPLY: Thankyou for this suggestion. We have revised both these sections to improve clarity of these descriptions in the preliminary revision, including making both consistent by enforcing a 90% limit. The merging and splitting scheme is introduced (page 6 line 7 of the revision), however we note the concern this is not described fully, and have referred to it where relevant now, but probably should consider a new sub-section.

41. P. 29, line 3 says “wind speed and fetch. . .calculated as”, while eq. 61 only shows the formula for fetch.

REPLY: The sentence introducing this Eq has been be re-worded to remove this ambiguity.

42. To help solve the problem of small print in Fig. 16, it may be useful to transfer some of the information to a table instead.

REPLY: Thankyou, we have re-drafted this figure, to prevent the small fonts.

43. P. 34, line 19 has a placeholder for a citation. This is evidence of a poor final edit on the part of the authors.

REPLY: Updated in the revision; apologies for this oversight.

44. P. 34, line 23: If you mention calibration, it would be well to describe this process more fully, in particular which parameters you consider adjustable for purposes of calibration. Where p. 35, line 10 mentions “compare”, I wonder whether this might also imply calibration.

REPLY: The initial line referred to is an introductory statement with the intent that the text in Section 5.2 would describe the calibration process more fully. We have mentioned in this section the link to our associated model validation paper (Bruce et al., 2018).

45. P. 48, line 12: “Anneville” misspelled?

REPLY: Updated in the revision

**Anonymous Referee #3**

General Comments

1. This paper describes the detailed functioning of the 1D physical lake model GLM 2.4 and its application potential. The model incorporates a broad range of physical processes as surface heat exchange, snow and ice dynamics, in- and outflow, submerged inflow and groundwater seepage and can be coupled with or embedded into other models. The authors explain how GLM 2.4 has emerged as a response to the need of standardized, yet flexible and computationally effective community lake model to interpret environmental data from a broad range of lakes collected within the Global Lake Ecological Observatory Network (GLEON). The model has been formulated as a new code in 2012, whereas layer structure, mixing algorithms and physical formulae are based on earlier peer reviewed work. The authors state that the code is computationally efficient and well suited for embedding in larger scale modelling frameworks. The authors present also an overview of pre- and post-processing utilities as well as an innovative cloud computing environment. Lastly, they elaborate on the educational use and gained experience in the classroom.

REPLY: Thankyou for this very accurate summary

2. I realized that this manuscript is for a major part equivalent to an earlier manual of GLM (V2 Manual, October 2014, accessed on the 08.01.2017 from http://aed.see.uwa.edu.au/ research/models/GLM/Pages/ documentation.html). I think the authors should mention this.

REPLY: It is our intent that this paper replaces the online manual and we have removed the available PDF cited above. The online manual was used as an interim resource to inform users until the model development efforts had stabilised. Now this is the case, the revised version of the present paper includes more detail and numerous improvements, extensions and fixes to errors and should become the key reference. Aspects of that manual associated with model-use & setup that are not covered in this (science-oriented) paper have been migrated to the website pages.

3a. The model in this paper represents with no doubt a tremendous effort in lake modelling and is of interest for modelers in various fields of environmental research. The publication of this model is a step towards better model documentation and contributes to the general scientific discussion and better lake model development. As such it falls within the scope of this journal. The paper is well written and the language is easily com- prehensible. Unfortunately, this manuscript has some structural problems and there are quite a few mistakes in equations and figures. After dealing with these issues, the manuscript should be good for publishing.

REPLY: Thank you for this recommendation. We have endeavoured to resolve the specific issues that you and the other reviewers have identified in this revision.

3b. The main problem of this very long manuscript is that it is missing an instant overview of what is in the paper and what not. Scanning through, the reader gets lost easily in the large chapter 2 'model overview' and might miss the subsequent chapters that elaborate more on the possibilities and significance of this model for the scientific community.

REPLY: We acknowledge this view, which is similar to a comment #2 by R2, and have updated the introduction significantly with the aim of providing a better "road-map" for the paper structure.

4. I think that this problem can be fixed with some changes in the introduction: âA˘c´ I suggest using subtitles in the introduction. (In the introduction, the authors describe the importance of the study of lakes, the importance of GLEON, the importance of lake models, the advantages of simple models, applications and features of 1D models, the need for a flexible open-source model, how GLM 2.4 answers this need and finally an overview of the paper) âA˘ c´ I suggest creating a new paragraph starting at p. 3 Line 19 ... "Nonetheless, there . . .". The need of an open source and flexible community model that can be applied to various lakes should be highlighted better. Another additional paragraph could explain how GLM 2.4 responds to this need. As I understand, GLM 2.4 is filling the gap because it provides a standard middle

complexity physics ‘shell’ (simple yet enough complex to be applied for various lakes) that can be connected individually to or implemented into various other models (e.g. water quality or land- climate models). I think this point could be emphasized. âA˘ c´ A figure could be helpful to draw attention to the significance of this model in the scientific community. This could also be combined with schematic overview of the model functioning (I agree with R2 that anything that gives an overview helps). âA˘ c´ The specific limitations of GLM 2.4 (not of 1D models in general) should be mentioned in the introduction. Like this, the reader may have a quick idea whether GLM is suitable for him/her. What are the key features of this model that set it apart from other models? âA˘ c´ On p. 4 lines 5-9, the authors explain the aims of the paper and in which of chapter 2-6 these aims are met. I think these lines are important and should be extended to a paragraph by itself to make sure the reader is fully aware what to expect from the paper. In the same paragraph, I would also expect some more information regarding what this paper is not about and mention that a companion paper by Bruce et al. (2017) is assessing the model’s error structure against 31 GLEON lakes.

REPLY: Thank you for this very useful suggestion and we have heavily modified the introduction in the revision, thought stopped short at adding another figure as our attempt at such a figure didn't seem worthy.

5. I think the authors did not carefully go through the complete manuscript. Many of the empirical equations are missing the definition of units for used variables. On other occasions variables where poorly described (see the examples listed below, as well as listed by R1 and R2). On several figures elevation and not the labeled depth is shown on y axis. The references are not formatted coherently. Like R2, I am of the opinion that many variable symbols are confusingly similar and that they should all be listed in a table. I also agree with R2 that all the subchapters of chapter 2 should have a small introduction paragraph. Further, I agree with the comments of R1 on the equations 1, 2, 3, 5, 9c, 12, 16 and with the comments of R2 on the equations 4, 7, 14, 26, 31, 52.

REPLY: Our sincere apologies that we didn’t identify these flaws in the original upload. In our responses to R1 and R2 we have detailed many fixes to these issues, including a significantly revised nomenclature and summary table with all variables and units. The revision addresses most of the issues, including updates to the nomenclature and figures, and improved contextual information in the Section 2 sub-sections.

Specific comments

6. I think it is not very clear how the amalgamating, expanding, contracting or splitting and adding of layers works. For example, in p. 23 L 21 it is not obvious what the mentioned ‘numerical criteria within the model’ are. I would explain these in detail somewhere in the beginning of chapter 2.

REPLY: We have revised Section 2.1 to add clarity to the layer scheme, and as also noted to R2 (specific comment #40), and also better descriptions in other module sections.

7. p. 6 eq 2 and eq 3: It seems odd that the interpolation of values between levels b-1 and b are depending on b-1, b and b+1 and not only on b-1 and b.

REPLY: This error is fixed in the revision

8. p. 10 Line 5-8: ϕSWS is defined only in text form and not as an equation, yet it is used in equation 6. There is the danger that ϕSW defined in eq 10 will be confused with ϕSWS. I suggest mentioning early on in this subchapter how you approach calculating ϕSWS.

REPLY: This notation for energy fluxes has been significantly improved and checked in the new revision; the extended Table 1 now makes the symbol definitions and units clear, and the text is updated accordingly.

9. p. 12 eq 17: formula only for forced convection? Wind speed at what height? What are the units? I would introduce first the concepts of sensible heat (free and forced con- vection) and latent heat (evaporation and condensation) before showing the equations.

REPLY: As per point #8 above, the notation for heat transfers has been significantly updated in the revised version. This makes explicit the reference height. As per the above suggestions for an opening paragraph in

the sub-sections, we have re-worded the opening and other parts of this sub-section to better introduce free and forced convection.

10. p. 18 L10: An intro with possible conceptual options to reproduce a surface mixed layer would be good. I would like to know how the chosen approach of a bulk mixed layer depth compares to other approaches in other models (e.g. k-epsilon turbulence closure with Fickian diffusion) and what the consequences of this approach are.

REPLY: We have not delved into a critical assessment of the model approach in this sub-section. We acknowledge your interest in the approach relative to alternatives but at 24000 words already we decided a review and critical assessment was not appropriate here, and the paper should focus on description. We have published a companion paper that compares the model performance in capturing stratification (Bruce et al, 2018) and others have done 1D model inter-comparisons.

11. p. 22 L 15 and eq 44 and eq 45: I think an explanation of the concept behind this numerical scheme is necessary

REPLY: We have provided some additional explanation to this description for this diffusion algorithm in the revised version.

12. p. 24. Figure 10: This figure is not enough self-explanatory to me.

REPLY: A revised version of this figure has now been included, better depicting the interaction of the inflow "parcels" with the lake layer structure, and using the updated notation (consistent with Table 1).

13. p. 28 eq 60: Shouldn't G not just be another term in eq 4 for all cases?

REPLY:

You are correct that the change in the thickness of the bottom layer then also leads to a downward vertical shift in the elevation of all the layers above (equivalent to advection, as also discussed with R2 specific comment #8). The wording of the seepage section is now updated. As this step occurs separately to the surface dynamics routine we had not included a term for this in Eq 4, and instead included a sentence describing this effect :

" However, in addition to the terms in Eq. 4, $h_S$ is modified due to volume changes associated with river inflows, withdrawals, seepage or overflows, which are described in subsequent sections."

14a. p. 40 lines 21-24: move this sentence to the intro

REPLY: In light of the proposed changes to the introduction discussed in comment #4, we have updated accordingly.

14b. p. 40 L 24 – 26: This needs to be better explained.

REPLY: We have removed this

List of Corrections

15. p. 1 lines 31-32. Consider splitting sentence as it contains different ideas.

REPLY: Thank you for the suggestion, we have revise the abstract.

16. p. 2. Line 1: write only 'standing' as this word is comprehensible and you don't use lentic in the rest of the text.

REPLY: Thank you for the suggestion, we have made this change.

17. p. 5 Line 17. Write the definite instead of the indefinite integral or otherwise phrase it in a sentence.

REPLY: We have updated the integral to be between $H_0$ and $H_max$.

18. p.6 eq 1: could be simplified

REPLY: Thank you for the suggestion, we have made this change.

19. p.6. Line 11-18: Should this go in the introduction?

REPLY: This section has been updated

20. p. 9 eq 9b: Contrary to R1, I managed to get the peak at 80◦SZA. The equation seems to be the same as used in fig 3.

REPLY: Fig 3 is updated and checked - problem with the bracket location!

21. p. 9 eq 9c: Specify units, also see comments of R1.

REPLY: This is updated in the revised version and also see the reply to R1.

22. p. 9. L 6: Ux is wind speed at which height?

REPLY: Within the revised vresion, all meteorological variables are now referenced to 10m, $U_10$. This is computed from the user input data ($U_x$) as $U_10 = f_UU_x$. The updated equation in the preliminary revision (now Eq 12c) however still needs correcting from $U_x$ to $U_10$.

23. p.9 figure 3: Specify the values of relative humidity, wind speed and atmospheric diffusive radiation used for eq 9c. I agree with R1 that the label is wrong, but I think it should be SZA = 360◦ Φzen/(2π) = 180◦ Φzen/π

REPLY: This figure is updated in the revision, and we have extended the caption to specify the values.

24. p. 11 eq 16 a-d: Use either only ◦C or only K in equations, now they are mixed. I found eq 16 c in Henderson-Sellers (1986) but strangely I couldn't find this equation in Brutseart (1975).

REPLY: The notation is now updated so as to distinguish between them ($T$ and $\theta$, respectively).

25. p. 12 L 12: no units specified for latent heat of vaporization

REPLY: Table 1 in the revision has been updated to have unit descriptions of ALL variables.

26. p. 13 L 9 and L 13: I guess the authors meant eq 17 -18 and not eq 16-17?

REPLY: Yes, corrected in the revision.

27. p. 16 L 6: 'penetrating the surface', which surface?

REPLY: This is referring to the ice/snow surface, now corrected in the revision.

28. p. 20 eq 35: What is u0?

REPLY: Following our updates to the notation in this revision, it is now $u_b_old$; it is the layer velocity at the previous time-step. We have added to Table 1 as it has been overlooked.

29. p. 22 eq 39: Please explain the variables in this equation.

REPLY: Apologies for this oversight and confusing notation. The revision includes the description of $\tildaV$ further down (and in Table 1), however we have moved this first description up to this point. The symbol for the surface layer thickness is also now matching the earlier use. However, we noted a further error since the k in this expression should be squared and it is now updated.

30. p. 22 eq 43: check index, should be hl not hi

REPLY: This is updated in the revision (now Eq 53).

31. p. 23 L 17: typo: entrain (not entrains)

REPLY: This is updated in the revision.

32. p. 23 L 18: typo: the (not th)

REPLY: This is updated in the revision.

33. p. 34 figure 17: increase font size and size of arrows.

REPLY: We have updated the resolution and fonts in this figure in the revision.

34. p. 34 L 19: Insert the references into the place holder

REPLY: This is updated in the revision.

35. p. 35 L 26: Who is testing these 'Wrappers' and examples? What is a wrapper?

REPLY: Updated to remove wrappers.

36. p. 37 L 13: What is HTCondor?
REPLY: Updated.

37. p. 27 L 16: Start a new paragraph at 'GRAPLEr's Web service . . .' to highlight this idea.
REPLY: Agreed

38. p. 40 L 24 – 26: Explain better.
REPLY: See the reply to comment #14b above

39. References Formatting: Some parts are underlined, remove it. Change all to coherent formatting.
REPLY: The reference formatting has been refined in the revision.

40. P. 49 L 23, 25 same author, write same initials.
REPLY: Agreed

41. P. 51 L 13, is there a translation of this Japanese paper? Check the year (2014 in text, here 2015)
REPLY: Unfortunately there is no English translation of this article, however, Yajima pers comm provided an English summary of the algorithm performance and coefficients. Year has been corrected in the revision.

42. Table 1: If there is no default variable, can you give a range for snow density, compaction coefficient, and thermal conductivity of snow?
REPLY: Table 1 has been updated to specify "computed" and in the comments the relevant equation is now referred to.

43. Table 1: Latent heat of fusion: remove the trailing zero 334
REPLY: Updated in the revision.

Geosci. Model Dev. Discuss., https://doi.org/10.5194/gmd-2017-257
Manuscript under review for journal Geosci. Model Dev.
Discussion started: 20 November 2017


Geoscientific Model Development Discussions

Revision 8 Mar 2018

# A General Lake Model (GLM ~~2.4~~3.0) for linking with high-frequency sensor data from the Global Lake Ecological Observatory Network (GLEON)

Matthew R Hipsey[1,*], Louise C Bruce[1], Casper Boon[1], Brendan Busch[1], Cayelan C. Carey[2], David P Hamilton[3], Paul C. Hanson[4], Jordan S. Read[5], Eduardo de Sousa[1], Michael Weber[6], Luke A. Winslow[7]

[1] UWA School of Agriculture & Environment, The University of Western Australia, Crawley WA, 6009, Australia
[2] Department of Biological Sciences, Virginia Tech, Blacksburg VA, USA
[3] Australian Rivers Institute, Griffith University, Nathan QLD, 4111, Australia
[4] Center for Limnology, University of Wisconsin - Madison, Madison WI, USA
[5] Center for Integrated Data Analytics, U.S. Geological Survey, Middleton WI, USA
[6] Department of Lake Research, Helmholtz Centre for Environmental Research - UFZ, Magdeburg, Germany
[7] Department of Biological Sciences, Rensselaer Polytechnic Institute, Troy NY, USA

[*] *Correspondence to*: Matthew R. Hipsey (matt.hipsey@uwa.edu.au)

*Keywords:* lake, stratification, mixing, water balance, climate change, water quality, observatory network,
*Word count*: ~~12~~13,000 words (text); ~~18~~24,000 words (text+references+figures&tables+~~appendix~~appendicies)

**Abstract.** The General Lake Model (GLM) is a one-dimensional open-source ~~model~~ code designed to simulate the hydrodynamics of lakes, reservoirs and wetlands. GLM was developed to support the science needs of the Global Lake Ecological Observatory Network (GLEON), a network of ~~lake sensors and~~ researchers attempting to use lake sensors to understand lake functioning and address questions about how lakes around the world ~~vary in response~~respond to climate and land-use change. The scale and diversity of lake types, locations and sizes, as well as the expanding observational ~~data within GLEON~~datasets, created the need for a robust community model of lake dynamics with sufficient flexibility to accommodate a range of scientific and management ~~needs of~~questions relevant to the GLEON community. This paper summarises the scientific basis and numerical implementation of the model algorithms, including details of sub-models that simulate surface heat exchange and ice-cover dynamics, vertical mixing and inflow/outflow dynamics. ~~A summary of typical parameter values for lakes and reservoirs collated from a range of sources is included.~~We demonstrate the suitability of the model for different lake types, that vary substantially in their morphology, hydrology and climatic conditions. GLM supports a dynamic coupling with biogeochemical and ecological modelling libraries for integrated simulations of water quality and ecosystem health~~. An overview of approaches~~, and options for integration with other environmental models~~, and~~ are outlined. Finally, we discuss utilities for the analysis of model outputs and ~~for undertaking sensitivity and~~ uncertainty assessments ~~is also provided. Finally,~~

Geosci. Model Dev. Discuss., https://doi.org/10.5194/gmd-2017-257
Manuscript under review for journal Geosci. Model Dev.
Discussion started: 20 November 2017


Geoscientific Model Development Discussions

Revision 8 Mar 2018

~~we discuss application of the,~~ model operation within a distributed cloud-computing environment, and as a tool to support learning of network participants.

## 1 Introduction

Lakes and other ~~lentic (~~standing~~)~~ waters support extensive ecosystem services such as water supply, flood mitigation, hydropower, aesthetic and cultural benefits, as well as fisheries and biodiversity (Mueller et al., 2016). Lakes are often considered to be "*sentinels of change*", providing a window into the sustainability of activities in their associated river basins (Williamson et al., 2009). They are also particularly susceptible to impacts from invasive species and land use development, which often lead to water quality deterioration and loss of ecosystem integrity. Recent estimates have demonstrated their significance in the earth system, contributing to heterogeneity in land surface properties and feedbacks to regional and global climate through energy, water and biogeochemical transfers (Martynov et al., 2012, Cole et al., 2007). For example, Tranvik et al. (2009) ~~suggested~~suggest carbon burial in lakes and reservoirs is substantial on ~~the~~a global scale, on the order of 0.6 Pg $yr^{-1}$, or four times the oceanic burial rate.

Given the diversity of lakes among continents, region-specific pressures and local management approaches, the Global Lake Ecological Observatory Network (GLEON: gleon.org) was initiated in 2004 as a grass-roots science community with a vision to observe, understand and predict freshwater systems at a global scale (Hanson et al., 2016). In doing so, GLEON has been a ~~leading~~successful example of collaborative research within the hydrological and ecological science disciplines. ~~-~~ GLEON aims to bring together environmental sensor networks, numerical models, and information technology to explore ecosystem dynamics across a vast range of scales - from ~~an~~ individual ~~lake~~lakes or ~~reservoir~~reservoirs (Hamilton et al., 2015) to regional (Read et al., 2014; Klug et al., 2012), and even global ~~trends~~extents (Rigosi et al., 2015; O´Reilly et al., 2015). Ultimately, it is the aim of the network to facilitate ~~primary~~ discovery and synthesis, and to provide an improved scientific basis for sustainable freshwater resource management.

Environmental modelling forms a critical component of observing systems, as a way to make sense of the "data deluge" (Porter et al., 2012), allowing users to build virtual domains to support knowledge discovery at the system ~~-~~ scale (Ticehurst et al., 2007; Hipsey et al., 2015). In lake ecosystems, the tight coupling between physical processes and water quality and ecological dynamics has long been recognised~~, and models~~. Models have capitalized on comprehensive understanding of physical processes (e.g., Imberger and Patterson, 1990; Imboden and Wüest, 1995) to use hydrodynamic models as an underpinning basis for coupling to ecological models ~~that~~. Such models have contributed to our understanding of lake dynamics, including aspects such as ~~mixing regimes,~~climate change (Winslow et al., 2017), eutrophication dynamics (Matzinger et al., 2007), harmful algal bloom dynamics (Chung et al., 2014), and fisheries (Makler-Pick et al., 2009).

In recent decades a range of 1, 2, and 3-dimensional hydrodynamic models has emerged for lake simulation ~~across a diverse range of time scales.~~ Depending on the dimensionality, the horizontal resolution of these models may vary from metres to tens of kilometres~~, and the spatial resolution~~ with vertical resolutions from sub-metre to several metres. As in all modelling

Geosci. Model Dev. Discuss., https://doi.org/10.5194/gmd-2017-257
Manuscript under review for journal Geosci. Model Dev.
Discussion started: 20 November 2017


Geoscientific Model Development Discussions



disciplines, identifying the most parsimonious model structure and degree of complexity and resolution is challenging, and users in the lake modelling community often tend to rely on heuristic rules or practical reasons for model choice (Mooij et al., 2010). High-resolution models are suited to studying events that occur at the time- scale of flow dynamics, but are not always desirable for ecological studies over longer time scales due to their computational demands and level of over-parameterisation. On the other hand, simple models may be more agile for a particular application, and more suited to parameter identification and scenario testing workflows. However, it has been the case within GLEON that simple models are often less applicable across a wide variety of domains, making them less generalizable, which is a key requirement of synthesis studies. Despite the fact that there is a relatively large diversity of models and approaches for aquatic ecosystem simulation (Janssen et al., 2015), it is generally agreed that to improve scientific collaboration within the limnological modelling community, there is an increasing need for flexible, open-source community models (Trolle et al., 2012). Whilst acknowledging that there is no single model suitable for all applications, a range of open-source community models and tools can enhance scientific capabilities, and foster scientific collaboration and combined efforts (Read et al., 2016). ~~, but are often less applicable across a wide variety of domains, making them less generalizable.~~ There are several examples of such initiatives being successful in the oceanography, hydrology and climate modelling communities.

With this in mind, the General Lake Model (GLM), a one-dimensional (1D) hydrodynamic model for enclosed aquatic ecosystems, was developed. The lake modelling community has often relied on ~~1-dimensional (~~1D~~)~~ models, which originated to capture lake water balance and thermal stratification dynamics (e.g., Imberger and Patterson, 1981; ~~Peeters et al., 2007;~~ Saloranta and Andersen, 2007; Perroud et al., 2009; Kirillin et al., 2011; ~~Stepanko~~Stepanenko et al., 2013). ~~Their~~The use of 1D structure is justified across a diverse range of lake sizes given the dominant role of seasonal changes in vertical stratification on lake dynamics, including oxygen ~~dynamics~~, nutrient and metal cycling and plankton dynamics (Hamilton and Schladow, 1997; Gal et al., 2009). Despite advances in computing power and more readily available 3D hydrodynamic drivers, ~~they~~1D models continue to remain attractive as they are easily linked with biogeochemical and ecological modelling libraries for complex ecosystem simulations~~, allowing them~~. This allows 1D models to be used to capture the long-term trajectory and resilience of lakes and reservoirs ~~in response~~ to climate change, hydrologic change and land use change~~; for~~. For example, such models have been used to model long-term changes to oxygen ~~and~~, nutrient cycles, and the ~~increasing~~changing risk of algal blooms (e.g., Peeters et al., 2007; Hu et al., 2016; Snortheim et al., 2017). Furthermore, ~~their~~the low computational requirements of this approach relative to 3D models ~~allow for their use in~~ is more suited to parameter identification ~~routines~~and uncertainty analysis, making ~~them~~it an attractive balance between process complexity and computational intensity. ~~Nonetheless, there has been a continuing proliferation in the diversity of lake models (Mooij et al., 2010; Janssen et al., 2015), with no clear packages that are suited to the broad range of geographic contexts, time scales, and science questions and management issues being addressed by the network participants. In acknowledging that there is no single model suitable for all lake applications, a range of open-source community models and tools can enhance scientific capabilities and foster scientific collaboration and combined efforts (Read et al., 2016). To improve scientific collaboration within the limnological modelling community, however, there is an increasing need for a flexible, open-source community model that limnologists~~

Geosci. Model Dev. Discuss., https://doi.org/10.5194/gmd-2017-257
Manuscript under review for journal Geosci. Model Dev.
Discussion started: 20 November 2017


Geoscientific Model Development Discussions
Open Access
EGU



~~can apply to their own lakes (Trolle et al., 2012), as has been common in oceanography, hydrology and climate modelling communities.~~

~~In response to this need, the General Lake Model (~~GLM~~), a one-dimensional hydrodynamic model for enclosed aquatic ecosystems was developed. The model~~ emerged as a new open-source code ~~from GLEON activities~~ in 2012, ~~and computes~~with the design goal of balancing the ~~lake water and energy balance by adopting a variable layer structure, allowing for simulation of vertical profiles~~complexity of ~~temperature, salinity and density, and considering the potential effects~~dimensional representation, applicability to a wide range of ~~inflows and outflows, surface heating and cooling, mixing and the effect of ice cover on heating and mixing of the lake. GLM is itself a hydrodynamic model, but has dynamic links~~standing waters, and availability to ~~biogeochemical models, allowing for exploration of stratification and vertical mixing on the dynamics of biogeochemical cycles, water quality attributes, and lake ecology.~~ a broad community (e.g., GLEON). The scope and capability of the model has ~~since~~ developed rapidly with application to numerous lakes and lake-types within the GLEON network and beyond (e.g., Read et al., 2014; Bueche et al., 2017, Snortheim et al., 2017; Weber et al., 2017; Menció et al., 2017; Bruce et al., 2017). ~~GLM has been designed to be an open-source community model suited to modelling studies across a broad spectrum of~~ It is unique in that its suitability now ranges from ephemeral wetlands and ponds to deep lakes, from natural systems to heavily managed man-made reservoirs ~~and wetlands. It balances complexity of dimensional representation, applicability to a wide range of standing waters~~, and ~~availability to a broad community (e.g., GLEON).~~across climatic regions. Given that individual applications of the model ~~are not able to describe~~rarely engage the full array of features ~~and~~or describe the full details of the model structure, the aim of this paper is to present a complete description of GLM, including the scientific background (Section 2), and model code organization (Section 3~~),~~). The approach to coupling with biogeochemical models is also discussed (Section 4~~), and~~ ) since a main objective of the model development is to intimately link with biogeochemical models to support exploration of stratification and vertical mixing on the dynamics of biogeochemical cycles and lake ecology. Finally, an overview of the use of the model within the context of GLEON specific requirements for model analysis, integration and education (Section 5-6) is described. In order to better define the typical level of model performance across these diverse lake types, a companion paper by Bruce et al. ~~)~~ (2018) has undertaken a systematic assessment of the model's error structure against 31 lakes from across GLEON.

## 2 Model Overview

### 2.1 Background and layer structure

~~GLM adopts a~~The 1D approach ~~for simulating lake mixing processes~~adopted by ~~resolving~~GLM resolves a vertical series of layers that ~~describe~~capture the variation in water column properties. Users may configure any number of inflows and outflows, and more advanced options exist for simulating aspects of the water and heat balance~~.~~ (Figure 1). Depending on the context of the simulation, either daily or hourly meteorological time~~-~~ series data for surface forcing is required, and daily time~~-~~ series of volumetric inflow and outflow rates can also be supplied. The model is suitable for operation in a wide range of climate conditions and is able to simulate ice formation, as well as accommodating a range of atmospheric forcing conditions.

Geosci. Model Dev. Discuss., https://doi.org/10.5194/gmd-2017-257
Manuscript under review for journal Geosci. Model Dev.
Discussion started: 20 November 2017




Revision 8 Mar 2018

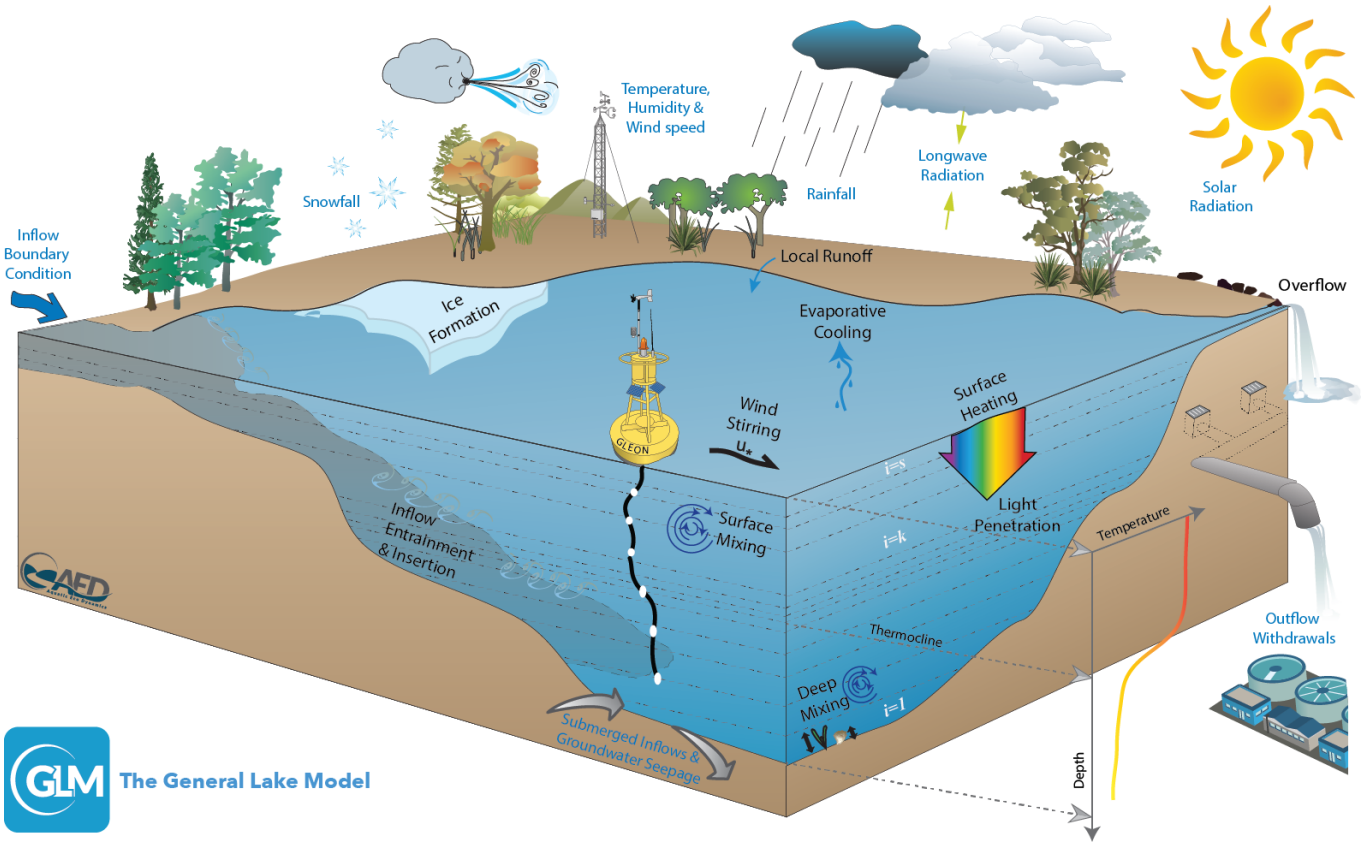


**Figure 1: Schematic of a GLM simulation domain, input information (blue text) and key simulated processes (black text).**

Although GLM is a new model code written in the C programming language, the core layer structure and mixing algorithms ~~is~~are founded on principles and experience from model platforms including the Dynamic Reservoir Simulation Model (DYRESM; Imberger and Patterson, 1981; Hamilton and Schladow, 1997) and the Dynamic Lake Model (DLM; Chung et al., 2008). Other variations have been introduced to extend this underlying approach through applications to a variety of lake and reservoir environments~~, to which the reader is also referred~~ (e.g., Hocking & Patterson, 1991; McCord & Schladow, 1998; Gal et al., 2003; Yeates and Imberger, 2003). The layer structure is numbered from the lake bottom to the surface, and adopts the flexible Lagrangian layer scheme first introduced by Imberger et al. (1978) and Imberger ~~&~~and Patterson (1981). The approach defines each layer, $i$, as a 'control volume' that can change thickness by contracting and expanding in response to inflows, outflows, mixing with adjacent layers, and surface mass fluxes, as depicted schematically in Figure 1. As the model simulation progresses, density changes due to surface heating, vertical mixing, and inflows and outflows lead to dynamic changes in the layer structure, associated with layers amalgamating, expanding, contracting or splitting. Notation used throughout the model description is provided in Table 1.

As layers change, their volumes change based on the site-specific hypsographic curve, whereby the overall lake volume, $V_{max}$, is defined as $\int_{H_0}^{H_{max}} A[H]\, dH$, with the elevation ($H$), and area ($A$) relationship provided as a series of points based on

Geosci. Model Dev. Discuss., https://doi.org/10.5194/gmd-2017-257
Manuscript under review for journal Geosci. Model Dev.
Discussion started: 20 November 2017


Geoscientific Model Development Discussions
Open Access
EGU



bathymetric data. This computation requires the user to provide a number, $N_{BSN}$, of heights with corresponding areas. The cumulative volume at any lake elevation is first estimated as:

$$V_b = V_{b-1} + [A_{b-1} + 0.5(A_b - A_{b-1})](H_b - H_{b-1}) \quad (1)$$

where $2 \leq b \leq N_{BSN}$. Using this raw hyposgraphic data, a refined height-area-volume relationship is then internally computed using finer height increments (e.g., $\Delta H_{mi} \simeq 0.1$ m), giving $N_{MORPH}$ levels that are used for subsequent calculations. The area and volume at the height of each increment, $H_{mi}$, are interpolated from the supplied information as:

$$V_{mi} = V_{b-1}\left(\frac{H_{mi}}{H_{b-1}}\right)^{\alpha_{b-1}} \quad \text{and} \quad A_{mi} = A_{b-1}\left(\frac{H_{mi}}{H_{b-1}}\right)^{\beta_{b-1}} \quad (2)$$

where $V_{mi}$ and $A_{mi}$ are the volume and area at each of the elevations of the interpolated depth vector, and $V_{b-1}$ and $A_{b-1}$ refer to the nearest $b$ level below $H_{mi}$ such that $H_{b-1} < H_{mi}$. The interpolation coefficients are computed as:

$$\alpha_b = \left[\frac{log_{10}\left(\frac{V_{b+1}}{V_b}\right)}{log_{10}\left(\frac{H_{b+1}}{H_b}\right)}\right] \quad \text{and} \quad \beta_b = \left[\frac{log_{10}\left(\frac{A_{b+1}}{A_b}\right)}{log_{10}\left(\frac{H_{b+1}}{H_b}\right)}\right]. \quad (3)$$

Within this lake domain, the model solves the water balance by including several user configurable water fluxes that change the layer structure. Initially, the layers are assumed to be of equal thickness, and the initial number of layers, $N_{LEV}(t = 0$~~. Layer thickness limits are enforced to adequately resolve the vertical density gradient with fine resolution occurring in the metalimnion and thicker cells where mixing is occurring, as depicted schematically in Figure 1. Unlike fixed grid (Eulerian) design of most 1D lake and ocean models, where mixing algorithms are typically based on resolving vertical velocities, it has been reported that numerical diffusion at the thermocline can be restricted by this approach (depending on the user-defined minimum ($h_{min}$) and maximum ($h_{max}$) layer thickness limits set by the user), making it particularly suited to long term investigations, and requiring limited site-specific calibration (Patterson et al., 1984; Hamilton & Schladow, 1997; Bruce et al., 2017). Layers each have a unique density computed based on the local salinity and temperature, and when~~) is computed based on the initial water depth. Water fluxes include surface mass fluxes (evaporation, rainfall and snowfall), inflows (surface inflows, submerged inflows and local runoff from the surrounding exposed lake bed area) and outflows (withdrawals, overflow and seepage). Surface mass fluxes operate on a sub-daily time step, $\Delta t$, by impacting the surface layer thickness (described in Section 2.2), whereby the dynamics of inflows and outflows modify the overall lake water balance and layer structure on a daily time step, $\Delta t_d$, by adding, merging or removing layers (described in Section 2.6). Depending on whether a surface (areal) mass flux or volumetric mass flux is being applied, the layer volumes are updated by interpolating changes in layer heights, whereby $V_i = f[h_i]$, and $i$ is the layer number, or layer heights are updated by interpolating changes in layer volumes, whereby $h_i = f[V_i]$.

Each layer also contains heat, salt ($S$) and other constituents ($C$) which are generically referred to as scalars. These are subject to mass conservation as layers change thickness or are merged or split. The specific number of other constituents depends on the configuration of the associated water quality model, but typically includes attributes such as oxygen, nutrients and phytoplankton. Layer density is computed from the local salinity and temperature according to TEOS-10, whereby $\rho_i = \rho[T_i, S_i]$. When sufficient energy becomes available to overcome density instabilities between adjacent layers, ~~they will~~the layers merge, thereby accounting for the process of mixing~~.~~ (Section 2.5). For deeper systems, a stable vertical density gradient

Geosci. Model Dev. Discuss., https://doi.org/10.5194/gmd-2017-257
Manuscript under review for journal Geosci. Model Dev.
Discussion started: 20 November 2017






will form in response to periods of high solar radiation creating warm, ~~less-dense conditions near the surface with~~ buoyant water overlying cooler ~~conditions deeper in the~~, denser water, separated by a metalimnion region which includes the thermocline. Layer thickness limits, $\Delta z_{min}$ and $\Delta z_{max}$, are enforced to adequately resolve the vertical density gradient, generally with fine resolution occurring in the metalimnion and thicker cells where mixing is active. The number of layers, $N_{LEV}(t)$, is adjusted throughout the simulation to maintain homogenous properties within a layer. It has been reported that numerical diffusion at the thermocline can be restricted using this layer structure and mixing algorithm (depending on the minimum and maximum layer thickness limits set by the user), making it particularly suited to long-term investigations, and ideally requiring limited site-specific calibration (Patterson et al., 1984; Hamilton and Schladow, 1997; Bruce et al., 2018). ~~Initially, the layers are assumed to be of equal thickness, and the initial number of layers, $N_{LEV}(t = 0)$. As the model simulation progresses, density changes due to surface heating, vertical mixing, and inflows and outflows lead to dynamic changes in the layer structure, associated with layers amalgamating, expanding, contracting or splitting.~~

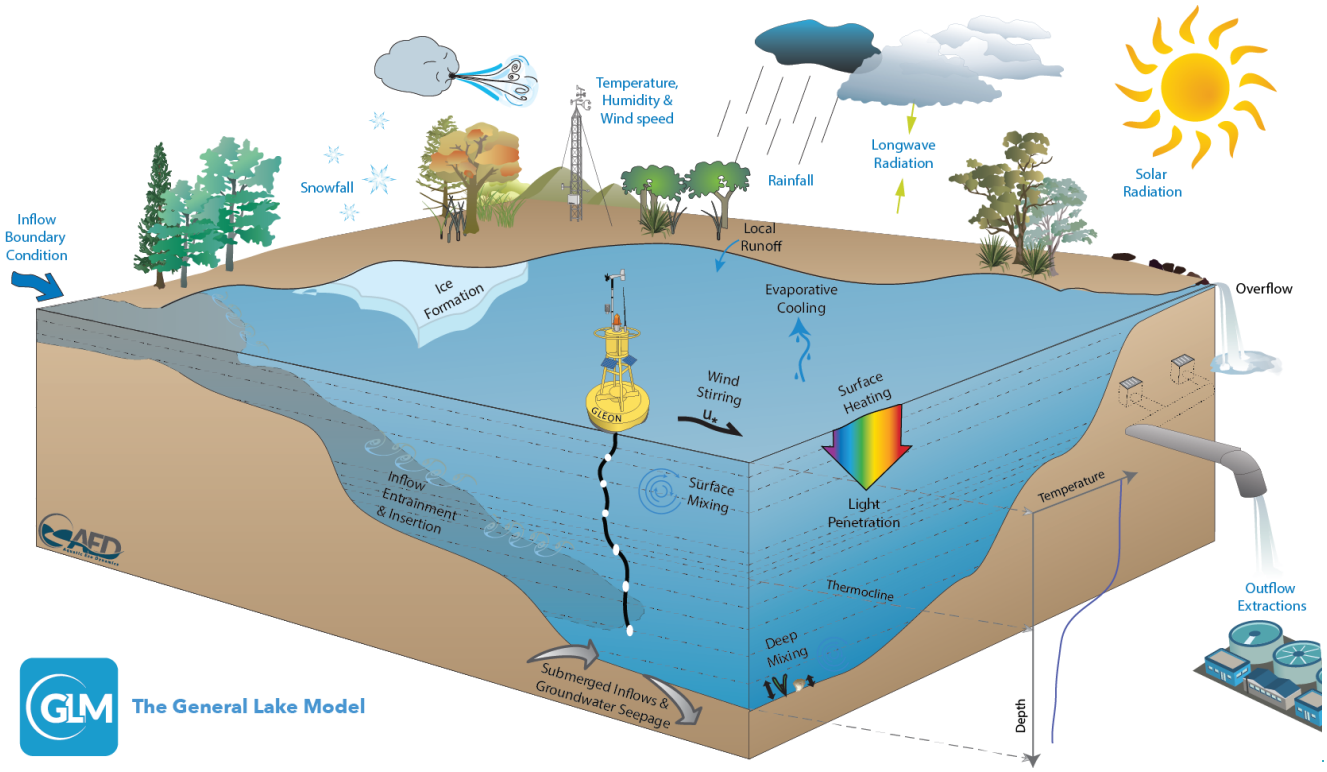


~~**Figure 1: Schematic of a GLM simulation domain, input information (blue text) and key simulated processes (black text).**~~

~~As layers change, their volumes change based on the site-specific hypsographic curve, whereby the overall lake volume~~ is ~~defined as $\int A(h)dh$, and the elevation ($h$), and area ($A$) relationship must be provided as a series of points based on bathymetric data. Layer volumes are determined by interpolating layer area at the appropriate height in the lake basin, whereby~~

Geosci. Model Dev. Discuss., https://doi.org/10.5194/gmd-2017-257
Manuscript under review for journal Geosci. Model Dev.
Discussion started: 20 November 2017


Geoscientific Model Development Discussions



~~$A_i = f(h_i)$, and $i$ is the layer number. This computation requires the user provides a number $N_{BSN}$ of depths with corresponding areas, and the volumes are estimated as:~~

$$V_b = V_{b-1} + [A_{b-1} + 0.5(A_b - A_{b-1})](h_b - h_{b-1}) \quad (1)$$

~~where $1 < b \leq N_{BSN}$. Using the raw hyposgraphic data, a refined depth–area–volume relationship is internally computed using finer depth increments (e.g., 0.1 m), giving $N_{MORPH}$ levels that are used for subsequent calculations. The area and volume at the depth of each increment, $h_z$ is interpolated from the supplied information as:~~

$$V_z = V_{b-1}\left(\frac{h_z}{h_{b-1}}\right)^{\alpha_b} \text{ and } A_z = A_{b-1}\left(\frac{h_z}{h_{b-1}}\right)^{\beta_b} \quad (2)$$

~~where $V_z$ and $A_z$ are the volume and area at each of the elevations of the refined depth vector, and $V_z$ refers to the nearest $b$ level below $h_z$ such that $h_{b-1} < h_z$. The interpolation coefficients are computed as:~~

$$\alpha_b = \left[\frac{log_{10}\left(\frac{V_{b+1}}{V_b}\right)}{log_{10}\left(\frac{h_{b+1}}{h_b}\right)}\right] \text{ and } \beta_b = \left[\frac{log_{10}\left(\frac{A_{b+1}}{A_b}\right)}{log_{10}\left(\frac{h_{b+1}}{h_b}\right)}\right] \quad (3)$$

~~The density in each layer $i$ is computed based on the temperature, $T$, and salinity, $S$, at any given time according to the UNESCO (1981) equation of state whereby $\rho_i = \rho(T_i, S_i)$. Density calculations can also be customised as required.~~

Because this approach assumes layer properties are laterally averaged, the model is suitable for investigations where resolving the horizontal variability is not a requirement of the study. This is often the case for ecologists and biogeochemists studying central basins of natural lakes (e.g., Gal et al., 2009), managers simulating drinking water reservoirs (e.g., Weber et al., 2017), or mining pit lakes (e.g., Salmon et al., 2017), or for analyses exploring the coupling between lakes and regional climate (e.g., Stepanenko et al., 2013). Further, whilst the model is able to resolve vertical stratification, ~~it may~~the approach is also able to be used to simulate shallow lakes, wetlands, wastewater ponds and other small waterbodies that experience well-mixed conditions. In this case, the layer resolution, with upper and lower layer bounds specified by the user, will automatically ~~simplify~~be reduced, and the mass of water and constituents, and energy will continue to be conserved. The remainder of this section outlines the model components and provides example outputs for five water bodies that experience a diverse hydrology (Figure 2).

### 2.2 ~~Water balance~~

#### ~~The model solves the~~Surface water balance

The mass balance of the ~~lake domain by including several user-configurable water fluxes. The components include surface mass fluxes (evaporation, rainfall and snowfall), inflows (surface inflows, submerged inflows and local runoff from the surrounding exposed lake bed area) and outflows (withdrawals, overflow and seepage). The dynamics of inflows and outflows modify the overall lake water balance on a daily time step, and may impact upon the layer structure by adding, merging or removing layers (described in Sect. 2.6). In addition, the mass balance the~~ surface layer is computed at each model time step ($\Delta t$; usually hourly), by modifying the surface layer height according to:

Geosci. Model Dev. Discuss., https://doi.org/10.5194/gmd-2017-257
Manuscript under review for journal Geosci. Model Dev.
Discussion started: 20 November 2017




$$\frac{dh_s}{dt} = E + S + f_R R + Q_R/A_s \quad \frac{dh_S}{dt} = R_F + S_F + \frac{Q_R}{A_s} - E - \frac{d\Delta z_{ice}}{dt} \tag{4}$$

where $h_s h_S$ is the top height of the surface layer (m), $t$ is the time (days s), $E$ is the evaporation mass flux computed from the heat flux $\phi_E$ (W m$^{-2}$), described below, $R$ ($E = -\phi_E/\lambda_v \rho_s$ ; m s$^{-1}$), $R_F$ is rainfall and $S S_F$ is snowfall (m days$^{-1}$). $R_F$ and $S_F$ both affect the water surface height depending on the presence of ice cover:

$$R_F = \begin{cases} f_R R_x / c_{secday} , & \text{if } \Delta z_{ice} = 0 \\ f_R R_x / c_{secday} , & \text{if } \Delta z_{ice} > 0 \text{ and } T_a > 0 \\ 0 , & \text{if } \Delta z_{ice} > 0 \text{ and } T_a \le 0 \end{cases} \tag{5}$$

and

$$S_F = \begin{cases} f_S f_{SWE} S_x / c_{secday} , & \text{if } \Delta z_{ice} = 0 \\ 0, & \text{if } \Delta z_{ice} > 0 \end{cases} \tag{6}$$

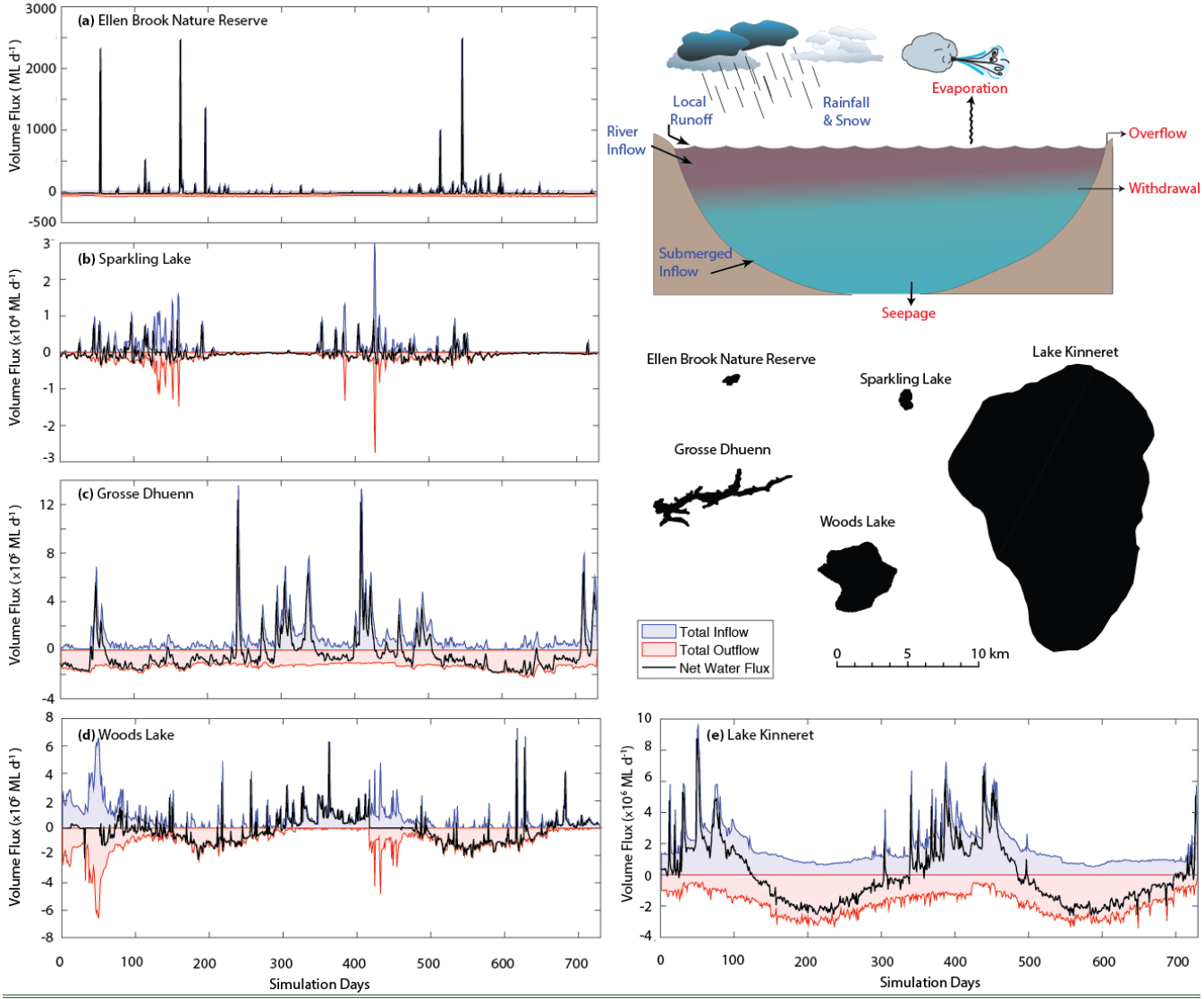


Figure 2: A two-year times-series of the simulated daily water balance for five example lakes, a-e, that range in size and hydrology. The water balance components summarised are depicted schematically in the inset $f_R$, and partitioned into inputs and outputs.

Geosci. Model Dev. Discuss., https://doi.org/10.5194/gmd-2017-257
Manuscript under review for journal Geosci. Model Dev.
Discussion started: 20 November 2017


Geoscientific Model Development Discussions



**The net water flux in a time step is ~~a~~: $dV/dt = \Delta h_s A_s + \sum_I^{N_{INF}} Q_{inf_{0_I}} - \sum_O^{N_{OUT}} Q_{outf_O} - Q_{ovfl} - Q_{seepage}$. For more information about each lake, the simulation configuration and input data, refer to the Data availability section.**

Here $f_R$ and $f_S$ are user- definable scaling ~~factor~~factors that may be applied to ~~increase~~adjust the input data values, $R_x$ and $S_x$ respectively. The surface height of the water column is also impacted by ice formation or ~~reduce the rainfall data (default = 1).~~ melting, according to $d\Delta z_{ice}/dt$, as described in Section 2.4.

$Q_R$ is an optional term to account for runoff to the lake from the exposed riparian banks, which may be important in reservoirs with a large drawdown range, or wetlands where periodic drying of the lake may occur. The runoff volume generated is averaged across the ~~current~~area that the active lake surface area ($A_s$~~),~~) is not occupying, and the amount is calculated using a simple model based on exceedance of a ~~threshold~~ rainfall intensity threshold, $R_L$ (m day$^{-1}$), and runoff coefficient:

$$~~Q_R = f_{ro}(f_R R - R_L)(A_{max} - A_s)~~ Q_R = max\left[0, f_{ro}\left(R_F - R_L/c_{secday}\right)\right](A_{max} - A_s) \quad (~~5~~7)$$

where $f_{ro}$ is the runoff coefficient, defined as the fraction of rainfall that is converted to runoff at the lake's edge, and $A_{max}$ is the maximum possible area of inundation of the lake (~~as defined by~~ the area provided by the user ~~at~~as the $N_{BSN}$ ~~area~~ value).

Note that mixing dynamics (i.e., the merging or splitting of layers to enforce the layer thickness limits), will impact the thickness of the surface mixed layer, ~~$z_{SML}$~~$z_{sml}$, but not change the overall lake height. However, in addition to the terms in Eq. 4, ~~$h_S$ will also be~~$h_S$ is modified ~~as a result of ice formation/melt, and~~due to volume changes associated with river inflows, withdrawals, seepage or overflows ~~impacting upon the surface layer~~, which are described in subsequent sections~~; these are in addition to the above described terms~~.

## 2.3 Surface energy balance

A balance of shortwave and longwave radiation fluxes, and sensible and evaporative heat fluxes ~~determine~~(all W m$^{-2}$) determines the net cooling and heating ~~for GLM.~~across the surface. The general heat budget equation for the upper most layer is described as:

$$~~\left[\frac{c_p}{A_s z_{sml}}\right]\frac{dT_s}{dt}~~ c_w \rho_s z_s \frac{dT_s}{dt} = \phi_{SW_S} - \phi_E + \phi_H + \phi_{LWin} - \phi_{LWout} \quad (~~6~~8)$$

where ~~$c_p$~~$c_w$ is the specific heat capacity of water ~~(4186 J kg$^{-1}$ °C$^{-1}$),~~ ~~$T_S$~~$T_s$ is the surface temperature, and $z_s$ and $\rho_s$ are the depth and density of the surface ~~mixed~~ layer ~~and $z_{sml}$ is the depth of the surface mixed layer.~~($i = N_{LEV}$), respectively. The RHS heat flux terms~~, including~~ are computed at each time step, and include several options for customizing the individual surface heat flux components, which are expanded upon ~~individually~~ below.

### 2.3.1 Solar heating and light penetration

Solar radiation is the key driver of the lake thermodynamics~~, however, data~~ and may ~~not always~~ be ~~available~~ input based on daily or hourly measurements from a nearby pyranometer. ~~Users~~If data is not available then users may choose to either have

Geosci. Model Dev. Discuss., https://doi.org/10.5194/gmd-2017-257
Manuscript under review for journal Geosci. Model Dev.
Discussion started: 20 November 2017


Geoscientific Model Development Discussions

**Revision 8 Mar 2018**

GLM compute surface irradiance from a theoretical approximation based on the Bird Clear Sky insolation model (BCSM) (Bird, 1984), modified for cloud cover and latitude~~, or alternatively, hourly or daily solar radiation intensity data may be specified directly. If the BCSM is used, then $\hat{\phi}_{SW}$ is calculated from (Bird, 1984; Luo et al., 2010):~~. Therefore the options for input are summarised as:

$$\hat{\phi}_{SW} = \frac{\hat{\phi}_{DB} + \hat{\phi}_{AS}}{1 - (\alpha_{SW}\,\alpha_{SKY})} f(C)\phi_{SW_0} \qquad (7)$$

$$= \begin{cases} (1-\alpha_{SW})\, f_{SW}\, \phi_{SW_x}\, f[d, t - \lfloor t \rfloor], & \text{Option 1: daily insolation data provided} \\ (1-\alpha_{SW})\, f_{SW}\, \phi_{SW_x}, & \text{Option 2: sub-daily input data provided} \\ (1-\alpha_{SW})\, \hat{\phi}_{SW}, & \text{Option 3: data is computed from the BCSM} \end{cases} \qquad (9a\text{-}c)$$

~~where the model computes total irradiance, $\hat{\phi}_{SW}$ (W m$^{-2}$)~~where $\phi_{SW_0}$ is the solar radiation flux entering the surface layer, $\phi_{SW_x}$ is the incoming shortwave radiation flux supplied by the user, $f_{SW}$ is a scaling factor that may be applied and adjusted as part of the calibration process, and $\alpha_{SW}$ is the albedo for shortwave radiation. If daily data is supplied (Option 1), the model continues to run at a sub-daily time step, but applies the algorithm outlined in Hamilton and Schladow (1997) to distribute the daily solar energy flux over a diurnal cycle, based on the day of the year, $d$, and time of day, $t - \lfloor t \rfloor$. For Option 3 the BCSM is used (Bird, 1984; Luo et al., 2010):

$$\hat{\phi}_{SW} = \frac{\hat{\phi}_{DB} + \hat{\phi}_{AS}}{1 - (\alpha_{SW}\,\alpha_{SKY})} f[C] \qquad (10)$$

where the total irradiance, $\hat{\phi}_{SW}$, is computed from direct beam $\hat{\phi}_{DB}$, and atmospheric scattering $\hat{\phi}_{AS}$ components (refer to Appendix A for a detailed outline of the BCSM equations and parameters). In GLM, the clear sky value is then reduced according to the cloud cover~~, $C$~~ data provided by the user, $C_x$, according to:

$$f[C] = 0.66182\, C_x^{\,2} - 1.5236\, C_x + 0.98475 \qquad (11)$$

which is based on a polynomial regression of cloud data from Perth Airport, Australia, compared against nearby sensor data ($R^2 = 0.952$; see also Luo et al., 2010).

Geosci. Model Dev. Discuss., https://doi.org/10.5194/gmd-2017-257
Manuscript under review for journal Geosci. Model Dev.
Discussion started: 20 November 2017






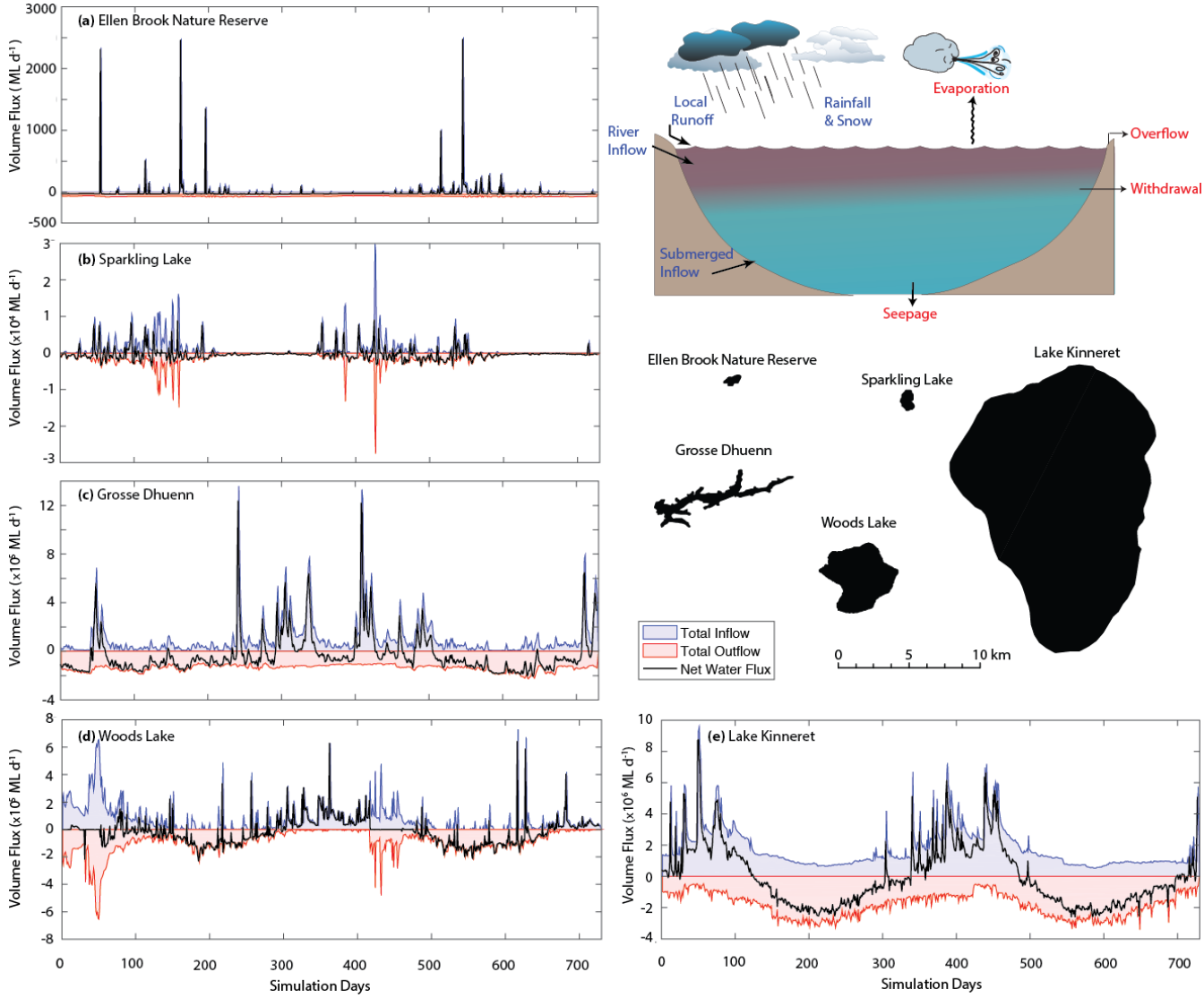


~~**Figure 2: A two-year times-series of the simulated daily water balance for five example lakes, a-e, that range in size and hydrology. The water balance components summarised are depicted schematically in the inset. For more information about each lake and the simulation configuration refer to the Data availability section.**~~

5

The albedo, $\alpha_{SW}$, is the reflected fraction of ~~$\hat{\phi}_{SW}$, with several computation options based~~the incoming radiation and depends on ~~the~~ surface conditions including the presence of ice, waves and the angle of incident radiation~~, selected via the `radmode` option in the model configuration file~~. For open water conditions, users may configure:

~~Option 1 : Daily approximation, Hamilton & Schladow (1997)~~

$$\alpha_{SW} = \begin{cases} 0.08 + 0.02\ sin\left[\frac{2\pi}{365}d - \frac{\pi}{2}\right] & \text{:northern hemisphere} \\ 0.08 & \text{:equator} \\ 0.08 - 0.02\ sin\left[\frac{2\pi}{365}d - \frac{\pi}{2}\right] & \text{:southern hemisphere} \end{cases} \quad (9a)$$

Geosci. Model Dev. Discuss., https://doi.org/10.5194/gmd-2017-257
Manuscript under review for journal Geosci. Model Dev.
Discussion started: 20 November 2017




~~Option 2 : Briegleb et al. (1986)~~

$$\alpha_{SW} = \frac{1}{100}\left(\frac{2.6}{1.1cos(\Phi_{zen})^{1.7}+0.065} + 15[cos(\Phi_{zen}) - 0.1][cos(\Phi_{zen}) - 0.5][cos(\Phi_{zen}) - 1]\right) \quad (9b)$$

~~Option 3 : Yajima and Yamamoto (2014)~~

$$\alpha_{SW} = 0.001\ RH\ [\cos(\Phi_{zen})]^{0.33} - 0.001\ U_x\ [\cos(\Phi_{zen})]^{-0.57} - 0.001\ \varsigma\ [\cos(\Phi_{zen})]^{0.829} \quad (9c)$$

Option 1 : Daily approximation, Hamilton and Schladow (1997)

$$\alpha_{SW} = \begin{cases} 0.08 - 0.02\ sin\left[\frac{2\pi}{365}d - \frac{\pi}{2}\right] & \text{:northern hemisphere} \\ 0.08 & \text{:equator} \\ 0.08 - 0.02\ sin\left[\frac{2\pi}{365}d + \frac{\pi}{2}\right] & \text{:southern hemisphere} \end{cases} \quad (12a)$$

Option 2 : Briegleb et al. (1986)

$$\alpha_{SW} = \frac{1}{100}\left(\frac{2.6}{cos[\Phi_{zen}]^{1.7}+0.065} + 15(cos[\Phi_{zen}] - 0.1)(cos[\Phi_{zen}] - 0.5)[cos[\Phi_{zen}] - 1]\right) \quad (12b)$$

Option 3 : Yajima and Yamamoto (2015)

$$\alpha_{SW} = max\left[0.02, 0.001\ \frac{RH_x}{100}\ [1 - \cos(\Phi_{zen})]^{0.33} - 0.001\ U_{10}\ [1 - \cos(\Phi_{zen})]^{-0.57} - 0.001\ \varsigma\ [1 - \cos(\Phi_{zen})]^{0.829}\right] \quad (12c)$$

where ~~$d$ is the day of the year, and~~ $\Phi_{zen}$ is the solar zenith angle (radians) as outlined in Appendix A, ~~$RH$~~$RH_x$ is the relative humidity, $\varsigma$ is the atmospheric diffuse radiation, $d$ is the day of year, and $U_x$ is wind speed. The second (oceanic) and third (lacustrine) options are included to allow for diel and seasonal variation of albedo from approximately 0.01 to 0.4 depending on the sun-angle (Figure 3). Albedo is calculated separately during ice cover conditions using a customised algorithm, outlined below in Section 2.4.

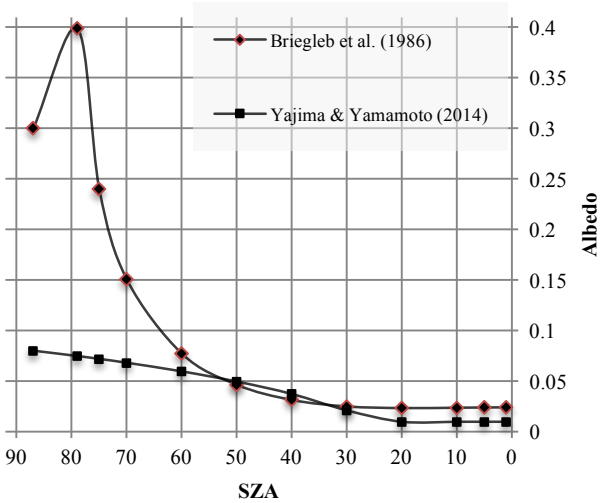

Geosci. Model Dev. Discuss., https://doi.org/10.5194/gmd-2017-257
Manuscript under review for journal Geosci. Model Dev.
Discussion started: 20 November 2017


Geoscientific Model Development Discussions



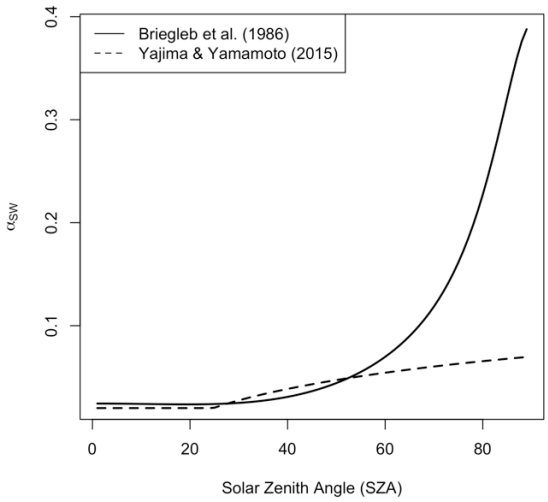


**Figure 3: Variation of albedo ($\alpha_{SW}$) with solar zenith angle (SZA = ~~$2\pi\,\Phi_{zen}/180\,\Phi_{zen}180/\pi$~~, degrees) for ~~radmode~~albedo_mode 2 and 3 (Eq. 12). For option 3, settings of RH = 80 % and U = 6 m s$^{-1}$ were assumed.**

~~Shortwave radiation~~ The depth of penetration of shortwave radiation into the lake is wavelength specific, and ~~through~~depends on the ~~layers is modelled according to~~water clarity via the light extinction coefficient, $K_w$ (m$^{-1}$). Two approaches are supported in GLM. The first option assumes the Photosynthetically Active Radiation (PAR) fraction of the incoming light is the most penetrative, and follows the Beer-Lambert Law:

$$\phi_{SW}(z)\phi_{PAR}[z] = (1-\alpha_{SW})\, f_{SW} f_{PAR}\, \hat{\phi}_{SW} f_{PAR}\, \phi_{SW_0}\, exp[-K_w z] \qquad (10\,13)$$

where $z$ is the depth of ~~the~~any layer from the surface, ~~$f_{SW}$ is a scaling factor that may be applied and adjusted as part of the calibration process, and $K_w$ is the light extinction coefficient (m$^{-1}$). $K_w$.~~ $K_w$ may be set by the user as constant or linked to the water quality model (e.g., FABM or AED2, see ~~Sect~~Section 4) in which case the extinction coefficient will change as a function of depth and time according to the concentration of dissolved and particulate constituents. For this option Beer's Law is only applied for the photosynthetically active fraction ~~(PAR) component~~, $f_{PAR}$, which is set as 45% of the incident light. The amount of ~~light~~radiation heating the surface layer, $\phi_{SW_S}$, is therefore the ~~above~~ photosynthetically ~~average~~active fraction that is attenuated across ~~$z_{SML}$~~$z_{sml}$, plus the ~~remaining~~entire $(1 - f_{PAR})$ fraction, which accounts for near infra-red and ultraviolet bandwidths of the incident shortwave radiation ~~with~~ $\phi_{SW_S} = \phi_{SW_0} - \phi_{PAR}[z_{sml}]$. and implicitly assumes these have significantly higher attenuation coefficients (Kirk, 1994). The second option adopts a more complete light adsorption algorithm that integrates the attenuated light intensity across the bandwidth spectrum:

~~In some applications, the extent to which the benthos has a suitable light climate is a good~~

$$c_w \rho_s \Delta z_i \frac{dT_i}{dt} = \sum_{k=1}^{N_{SW}} \phi_{SW_{i_k}}[z_i] - \sum_{k=1}^{N_{SW}} \phi_{SW_{i-1_k}}[z_{i-1}] \qquad (14)$$

Geosci. Model Dev. Discuss., https://doi.org/10.5194/gmd-2017-257
Manuscript under review for journal Geosci. Model Dev.
Discussion started: 20 November 2017




where $k$ is the bandwidth index $\phi_{SW_{i_k}}[z_i]$ is the radiation flux at the top of the $i^{th}$ layer. For this option, the model by Cengel and Ozisk (1984) is adopted to compute $\phi_{SW_{i_k}}(z_i)$, which more comprehensively resolves the light climate including incident and diffuse radiation components, the angle of incident light and transmission across the light surface (based on the Fresnel equations), and reflection off the bottom. These processes are wavelength specific and the user must specify the number of simulated bandwidths, $N_{SW}$, and their respective absorption coefficient.

The light reaching the benthos may be used in some applications as an indicator of benthic productivity, and a proxy for the type of benthic habitat that might emerge. In addition to the light profiles, GLM also predicts the benthic area of the lake where light intensity exceeds a user defined ~~value~~fraction of the surface irradiance, $f_{BEN_{crit}}$ (Figure 4~~, $\phi_{BEN_{crit}}$~~):

$$A_{BEN} = A_s - A_{(h_{BEN})}[h_{BEN}] \quad (1115)$$

where $h_{BEN} = h_{SURF} h_S - z_{BEN}$, and $z_{BEN}$ is calculated from Beer's law:

$$z_{BEN} = \frac{ln\left[\frac{\phi_{BEN_{crit}}}{\phi_{SW_S}}\right]}{K_w} - \frac{ln[f_{BEN_{crit}}]}{K_w} \quad (1216)$$

The and the daily average benthic area above the threshold is then reported ~~in the `lake.csv` summary file~~ as a percentage ($A_{BEN}/A_s$).

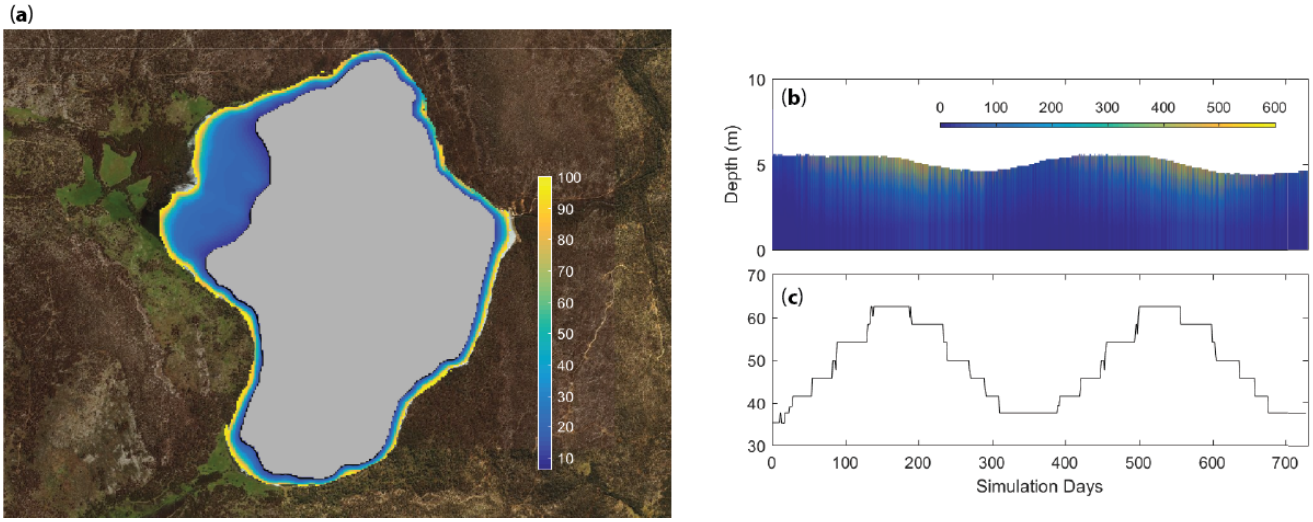


~~**Figure 4: Example light data outputs from a GLM application to Woods Lake, Australia, showing a) the ratio of benthic to surface light, $\phi_{SW_{BEN}}/\phi_{SW_S}$ (%), overlain on the lake map based on the bathymetry, b) a time-series of the depth variation in light (W m$^{-2}$), and c) a time-series of $A_{BEN}/A_S$ (%).**~~

### 2.3.2 Longwave radiation

Longwave radiation can ~~either~~ be ~~specified~~provided as a net flux, an incoming flux or, if there is no radiation data from which longwave radiation can be computed, then it may be calculated by the model internally based on the cloud cover fraction and air temperature. Net longwave radiation is described as:

Geosci. Model Dev. Discuss., https://doi.org/10.5194/gmd-2017-257
Manuscript under review for journal Geosci. Model Dev.
Discussion started: 20 November 2017






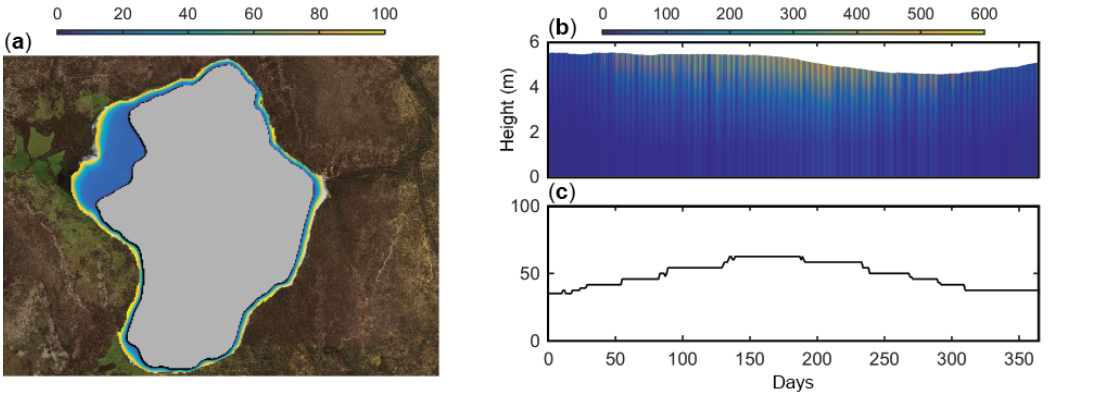


**Figure 4: Example light data outputs from a GLM application to Woods Lake, Australia, showing a) the ratio of benthic to surface light, $\phi_{PAR_{BEN}}/\phi_{SW_0}$ (%), overlain on the lake map based on the bathymetry, b) a time series of the depth variation in light (W m$^{-2}$), and c) a time series of $A_{BEN}/A_s$ (as %) for $f_{BEN_{crit}} = 0.2$.**

$$\phi_{LW_{net}} = \phi_{LW_{in}} - \phi_{LW_{out}} \quad (13\,17)$$

where

$$\phi_{LW_{out}} = \varepsilon_w \sigma [T_s + 273.15]^4 (\theta_s)^4 \quad (14\,18)$$

and $\sigma$ is the Stefan-Boltzman constant and $\varepsilon_w$ the emissivity of the water surface, assumed to be 0.985. If the net or incoming longwave flux is not provided, the model will compute the incoming flux from:

$$\phi_{LW_{in}} = (1 - \alpha_{LW})\, \varepsilon_a^*\, \sigma\, [T_a + 273.15]^4 (\theta_a)^4 \quad (15\,19)$$

where $\alpha_{LW}$ is the longwave albedo (0.03~~), and the~~). The emissivity of the atmosphere ~~is~~can be computed considering emissivity of cloud-free conditions ($\varepsilon_a$), based on air temperature ($T_a$) and vapour pressure, and extended to account for reflection from clouds, such that $\varepsilon_a^* = f$~~($T_a$, $C$) calculated from ($[T_a, C_x, e_a]$~~ (see Henderson-Sellers, 1986~~);~~; Flerchinger, 2009). Options available in GLM include:

$$\varepsilon_a^* = \begin{cases} (1 + 0.275C)\left(1 - 0.261 \exp\left[-0.000777\, T_a^{\,2}\right]\right) & \text{Option 1: Idso and Jackson (1969)} \\ (1 + 0.17\, C^2)\,(9.365\times10^{-6}[T_a + 273.15]^2) & \text{Option 2: Swinbank (1963)} \\ (1 + 0.275\, C)\, 0.642 \left(\frac{e_a}{T_a}\right)^{\frac{1}{7}} & \text{Option 3: Brutseart (1975)} \\ \left[(1 - C^{2.796})\, 1.24 \left(\frac{e_a}{T_a}\right)^{\frac{1}{7}} + 0.955\, C^{2.796}\right] & \text{Option 4: Yajima and Yamamoto (2014)} \end{cases} \varepsilon_a^* \quad (16a\,20a\text{-d})$$

$$= \begin{cases} (1 + 0.275\, C_x)\left(1 - 0.261 \exp\left[-0.000777\, T_a^{\,2}\right]\right), & \text{Option 1: Idso and Jackson (1969)} \\ (1 + 0.17\, C_x^2)\,(9.365\times10^{-6}(\theta_a)^2), & \text{Option 2: Swinbank (1963)} \\ (1 + 0.275\, C_x)\, 0.642\, (e_a/\theta_a)^{1/7}, & \text{Option 3: Brutsaert (1975)} \\ (1 - C_x^{2.796})\, 1.24\, (e_a/\theta_a)^{1/7} + 0.955\, C_x^{2.796}, & \text{Option 4: Yajima and Yamamoto (2015)} \end{cases}$$

where, ~~$C$~~$C_x$ is the cloud cover fraction (0-1), $e_a$ the air vapour pressure calculated from relative humidity, and options 1-4 are chosen via the ~~cloudmode~~`cloud_mode` variable. Note that cloud cover is typically reported in octals (~~1~~0-8) with each value depicting a fraction of 8~~. So~~, thus a value of 1 would correspond to a fraction of 0.125. Some data may also include cloud type

Geosci. Model Dev. Discuss., https://doi.org/10.5194/gmd-2017-257
Manuscript under review for journal Geosci. Model Dev.
Discussion started: 20 November 2017




and their respective heights. If this is the case, good results have been reported by averaging the octal values for all cloud types to get an average ~~value of~~ cloud cover.

If longwave radiation data does not exist and cloud data is also not available, but solar irradiance is measured, then ~~it is possible to get~~ GLM `rad mode setting 3 will instruct the model` to compare the measured and theoretical ~~(BCSM)~~clear-sky solar irradiance (estimated by the BCSM; Eq. 10) to approximate the cloud cover fraction~~. This option utilises the above relation in Eq. 7 to compute $\hat{\phi}_{SW}$, and clouds are approximated~~ by assuming that $\hat{\phi}_{SW_{OBS}}/\hat{\phi}_{SW_{BCSM}}\phi_{SW_x}/\hat{\phi}_{SW} = f$~~(C)~~$[C_x]$. Note that if neither shortwave or longwave radiation ~~are~~is provided, then the model will use the BCSM to compute incoming solar irradiance, and cloud cover will be assumed to be 0~~.~~ (noting that this is likely to be an overestimate of downwelling shortwave radiation).

### 2.3.3 Sensible and latent heat transfer

The model accounts for the surface fluxes of sensible heat and latent heat using commonly adopted bulk aerodynamic formulae. For sensible heat:

$$\phi_H = -\rho_a \text{~~}c_p\text{~~} c_a C_H \text{~~}U_x\text{~~} U_{10}(T_s - T_a) \quad (\text{~~17~~}21)$$

where ~~$c_p$~~ $c_a$ is the specific heat capacity of air~~ (, $C_H$ 1005 J kg$^{-1}$ °C$^{-1}$), $C_H$~~ is the bulk aerodynamic coefficient for sensible ~~hear~~heat transfer~~ ( 1.3x10$^{-3}$), $T_a$,~~ $T_a$ the air temperature ~~(°C)~~ and ~~$T_s$~~ $T_s$ the temperature of the water surface layer~~ (°C).~~. The air density ~~is in~~ (kg m$^{-3}$ ~~and)~~ is computed from $\rho_a = 0.348\,(1 + r)/(1 + 1.61r)\,p/T_a$, where $p$ is air pressure (hPa) and $r$ is the mixing ratio, which is used to compute the gas constant.

For latent heat:

$$\phi_E = -\rho_a C_E \text{~~}\lambda U_x \frac{\kappa}{p}\text{~~}\lambda_v\, U_{10}\, \frac{\omega}{p}\, (e_s[T_s] - e_a[T_a]) \quad (\text{~~18~~}22)$$

where ~~$C_E$~~ $C_E$ is the bulk aerodynamic coefficient for latent heat transfer, $e_a$ the air vapour pressure, $e_s$ the saturation vapour pressure (hPa) at the surface layer temperature (°C), ~~$\kappa$ is~~$\omega$ the ratio of molecular ~~weight~~mass of water to molecular ~~weight~~mass of dry air ( = 0.622) and ~~$\lambda$ is~~$\lambda_v$ the latent heat of vaporisation. The vapour pressure can be calculated by the following formulae:

~~$e_s[T_s] = exp\left[2.3026\left(7.5\frac{T_s}{T_s+237.3}\right) + 0.7858\right]$~~ ~~Option 1 : TVA (1972) - Magnus-Tetens~~ (~~19a~~23a)

~~$e_s[T_s] = exp\left[6.1094\left(\frac{17.625\,T_s}{T_s+243.04}\right)\right]$~~ ~~Option 2 : August-Roche-Magnus~~ (~~19b~~23b)

~~$e_s[T_s] = 10^{\left(9.28603523 - \frac{2322.37885}{T_s+273.15}\right)}$~~ ~~Option 3 : Tabata (1973) - Linear~~ (~~19c~~23c)

Geosci. Model Dev. Discuss., https://doi.org/10.5194/gmd-2017-257
Manuscript under review for journal Geosci. Model Dev.
Discussion started: 20 November 2017






$$e_s[T_s] = \begin{cases} exp\left[2.3026\left(7.5\frac{T_s}{T_s+237.3}\right)+0.7858\right], & \text{Option 1 : TVA (1972) - Magnus-Tetens} \\ exp\left[6.1094\left(\frac{17.625\,T_s}{T_s+243.04}\right)\right], & \text{Option 2 : August-Roche-Magnus} \\ 10^{\left(9.28603523\frac{2322.37885\,T_s}{T_s+273.15}\right)}, & \text{Option 3 : Tabata (1973) - Linear} \end{cases}$$

and

$$e_a[T_a] = \frac{RH}{100} e_s f_{RH} RH_x\, e_s[T_a] \qquad (20\ (24)$$

Correction for non-neutral atmospheric stability: For long-time (e.g., seasonal) integrations (i.e., seasonal), the bulk-transfer coefficients for momentum, $C_D, C_{D_z}$ sensible heat, $C_H, C_{H_z}$ and latent heat, $C_E, C_{E_z}$ can be assumed approximately constant because of the negative feedback between surface forcing and the temperature response of the water body (e.g., Strub and Powell, 1987). At finer timescales (hours to weeks), the thermal inertia of the water body is too great and so the transfer coefficients must be specified as a function of the degree of atmospheric stratification experienced in the internal boundary layer that develops over the water (Woolway et al. 2017). Monin and Obukhov (1954) parameterised the stratification in the air column using the now well-known stability parameter, $z/L, z/L_z$ which is used to define corrections to the bulk aerodynamic coefficients $C_H C_H$ and $C_E, C_{E_z}$ using the numerical scheme presented in Appendix B. The corrections may be optionally applied as options in the model within a simulation, and if enabled, the transfer coefficients used above are automatically updated. This option requires that the measurement of wind speed, air temperature and relative humidity within the internal boundary layer over the lake surface are, supplied at an hourly resolution.

Geosci. Model Dev. Discuss., https://doi.org/10.5194/gmd-2017-257
Manuscript under review for journal Geosci. Model Dev.
Discussion started: 20 November 2017




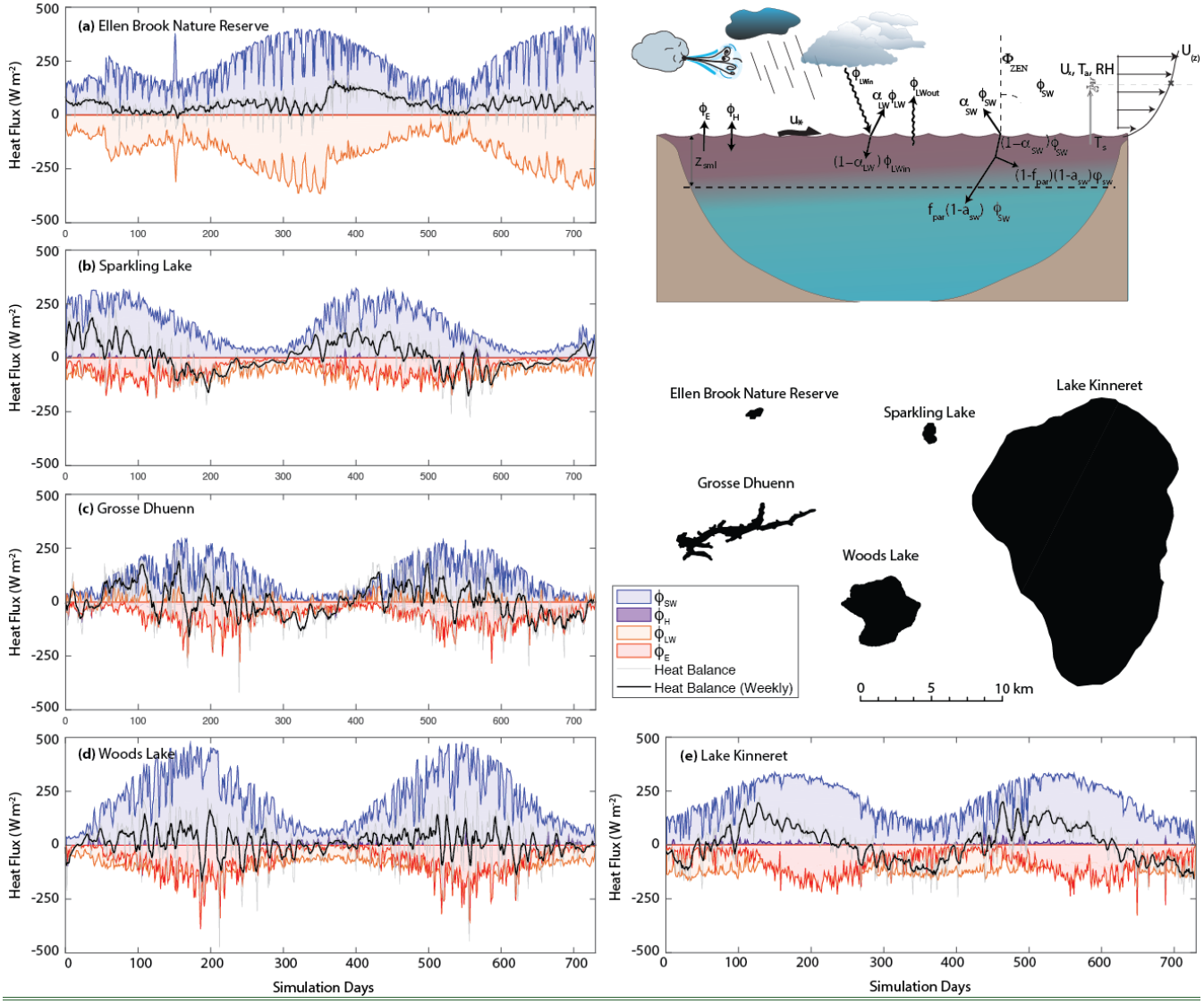


**Figure 5: A two-year times-series of the simulated daily heat fluxes for the five example lakes, a-e, that were depicted in Figure 2. The heat balance components summarised are depicted schematically in the inset, as described in Section 2.3 and the "Heat Balance" line refers to the LHS of Eq. 8.**

Wind sheltering: Wind sheltering may be important depending on the lake size and shoreline complexity, and is parameterised according to several methods based on the context of the simulation and data available. For example, Hipsey et al. (2003) presented a simple adjustment to the bulk transfer equation to account for the effect of wind sheltering in small reservoirs using a shelter index to account for the length scale associated with the vertical obstacle relative to the horizontal length scale associated with the water body itself. Markfort et al. (2009) estimate the effect of a similar sheltering length-scale on the overall lake area. Therefore, within GLM, users may specify the degree of sheltering or fetch limitation using either constant or direction-specific options for computing an "effective" area:

Geosci. Model Dev. Discuss., https://doi.org/10.5194/gmd-2017-257
Manuscript under review for journal Geosci. Model Dev.
Discussion started: 20 November 2017




**Revision 8 Mar 2018**

$$A_E = \begin{cases} A_S, & \text{Option 0: no sheltering (default)} \\ A_S \tanh\left(\frac{A_S}{A_{WS}}\right), & \text{Option 1: Yeates \& Imberger (2003)} \\ \frac{{L_D}^2}{2} cos^{-1}\left(\frac{{x_{WS}}^{\Phi}}{L_D}\right) - \frac{{x_{WS}}^{\Phi}}{L_D}\sqrt{{L_D}^2 - ({x_{WS}}^{\Phi})^2}, & \text{Option 2: Markfort et al. (2009)} \\ f_{WS}[\Phi_{wind}]\, A_S, & \text{Option 3: user} - \text{defined} \end{cases} \quad (25a\text{-}d)$$

where $A_{WS}$ is a user defined critical lake area for wind sheltering to dominate, $x_{WS}$ is a user defined sheltering distance, and $L_D$ the lake diameter ($L_D = 0.5(L_{crest} + W_{crest})$). For option 1, the sheltering factor is held constant for the simulation based on the size of the lake, whereas the latter two options require users to additionally input wind direction data, and a direction function, $f_{WS}[\Phi_{wind}]$, to allow for a variable sheltering effect over time. In the case of option 2, this function scales the sheltering distance, $x_{WS}$, as a function of wind direction, ${x_{WS}}^{\Phi} = x_{WS}\,(1 - min(f_{WS}[\Phi_{wind}], 1))$, whereas in the case of option 3 the function reads in an effective area scaling fraction directly.

The ratio of the effective area to the total area of the lake, $A_E/A_S$, is then used to scale the wind speed data input by the user, $U_x$, as a means of capturing the average wind speed over the entire lake surface, such that $U_{10} = f_U\, U_x\, A_E/A_S$, where $f_U$ is a wind speed adjustment factor that can be used to assist calibration, or to correct the raw wind speed data to the reference height of 10 m.

Still-air limit: The above formulations only apply when sufficient wind exists to create a defined boundary layer over the surface of the water. As the wind tends to zero (the 'still-air limit'), Eqs. ~~16-17 are no longer~~21-22 become less appropriate as they do not account for free convection directly from the water surface. This is a relatively important phenomenon for small lakes, cooling ponds and wetlands since they tend to have small fetches that limit the ~~build-up of~~energy input from wind ~~speed~~. These water bodies ~~are often~~may also have large areas sheltered from the wind and will develop surface temperatures warmer than the atmosphere for considerable periods. Therefore, ~~we~~users can optionally augment Eqs. ~~16-17~~21-22 with calculations ~~under~~for low wind- speed conditions by calculating the evaporative and sensible heat flux values for both the given ~~$U_* = 0$~~ $U_{10}$ and for an assumed ~~$U_* = 0$~~ $U_{10} = 0$. The chosen value for the surface energy balance (as applied in Eq. 8) is found by taking the maximum value of the two calculations:

~~$\phi^*_{H,E} = \max(\phi_{E,H}, \phi_{E,H_0})\phi^*_X$~~ (~~21~~26)

$$= \begin{cases} \max\left[\phi_X, \phi_{X_0}\right], & \text{Option 1: no} - \text{sheltering area} \\ \max\left[\phi_X, \phi_{X_0}\right] A_E/A_S + \phi_{X_0}\,(A_S - A_E)/A_S, & \text{Option 2: still} - \text{air sheltered area} \end{cases}$$

where ~~$\phi_0$~~$\phi_{X_0}$ is the zero-wind flux~~, given below, and applies~~ for ~~both~~either the evaporative ~~and~~or sensible heat ~~fluxes,~~ flux (and ~~$\phi_{E,H}$~~$\phi_X$ is calculated from Eqs. ~~16-17~~21-22). The two zero-wind speed heat flux equations are ~~taken~~ from TVA (1972), but modified ~~slightly~~ to return energy flux in SI units (W m$^{-2}$):

Geosci. Model Dev. Discuss., https://doi.org/10.5194/gmd-2017-257
Manuscript under review for journal Geosci. Model Dev.
Discussion started: 20 November 2017




**Revision 8 Mar 2018**

$$\phi_{E_0} = \rho_s \lambda\lambda_v \alpha_e (C_0 - C_a)(\vartheta_s - \vartheta_a) \qquad (22\underline{27a})$$

$$\phi_{H_0} = \alpha_h (T_s - T_a) \qquad \underline{b})$$

$$\alpha_e = 2.283\times10^{-3}\,\xi \frac{v}{c_p \rho_s}\left[g\frac{|\rho_a - \rho_o|}{\rho_a \nu_a}\right]^{1/3} 0.137\, f_0 \frac{K_{air}}{c_a \rho_s}\left(g\frac{|\rho_a - \rho_o|}{\rho_a\, \nu_a\, D_a}\right)^{1/3} \qquad (23\underline{28a})$$

$$\alpha_h = 2.283\times10^{-3}\,\xi\, v\left[g\frac{|\rho_a - \rho_o|}{\rho_a \nu_a}\right]^{1/3} 0.137\, f_0\, K_{air}\left(g\frac{|\rho_a - \rho_o|}{\rho_a\, \nu_a\, D_a}\right)^{1/3} \qquad \underline{b})$$

where $C\vartheta = \kappa\, e/p$, with the appropriate vapour pressure values, $e$, for both surface and ambient atmospheric values. Here, $\nu K_{air}$ is the molecular heat conductivity of air (0.1 kJ m$^{-1}$ hs$^{-1}$ C$^{-1}$ K$^{-1}$), $\nu$), $\nu_a$ is the kinematic viscosity of the air (0.0548 m$^2$ hs$^{-1}$),), $\rho_o$ is the density of the saturated air at the water surface temperature, $\rho_s$ is the density of the surface water, $\xi f_0$ is a dimensionless roughness correction coefficient for the lake surface (0.5) and $aD_a$ is the molecular heat diffusivity of air (0.077 m$^2$ hs$^{-1}$). Note that the impact of low wind speeds on the drag coefficient is captured by the modified Charnock relation (Eq. A24), which includes an additional term for the smooth flow transition (see also Figure A1).

Wind sheltering: Wind-sheltering maybe parameterised according to several methods based on the context of the simulation and data available. Hipsey et al. (2003) presented a simple adjustment to the bulk transfer equation to account for the effect of wind-sheltering in small reservoirs. The method employs the use of a shelter index by accounting for the length scale associated with the vertical obstacle relative to the horizontal length scale associated with the water body itself. Within

Geosci. Model Dev. Discuss., https://doi.org/10.5194/gmd-2017-257
Manuscript under review for journal Geosci. Model Dev.
Discussion started: 20 November 2017






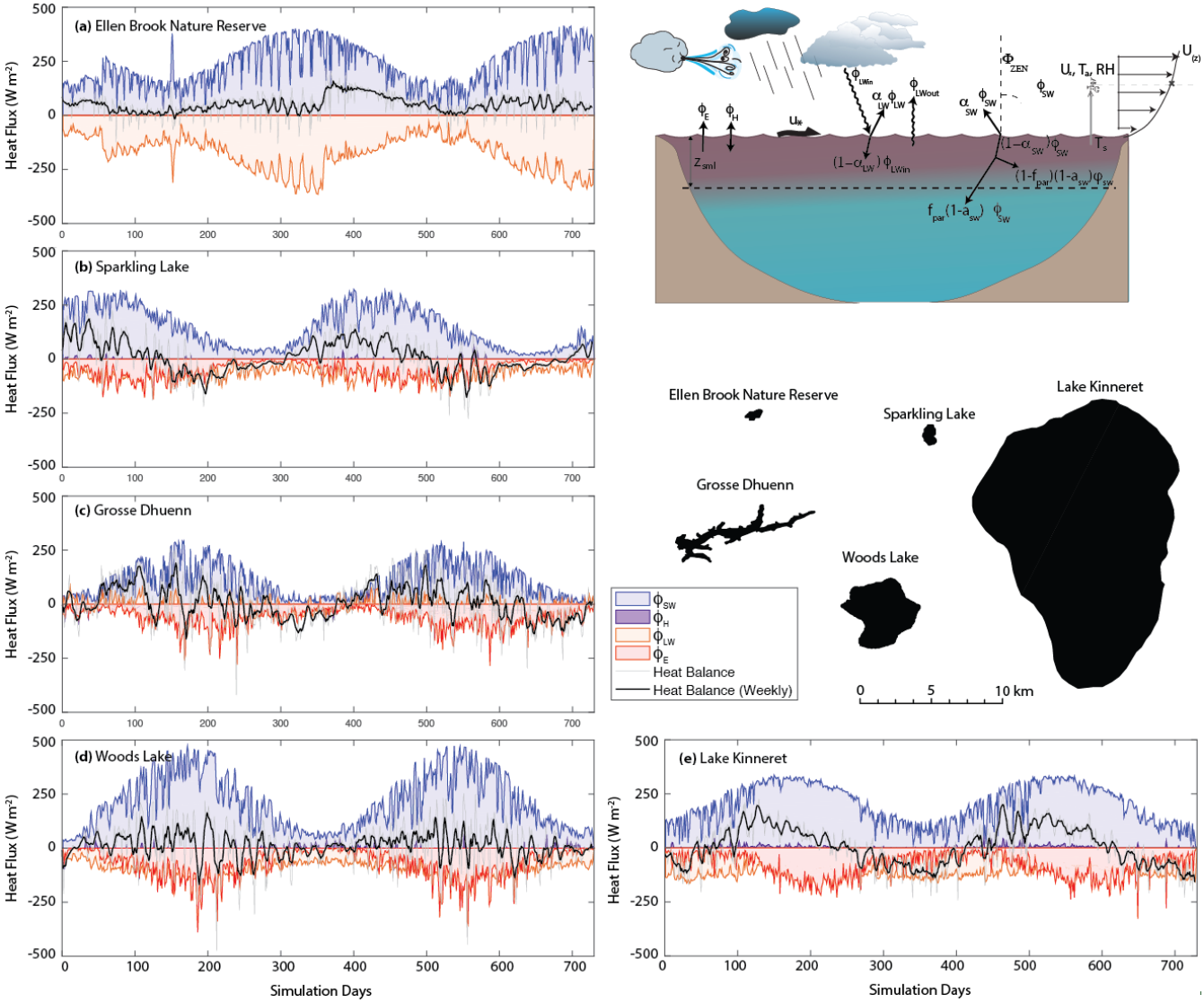


~~**Figure 5: A two-year times-series of the simulated daily heat fluxes for** five example lakes, a-e, that were depicted in Figure 2. The heat balance components summarised are depicted schematically in the inset, as described in Sect. 2.3.~~

~~GLM, users may specify the degree of sheltering or fetch limitation by optionally supplying the model with the wind direction, and a table linking direction and a wind scaling factor. Alternatively, if the direction-specific data is not available, an effective wind-sheltering coefficient has been implemented that reduces the effective surface area for heat and momentum fluxes:~~

$$A_E = \begin{cases} A_S \tanh\left(\frac{A_S}{A_C}\right) & \text{Yeates \& Imberger (2003)} \quad (24a) \\ \frac{D^2}{2}\cos^{-1}\left(\frac{x_f}{D}\right) - \frac{x_f}{D}\sqrt{D^2 - x_f^2} & \text{Markfort et al. (2009)} \quad (24b) \end{cases}$$

~~where $A_C$ is the critical area. In GLM, the ratio of the effective area to the total area of the lake $A_E/A_S$ is then used to scale $U_*$ as a means of capturing the average wind speed over the entire lake surface.~~

Geosci. Model Dev. Discuss., https://doi.org/10.5194/gmd-2017-257
Manuscript under review for journal Geosci. Model Dev.
Discussion started: 20 November 2017


Geoscientific Model Development Discussions
Open Access
EGU



### 2.4 Snow and ice dynamics

The algorithms for GLM ice and snow dynamics are based on previous ice modelling studies (Patterson and Hamblin, 1988; Gu and Stefan, 1993; Rogers et al., 1995; Vavrus et al., 1996; Launiainen and Cheng, 1998; Magee et al., 2016). To solve the heat transfer equation, the ice model uses a quasi-steady assumption that the time scale for heat conduction through the ice is short relative to the time scale of changes in meteorological forcing (Patterson and Hamblin, 1988; Rogers et al., 1995). The steady-state conduction equations~~, which allocate shortwave radiation into two components, a visible (A1=70%) and an infra-red (A2=30%) spectral band,~~ are used with a three-~~component~~layer ice model that includes blue ice (or black ice), white ice (or snow ice) and snow (see Eq. 1 and Fig. 5 of Rogers et al., 1995~~). White~~), and forced at the surface based on shortwave radiation which is partitioned into two components, a visible ($f_{VIS}$) and an infra-red ($1 - f_{VIS}$) spectral band. Blue ice is formed through direct freezing of lake water into ice whereas white ice is generated in response to flooding, when the mass of snow that can be supported by the buoyancy of the ice cover is exceeded (~~see Eq. 13 of~~ Rogers et al., 1995). By assigning appropriate boundary conditions to the interfaces and solving the quasi-steady state ~~of~~equation for heat transfer numerically, the model computes the upward conductive heat flux ~~from~~through the ice ~~or~~and snow cover to the atmosphere, termed $\phi_0$. The estimation of $\phi_0$ ~~involves the application of~~applies an empirical equation ~~(Ashton, 1986)~~ to estimate snow conductivity ~~($K_s$)~~, $K_{snow}$, from its density (Ashton, 1986; Figure 6).

At the solid surface (ice ~~(~~or snow~~) surface;~~), a heat flux balance is employed to provide the condition for surface melting:

$$\phi_0(T_0)[T_0] + \phi_{net}(T_0)[T_0] = 0 \qquad T_0 < T_m$$

$$\phi_{net}(T_0)[T_0] = -\rho L \frac{dh_i}{dt} = -\rho_{ice,snow}\,\lambda_f \frac{d\Delta z_{ice,snow}}{dt} \qquad T_0 = T_m \qquad (25)$$

(29)

(30)

where ~~$L\lambda_f$~~ is the latent heat of fusion ~~(see physical constants, Table 1), $h_i$,~~ $\Delta z_{ice,snow}$ is the height of the upper snow or ice layer, ~~$t$ is time, $\rho\rho_{ice,snow}$~~ is the density of either the snow or ice, determined from the surface medium properties, ~~$T_0$~~$T_0$ is the temperature at the solid surface, ~~$T_m$~~$T_m$ is the melt-water temperature (~~0°C~~0 °C) and ~~$\phi_{net}(T_0)$~~$\phi_{net}[T_0]$ is the net incoming heat flux~~,~~ for non-pentrative radiation at the solid surface:

$$\phi_{net}(T_0)[T_0] = \phi_{LWin} - \phi_{LWout}(T_0)[T_0] + \phi_H(T_0)[T_0] + \phi_E(T_0)[T_0] + \phi_R(T_0)[T_0] \qquad (26\,31)$$

where ~~$\phi_{LWin}$ and $\phi_{LWout}$ are incoming and outgoing longwave radiation, $\phi_H$ and $\phi_E$ are sensible and evaporative~~the heat fluxes between the solid boundary and the atmosphere~~, and $\phi_R$ is the heat flux due to rainfall. These heat fluxes~~ are calculated as ~~above~~outlined previously, but with modification for the determination of vapor pressure over ice or snow (Gill, 1982~~)~~), and the addition of the rainfall heat flux, $\phi_R$, (Rogers et al., 1995). ~~$T_0$~~$T_0$ is determined using a bilinear iteration until surface heat fluxes are balanced (i.e~~. $\phi_0(T_0) = -\phi_{net}(T_0)$ and $T_0$,~~ $\phi_0[T_0] = -\phi_{net}[T_0]$) and $T_0$ is stable (± 0.~~001°C). 001 °C).~~ In the presence of ice (or snow) cover, a surface temperature ~~$T_0 > T_m$~~$T_0 > T_m$ indicates that energy is available for melting. The amount of energy for melting is calculated by setting ~~$T_0 = T_m$~~$T_0 = T_m$ to determine the reduced thickness of snow or ice (as shown in Eq. 25~~30~~).

Geosci. Model Dev. Discuss., https://doi.org/10.5194/gmd-2017-257
Manuscript under review for journal Geosci. Model Dev.
Discussion started: 20 November 2017


Geoscientific Model Development Discussions



Accretion or ablation of ice is determined through the heat flux at the ice-water interface, ~~$q_f$, Solving~~$\phi_f$. Shortwave radiation is absorbed and attenuates with different extinction depths for snow, white ice, and blue ice, and these also depend on wavelength of the light. Assuming two light bandwidths, we solve for the heat conduction through ice ~~yields~~to yield:

$$\begin{aligned} \text{~~}q_f = q_0 - A_1\hat{\phi}_{SW}(1-\exp[-K_{s1}h_{snow}-K_{w1}h_{white}-K_{b1}h_{blue}]) - A_2\hat{\phi}_{SW}(1-\exp[-K_{s2}h_{snow}-Kh_{white}-K_{b2}h_{blue}]) - Q_{white}h_{snow}\phi_f\text{~~} \quad (\text{~~}27\text{32}) \\ = \phi_0 - f_{VIS}\,\phi_{SW_0}\,(1-\exp[-K_{s1}\Delta z_{snow}-K_{w1}\Delta z_{white}-K_{b1}\Delta z_{blue}]) \\ -(1-f_{VIS})\,\phi_{SW_S}\,(1-\exp[-K_{s2}\Delta z_{snow}-K_{w2}\Delta z_{white}-K_{b2}\Delta z_{blue}]) \\ -\phi^*_{white}\Delta z_{snow} \end{aligned}$$

where ~~$\hat{\phi}_{SW}\phi_{SW_0}$~~ is the shortwave radiation penetrating the ice/snow surface, $K$ refers to the light attenuation coefficient of the ice and snow components designated with subscripts *s, w* and ~~*eb*~~ *b* for snow, white ice and blue ice ~~and snow ice~~ respectively, and ~~$h\Delta z$~~ refers to the thickness of snow, white ice ~~(snow ice)~~ and blue ice. ~~$Q_{white}\phi^*_{white}$~~ is a volumetric heat flux for the formation of snow ice, which is given in Eq. 14 of Rogers et al. (1995). Ice and snow light attenuation coefficients in GLM are fixed to the same values as those given by Rogers et al. (1995). Shortwave albedo for the ice or snow surface is a function of surface medium (snow or ice), surface temperature and ice or snow thickness (see Table ~~2,~~1 of Vavrus et al., 1996). Values of albedo derived from these functions vary from 0.08 to 0.6 for ice and from 0.08 to 0.7 for snow, depending on the surface temperature and their layer thickness.

The imbalance between ~~$q_f\phi_f$~~ moving through the blue ice layer and the heat flux from the water ~~to~~into the ice, ~~$q_w\phi_w$~~ gives the rate of change of ice thickness at the interface with water:

$$\text{~~}\frac{dh_{blue}}{dt} = \frac{q_f - q_w}{\rho_{blue} L}\frac{d\Delta z_{blue}}{dt} = \frac{\phi_f - \phi_w}{\rho_{blue}\,\lambda_f}\text{~~} \quad (\text{~~}28\text{33}) \tag{33}$$

where ~~$\rho_{blue}$~~$\rho_{blue}$ is the density of blue ice and ~~$q_w\phi_w$~~ is given by a finite difference approximation of the conductive heat flux from water to ice:

$$\text{~~}q_w = -K_m\frac{\Delta T}{\Delta z}\text{~~},\phi_w = -K_{water}\,\frac{\Delta T}{\delta_{wi}}, \quad (\text{~~}29\text{34}) \tag{34}$$

where ~~$K_m$~~$K_{water}$ is molecular conductivity of water (assuming the water is stagnant), and $\Delta T$ is the temperature difference between the surface water of the lake and the bottom of the blue ice~~, which~~ layer, $T_m - T_s$. This occurs across an assigned ~~depth $\Delta z$. A~~length-scale $\delta_{wi}$, for which a value ~~for $\Delta z$~~ of 0.1-0.5 m is usual, based on the reasoning given in Rogers *et al.* (1995) and the typical vertical water layer resolution of a model simulation (0.125 – 1.5 m). Note that a wide variation in techniques and values is used to determine the basal heat flux immediately beneath the ice pack (e.g., Harvey, 1990~~).~~) which suggests that this may need careful consideration during calibration.

Figure 6 summarizes the algorithm to update ice cover, snow cover and water depth. The ice cover equations are applied when water temperature first drops below 0 °C. The ice thickness is set to its minimum value of 0.05 m, which is suggested by

Geosci. Model Dev. Discuss., https://doi.org/10.5194/gmd-2017-257
Manuscript under review for journal Geosci. Model Dev.
Discussion started: 20 November 2017




Patterson and Hamblin (1988) and Vavrus et al. (1996). The need for a minimum ice thickness relates primarily to horizontal variability of ice cover during the formation and closure periods. The ice cover equations are discontinued and open water conditions are restored in the model when the thermodynamic balance first produces ice thickness < 0.05 m.

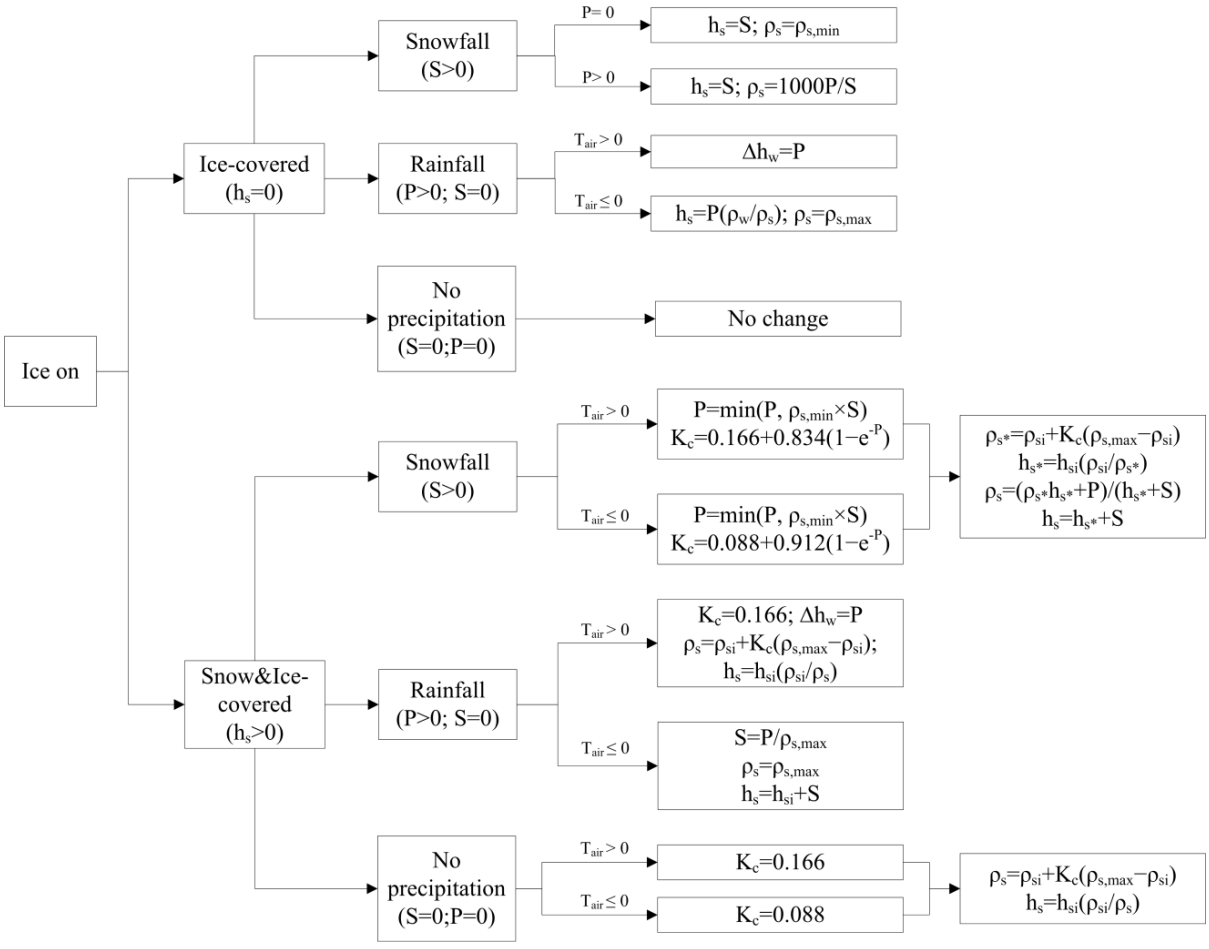

Geosci. Model Dev. Discuss., https://doi.org/10.5194/gmd-2017-257
Manuscript under review for journal Geosci. Model Dev.
Discussion started: 20 November 2017




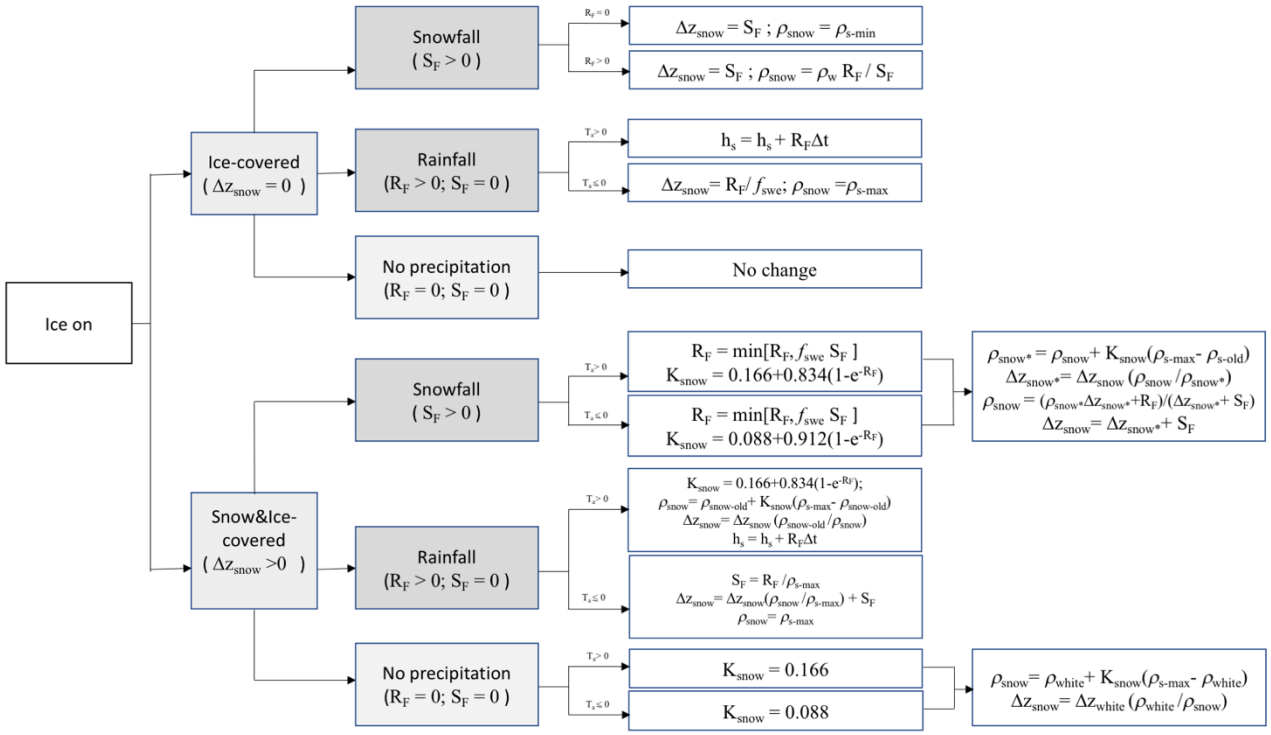


**Figure 6: Decision tree to update ~~ice cover,~~ snow cover and water depth according to snow compaction, rainfall (*~~P~~R_F*) and snowfall (~~*S*) on~~*S_F*) each ~~day, and depth of snow cover ($h_{si}$) and snow density ($\rho_{si}$) for the previous day.~~time step. Refer to text and Table 1 for definitions of other variables.**

After the change in ice thickness due to heat exchange is calculated, the effects of snowfall, rainfall, and compaction of snow are calculated through appropriate choice of one of several options, depending on the air temperature and whether ice or snow is the upper solid boundary (Figure 6). Density of fresh snowfall is determined as the ratio of measured snowfall height to water-equivalent height, with any values exceeding the assigned maximum or minimum snow density (defaults: $\rho_{s,max}$ = 300 kg m$^{-3}$, $\rho_{s,min}$ = 50 kg m$^{-3}$) truncated to the appropriate limit. ~~-~~The snow compaction model is based on the exponential decay formula of McKay (1968), with selection of snow compaction parameters based on air temperature (Rogers et al., 1995) as well as on rainfall or snowfall. The approach of snow compaction used by Rogers et al. (1995) is to set the residual snow density to its maximum value when there is fresh snowfall. This method is found to produce increases in snow density that are too rapid when there is only light snowfall. As a result, GLM uses a gradual approach where the new snowfall and the existing snow is used to form a layer with a combined mass and average density. Example outputs are shown in Figure 7, and see also Yao et al. (2014~~).~~) for a previous application.

Geosci. Model Dev. Discuss., https://doi.org/10.5194/gmd-2017-257
Manuscript under review for journal Geosci. Model Dev.
Discussion started: 20 November 2017


Geoscientific Model Development Discussions

Revision 8 Mar 2018

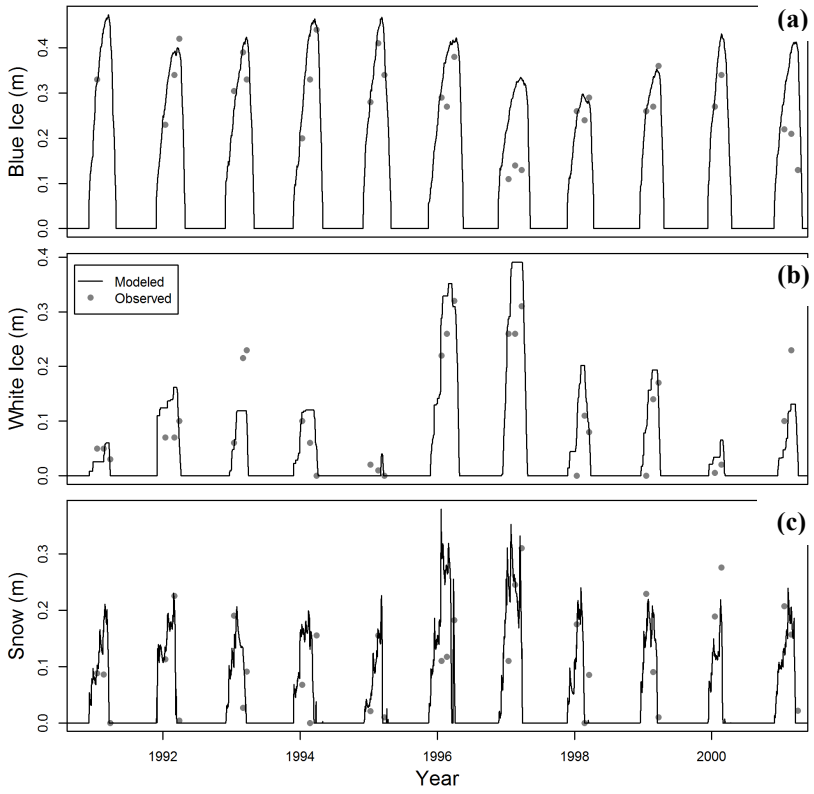


**Figure 7: Example of modelled and observed thickness of (a) blue ice ~~(a),~~ $\Delta z_{blue}$, (b) white ice ~~(b)~~ $\Delta z_{white}$, and ~~snow~~ (c) ~~thickness~~ snow, $\Delta z_{snow}$, for Sparkling Lake, Wisconsin. Lines are modelled thickness and points are average observed thicknesses.**

## 2.5 Sediment heating

The water column thermal budget may also be affected by heating or cooling from the soil/sediment below. For each layer, the rate of temperature change depends on the temperature gradient and the relative area of the layer volume in contact with bottom sediment:

$$c_w \rho_i \, \Delta V_i \frac{dT_i}{dt} = K_{soil} \frac{\left(T_{z_i} - T_i\right)}{\delta z_{soil}} \left(A_i - A_{i-1}\right) \quad (35)$$

where $K_{soil}$ is the soil/sediment thermal conductivity and $\delta z_{soil}$ is the length scale associated with the heat flux. The temperature of the bottom sediment varies seasonally, and also depending on its depth below the water surface, such that:

$$T_{z_i} = T_{z_{mean}} + \delta T_z \cos\left[\frac{2\pi}{365}\left(d - d_{T_z}\right)\right] \quad (36)$$

where $z$ is the soil/sediment zone that the $i^{th}$ layer overlays (see Section 4 for details), $T_{z_i}$ is the temperature of this zone, $T_{z_{mean}}$ is the annual mean sediment zone temperature, $\delta T_z$ is the seasonal amplitude of the soil temperature variation, and $d_{T_z}$ is the day of the year when the soil temperature peaks. By defining different sediment zones, the model can therefore allow

Geosci. Model Dev. Discuss., https://doi.org/10.5194/gmd-2017-257
Manuscript under review for journal Geosci. Model Dev.
Discussion started: 20 November 2017




for a different mean and amplitude of littoral waters compared to deeper waters. A dynamic sediment temperature diffusion model is also under development, which will be available when empirical data for the above parameters in Eq 36 is not possible.

## 2.6 Stratification and vertical mixing

### 2.56.1 Surface mixed layer

To compute mixing of layers, GLM works on the premise that the balance between the available energy, $E_{TKE}$, and the energy required for mixing to occur, $E_{PE}$, provides for the surface mixed layer (SMLsml) deepening rate ~~$dz_{SML}/dt$~~ $dz_{sml}/dt$, where $z_{sml}$ is the thickness of the surface mixed layer. For an overview of the dynamics, readers are referred to early works on bulk mixed layer depth models by Kraus and Turner (1967) and Kim (1976), which were subsequently extended by Imberger and Patterson (1981) as a basis for hydrodynamic model design. InUsing this modelapproach, the available kinetic energy is calculated due to contributions from wind stirring, convective overturn, shear production between layers, ~~convective overturn,~~ and Kelvin-Helmholtz (K-H) billowing. They may be combined and summarised for $E_{TKE}$ as (Hamilton and Schladow, 1997):

$$E_{TKE} = \underbrace{0.5C_K(w_*^3)\,\Delta t}_{convective\ overturn} + \underbrace{0.5C_K(C_W\,u_*^3)\,\Delta t}_{wind\ stirring} + \underbrace{0.5\,C_S\left[u_b^2 + \frac{u_b^2}{6}\frac{d\delta_{KH}}{dz_{sml}} + \frac{u_b\delta_{KH}}{3}\frac{du_b}{dz_{sml}}\right]}_{\substack{shear\ production \\ K-H\ production}} \Delta z_{k-1} \quad (3037)$$

where $\delta_{KH}$ is the K-H billow length scale (described below), $u_b$ is the shear velocity at the interface of the mixed layer, and $C_K$, $C_W$, and $C_S$ are mixing efficiency constants. For mixing to occur, the energy must be sufficient to lift up water atin the layer below the bottom of the mixed layer, denoted here as the layer $k-1$, with thickness ~~$\Delta h_{k-1}$~~ $\Delta z_{k-1}$, and accelerate it to the mixed layer velocity, $u_*$. This also accounts for energy consumption associated with K-H production and expressed as, $E_{PE}$:

$$E_{PE} = \left[\underbrace{0.5C_T(w_*^3 + C_W\,u_*^3)^{2/3}}_{acceleration} + \underbrace{\frac{\Delta\rho}{\rho_o}\,g\,z_{SML}}_{lifting} + \underbrace{\frac{g\delta_{KH}^2}{24\rho_o}\frac{d(\Delta\rho)}{dz_{sml}} + \frac{g\delta_{KH}\Delta\rho}{12\rho_o}\frac{d\delta_{KH}}{dz_{sml}}}_{K-H\ consumption}\right]\Delta z_{k-1}E_{PE} \quad (3138)$$

$$= \left[\underbrace{0.5C_T(w_*^3 + C_W\,u_*^3)^{2/3}}_{acceleration} + \underbrace{\frac{\Delta\rho}{\rho_o}\,g\,z_{SML}}_{lifting} + \underbrace{\frac{g\delta_{KH}^2}{24\rho_o}\frac{d(\Delta\rho)}{dz_{sml}} + \frac{g\delta_{KH}\Delta\rho}{12\rho_o}\frac{d\delta_{KH}}{dz_{sml}}}_{K-H\ consumption}\right]\Delta z_{k-1}$$

~~where $z_{SML}$ is the thickness of the surface mixed layer.~~

To numerically resolve Eq 37 and 38 the ~~above equations we~~model sequentially ~~compute~~computes the different components of the above expressions ~~in light of~~ with respect to the layer structure~~. Here~~, checking the available energy relative to the required amount. GLM follows the sequence of the algorithm ~~outlined~~presented in detail in Imberger and Patterson (1981~~)~~), whereby ~~cooling is computed so that~~ layers are combined due to convection~~, then~~ and wind stirring~~, and then~~ first, and then the resultant mixed layer properties are used when subsequently computing the extent of shear ~~and K-H~~ mixing ~~are computed~~and the effect of K-H instabilities.

Geosci. Model Dev. Discuss., https://doi.org/10.5194/gmd-2017-257
Manuscript under review for journal Geosci. Model Dev.
Discussion started: 20 November 2017


Geoscientific Model Development Discussions
Open Access
EGU

**Revision 8 Mar 2018**

To compute the mixing energy available due to ~~convective cooling~~convection, in the first step, the value for $w_*$ is calculated, which is the turbulent velocity scale associated with convection~~.~~ brought about by cooling at the air-water interface. The model adopts the algorithm used in Imberger and Patterson (1981), whereby the potential energy that ~~is~~would be released by mixed layer deepening is computed ~~by looking at~~as the difference in the moments of the ~~different~~ layers in the epilimnion (surface mixed layer~~(~~) about the lake bottom, which is numerically computed by summing from ~~layers *K*~~the bottom-most layer of the epilimnion, $k$, up to ~~$N_{LEV}$~~$N_{LEV}$:

$$~~w_*^3 = \frac{g}{\rho_{SML}\,\Delta t}\left(\sum_{k=K}^{N_{LEV}}[\rho_k\,\Delta z_k\,\widetilde{h_k}] - \widetilde{h_{SML}}\sum_{k=K}^{N_{LEV}}[\rho_k\,\Delta z_k\,]\right)w_*^3~~ \quad (3239)$$

$$= \frac{g}{\rho_{sml}\,\Delta t}\left(\sum_{i=k}^{N_{LEV}}[\rho_i\,\Delta z_i\,\widetilde{h_i}] - \widetilde{h_{sml}}\sum_{i=k}^{N_{LEV}}[\rho_i\,\Delta z_i\,]\right)$$

where ~~$\rho_{SML}$~~$\rho_{sml}$ is the mean density of the mixed layer including the combined layer, $\rho_k$ is the density of the $k^{th}$ layer, $\Delta$~~$z_k$~~$z_i$ is the height difference between two consecutive layers within the loop ($\Delta$~~$z_k$~~$z_i = $ ~~$h_k$~~$h_i - $ ~~$h_{k-1}$~~$h_{i-1}$), ~~$\widetilde{h_k}$~~$\widetilde{h_i}$ is the mean height of layers to be mixed ( ~~$\widetilde{h_k}$~~$\widetilde{h_i}$ ~~$= 0.5[$~~ $h_i$ ~~$+ h_{k-1}]$~~ ), and ~~$\widetilde{h_{SML}}$~~$\widetilde{h_{sml}}$ is the epilimnion ~~(surface mixed layer)~~ mid height, calculated ~~from~~as: ~~$\widetilde{h_{SML}}$~~$\widetilde{h_{sml}}$ $= 0.5$~~$[h_{SURF} + h_{k-1}]$~~$(h_s + h_{k-1})$.

The velocity scale $u_*$ is associated with wind stress and calculated according to the wind strength:

$$u_*{}^2 = C_D ~~U_*^2~~ U_{10}^2 \quad (3340)$$

where $C_D$ is the drag coefficient for momentum. The model first ~~has a check~~checks to see if the ~~stirring~~ energy available from Eqs. (39) and (40) can overcome the energy required to mix the ~~k-1~~$k-1$ layer~~,~~ into the surface mixed layer; i.e., mixing of $k-1$ occurs if:

$$~~C_K~~ C_K(w_*^3 + C_W\,u_*^3)\,\Delta t \geq \left(g'_k\,z_{SML} + C_T(w_*^3 + C_W\,u_*^3)^{2/3}\right)\Delta z_{k-1} \quad (3441)$$

~~and~~where $g'_k = \frac{\Delta\rho}{\rho_o}$ is the reduced gravity between the mixed layer and ~~k-1 layer.~~the $k-1$ layer, calculated as $(\rho_{sml} - \rho_{k-1})/(0.5(\rho_{sml} + \rho_{k-1}))$. If the mixing condition is met the layers are combined, the energy required to combine the layer is removed from the available energy, $k$ is adjusted, and the loop continues to the next layer. Where the mixing energy is substantial and the mixing reaches the bottom layer, then the mixing routine ends. If the condition in Eq. 41 is not met, then the energy is stored for the next time~~-~~ step~~-~~, and the mixing algorithm continues as outlined below.

Once stirring is completed, mixing due to velocity shear is applied. ~~Velocity shear at the interface is approximated from~~Parameterising the shear velocity in a one-dimensional model is difficult but the approximation used in Imberger and Patterson (1981) is applied as:

$$~~u_b = \frac{u_*^2 t}{z_{sml}} + u_{b_0}~~ u_b = \begin{cases} \frac{u_*{}^2 t}{z_{sml}} + u_{b_{old}}, & t \leq t_b + \delta t_{shear} \\ 0\ , & t > t_b + \delta t_{shear} \end{cases} \quad (3542)$$

~~where *t* is characteristic time scale over which~~such that there is a simple linear increase in the shear ~~has been operating~~velocity over time for a constant wind stress, considered relative to ~~$t_{shear}$~~$t_{shear}$, which is the cut-off time; beyond ~~which there~~this time

Geosci. Model Dev. Discuss., https://doi.org/10.5194/gmd-2017-257
Manuscript under review for journal Geosci. Model Dev.
Discussion started: 20 November 2017




it is assumed no further shear ~~production (*i.e.*,~~ induced mixing occurs for that event. The velocity ~~$u_b = 0$ if~~ $u_{b_{old}}$, is from the ~~time exceeds $t_{shear}$).~~ previous time step, and zeroed between shear events. This cut-off time assumes use of only the energy produced by shear at the interface during a period equivalent to half the basin-scale seiche duration, ~~$T_i$, and~~ $\delta t_{iw}$, which can be modified to account for damping~~:~~ (Spigel, 1978):

$$t_{shear} = T_i \left(1 + 0.59 \left[1 - cosh\left(\frac{T_d}{T_i} - 1\right)^{-1}\right]\right) \delta t_{shear} \quad (36\text{~~43~~})$$

$$= \begin{cases} 1.59\ \delta t_{iw} & \frac{\delta t_{damp}}{\delta t_{iw}} \geq 10 \\ \left(1 + 0.59 \left[1 - cosh\left(\frac{\delta t_{damp}}{\delta t_{iw}} - 1\right)^{-1}\right]\right) \delta t_{iw} & \frac{\delta t_{damp}}{\delta t_{iw}} < 10 \end{cases}$$

5

Geosci. Model Dev. Discuss., https://doi.org/10.5194/gmd-2017-257
Manuscript under review for journal Geosci. Model Dev.
Discussion started: 20 November 2017


Geoscientific Model Development Discussions

Revision 8 Mar 2018

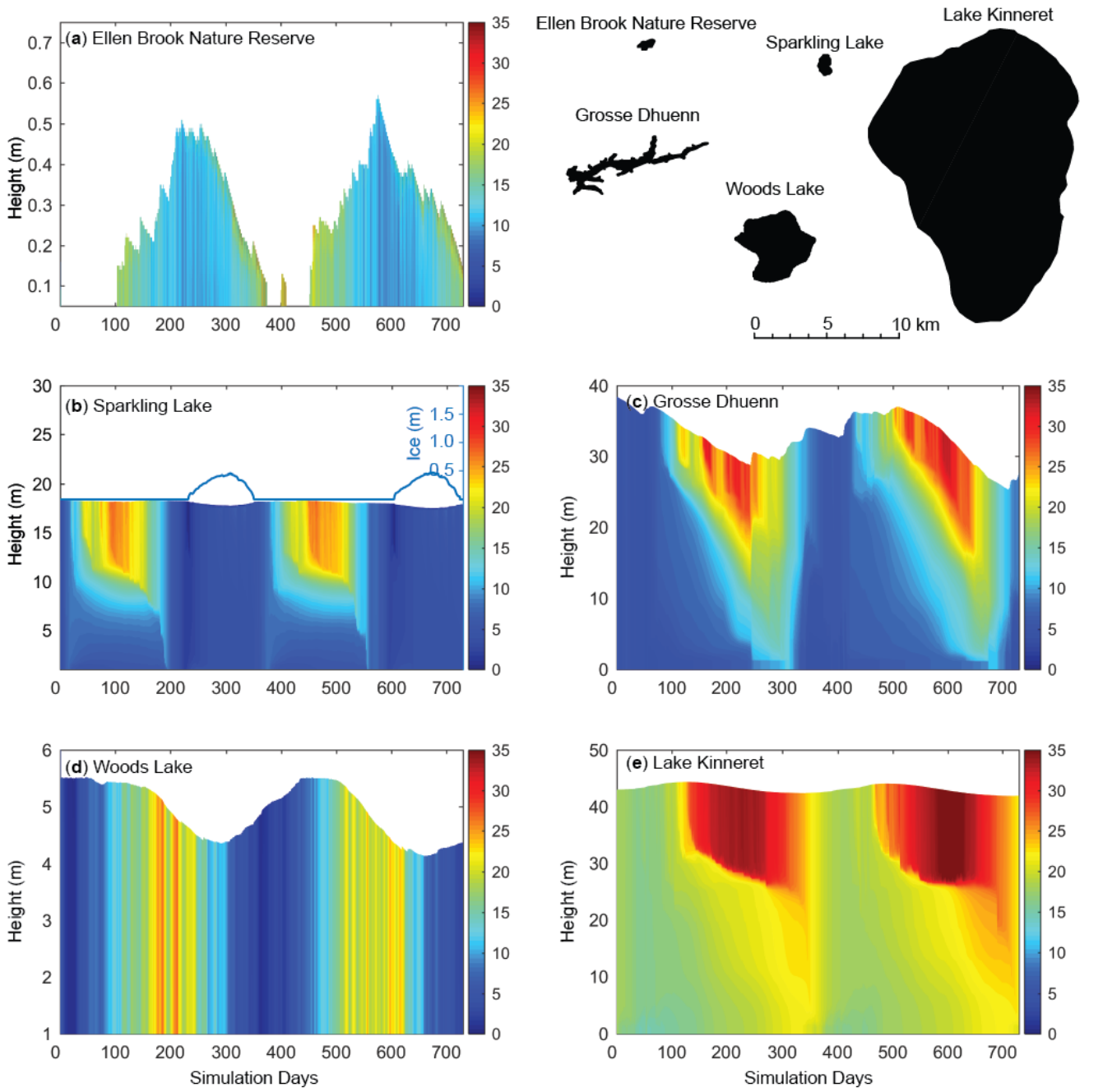


Figure 8: A two-year time-series of the simulated temperature profiles for five example lakes, a-e, that range in size and hydrology. For more information about each lake and the simulation configuration refer to the Data availability section (refer also to Fig. 2 and 5). Sparkling Lake (d) also indicates the simulated depth of ice on the RHS scale.

where ~~$T_d \delta t_{damp}$~~ is the time- scale of damping ~~(see Spigel, 1978).~~ The wave period is approximated based on the stratification as ~~$T_t$~~

Geosci. Model Dev. Discuss., https://doi.org/10.5194/gmd-2017-257
Manuscript under review for journal Geosci. Model Dev.
Discussion started: 20 November 2017




$\delta t_{iw} = L_{META}/2c$, where $L_{META}$ is the length of the basin at the thermocline, calculated from $\sqrt{A_{k-1}(4/\pi)(L_{crest}/W_{crest})}$, and $c$ is the internal wave speed~~.~~:

$$c = \sqrt{|g'_{EH}| \frac{\delta_{epi}\delta_{hyp}}{(\delta_{epi} + \delta_{hyp})}} \quad (44)$$

where $\delta_{epi}$ and $\delta_{hyp}$ are characteristic vertical length scales associated with the epilimnion and hypolimnion:

$$\delta_{epi} = \frac{\Delta V_{epi}}{0.5(A_s + A_{k-1})} \; ; \; \delta_{hyp} = \frac{V_{k-1}}{0.5A_{k-1}} \quad (45)$$

The time for damping of internal waves in a two-layer system can be parameterised by estimating the length scale of the oscillating boundary layer, through which the wave energy dissipates, and the period of the internal standing wave (see Spigel and Imberger, 1980):

$$\delta t_{damp} = \frac{\sqrt{\nu_w}}{c_{damp}\,\delta_{ss}} \frac{2(\delta_{epi} + \delta_{hyp})}{{u_*}^2} \sqrt{\frac{c}{2\,L_{META}}} \frac{\delta_{hyp}}{\delta_{epi}} (\delta_{epi} + \delta_{hyp}) \quad (46)$$

Once the velocity is computed from Eq. 42, the energy for mixing from velocity shear is compared to that required for lifting and accelerating the next layer down, and layers are combined if there is sufficient energy, *i.e.* when:

~~$$0.5\,C_S \left[\frac{u_b^2(\widetilde{z_{SML}} + \Delta\xi)}{6} + \frac{u_b \xi \Delta u_b}{3}\right] + \left[g'_k \xi \left(\frac{\xi \Delta z_{k-1}}{24 z_{SML}} - \frac{\Delta\xi}{12}\right)\right] \quad (37)$$~~

$$\geq \left(g'_k\, z_{SML} + C_T(w_*^3 + C_W\, u_*^3)^{2/3}\right)\Delta z_{k-1} \; 0.5\; C_S \left[\frac{u_b^2(\widetilde{z_{sml}} + \Delta\delta_{KH})}{6} + \frac{u_b \delta_{KH} \Delta u_b}{3}\right] + \left[g'_k \delta_{KH} \left(\frac{\delta_{KH}\Delta z_{k-1}}{24 z_{SML}} - \frac{\Delta\delta_{KH}}{12}\right)\right]$$

$$\geq \left(g'_k\, z_{sml} + C_T(w_*^3 + C_W\, u_*^3)^{2/3}\right)\Delta z_{k-1}$$

where the ~~K-H~~billow length scale is ~~$\xi = C_{KH} u_b^2/g'_{EH}$~~ $\delta_{KH} = C_{KH} u_b^2/g'_{EH}$ and ~~$\Delta\xi = 2\,C_{KH}\,u_b\,\Delta u_b/g'_{EH}$~~ $\Delta\delta_{KH} = 2\,C_{KH}\,u_b\,\Delta u_b/g'_{EH}$; in this case the reduced gravity is computed from the difference between the epilimnion and hypolimnion, and $C_{KH}$ is a measure of the billow mixing efficiency.

Once shear mixing is done, the model checks the resultant density interface to see if it is unstable to shear ~~(i.e., such that~~ K-H billows would be expected to form~~). This occurs~~, i.e., if the ~~gradient~~metalimnion thickness is less than the K-H length scale~~,~~ $\delta_{KH}$. If K-H mixing is required, layers are further split and ~~subject to mixing using an algorithm similar to above~~a linear density profile is set over the metalimnion.

Geosci. Model Dev. Discuss., https://doi.org/10.5194/gmd-2017-257
Manuscript under review for journal Geosci. Model Dev.
Discussion started: 20 November 2017






### 2.~~5~~6.2 Deep mixing

Mixing below the ~~SML~~epilimnion in lakes, in the deeper stratified regions of the water column, is modelled using a characteristic vertical diffusivity, ~~$K_Z = K_\varepsilon D_Z = D_\varepsilon + K_m D_m$~~, where ~~$K_m D_m$~~ is ~~the fixed~~a constant molecular diffusivity ~~of~~for scalars~~-~~ and $D_\varepsilon$ is the turbulent diffusivity. Three hypolimnetic mixing options are possible in GLM including: (~~i~~1) no diffusivity ~~(ii,~~ $D_Z = 0$, (2) a constant vertical diffusivity ~~$K_Z D_Z$~~ over the water depth below the thermocline or (~~iii~~3) a derivation by Weinstock (1981~~),~~) used in DYRESM, which is described as being suitable for regions displaying weak or strong stratification, whereby diffusivity increases with dissipation and decreases with heightened stratification.

Geosci. Model Dev. Discuss., https://doi.org/10.5194/gmd-2017-257
Manuscript under review for journal Geosci. Model Dev.
Discussion started: 20 November 2017




Revision 8 Mar 2018

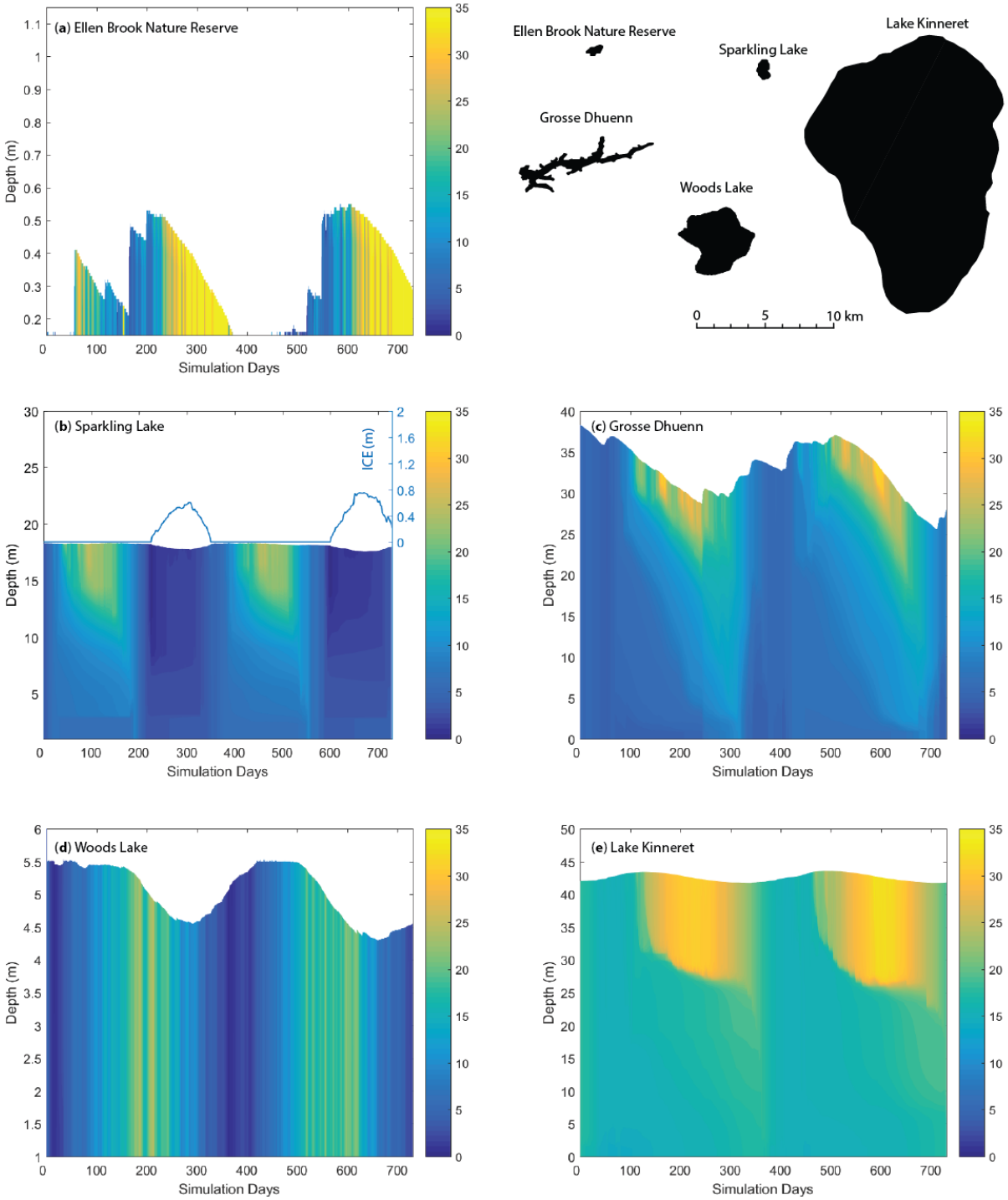


Figure 8: A two year time series of the simulated temperature profiles for five example lakes, a-e, that range in size and hydrology. For more information about each lake and the simulation configuration refer to the Data availability section (refer also to Fig. 2 and 5). Sparkling Lake (d) also indicates the simulated depth of ice.

Geosci. Model Dev. Discuss., https://doi.org/10.5194/gmd-2017-257
Manuscript under review for journal Geosci. Model Dev.
Discussion started: 20 November 2017




For the constant vertical diffusivity option, the coefficient $\alpha_{TKE}$ is interpreted as ~~a~~the vertical diffusivity (m~~$^2$~~/~~2~~ s~~)~~$^{-1}$), i.e., $D_z = C_{HYP}$. For the Weinstock (1981) model, the diffusivity is computed according to:

~~$$K_z = \frac{\alpha_{TKE} \varepsilon_{TKE}}{N^2 + 0.6\, k_{TKE}^{\ 2} u_*^{\ 2}}$$~~ ~~(38)~~

$$D_z = \frac{C_{HYP}\, \varepsilon_{TKE}}{N^2 + 0.6\, k_{TKE}^{\ 2}\, u_*^{\ 2}} \quad (48)$$

where ~~$\alpha_{TKE} C_{HYP}$~~ in this case is the mixing efficiency of hypolimnetic TKE (~0.8 in Weinstock, 1981) and ~~$k_{TKE}$ is the turbulence wavenumber:~~

~~$$k_{TKE} = \frac{12.4\, A_{top}}{\tilde{V}\, \Delta z_{top}\, 10^3}$$~~ ~~(39)~~

~~and $u_* = \sqrt{1.612 \times 10^{-6}\, U_x^{\ 2}}$. The term~~ is defined as above. $N^2$ is the Brunt–Väisälä (buoyancy) frequency defined for a given layer as:

$$N^2{}_i = \frac{g \Delta\rho}{\rho \Delta z} \approx \frac{g(\rho_{i+2} - \rho_{i-2})}{\rho_{ref}(h_{i+2} - h_{i-2})} \quad (49)$$

where $\rho_{ref}$ is the average of the layer densities. This is computed from layer 3 upwards, averaging over the span of 5 layers, until the vertical density gradient exceeds a set tolerance. $k_{TKE}$ is the turbulence wavenumber:

~~$$N^2 = \frac{g \Delta\rho}{\rho \Delta z} \approx \left[\frac{g(\rho_{i+2} - \rho_{i-2})}{\rho_{ref}(h_{i+2} - h_{i-2})}\right]$$~~ ~~(40)~~

~~Estimating the~~

$$k_{TKE}^2 = \frac{c_{wn}\, A_s}{\tilde{V}_{N^2}\, \Delta z_{sml}} \quad (50)$$

where $\tilde{V}_{N^2}$ is a fractional volume of the lake that contains 85% of $N^2$. The turbulent dissipation rate can be complex ~~and~~in stratified lakes, however, GLM adopts a simple approach as described in Fischer et al. (~~1980~~1979) where a "net dissipation" is approximated by assuming dissipation is in equilibrium with energy inputs from external drivers:

$$\varepsilon_{TKE} \approx \overline{\varepsilon_{TKE}} = E_{WIND}\varepsilon_{WIND} + E_{INFLOW}\varepsilon_{INFLOW} \quad (41\text{~~}51)$$

which is expanded and calculated per unit ~~volume~~mass as:

~~$$\varepsilon_{TKE} = \underbrace{\frac{1}{(\tilde{V}\bar{\rho})10^3} \frac{m\, C_D \rho_a\, f_S\, U_x^{\ 3}\, A_t}{10^6}}_{\text{rate of working by wind}} + \underbrace{\frac{1}{(V_{mix}\bar{\rho})10^3} \sum_t^{N_{INF}} g\, \Delta\rho_t\, Q_t (h_{top} - h_t)}_{\text{rate of work done by inflows}} \overline{\varepsilon_{TKE}}$$~~ ~~(42~~52)

$$= \underbrace{\frac{1}{\tilde{V}_{N^2}\, \bar{\rho}}\, m\, C_D\, \rho_a\, U_{10}^{\ 3}\, A_s}_{\text{rate of working by wind}}$$

$$+ \underbrace{\frac{1}{(\tilde{V}_{N^2} - \Delta V_s)\, \bar{\rho}} \sum_I^{N_{INF}} g \left(\rho_{ins_I} - \rho_{i_{ins_I}}\right) Q_{inf_{ins_I}} \left(\left(h_s - z_{inf_{ins_I}}\right) - h_{i_{ins_I}-1}\right)}_{\text{rate of work done by inflows}}$$

Geosci. Model Dev. Discuss., https://doi.org/10.5194/gmd-2017-257
Manuscript under review for journal Geosci. Model Dev.
Discussion started: 20 November 2017






~~The diffusivity is calculated according to Eq. 42, but since~~where $\bar{\rho} = 0.5(\rho_1 + \rho_{N_{LEV}})$ is the mean density of the water column. The work done by inflows is computed based on the flow rate, the depth the inflow plunges to, and the density difference, summed over all configured inflows.

Since the dissipation is assumed to concentrate close to the level of strongest stratification, the "mean" diffusivity from Eq. 48 is modified to decay exponentially ~~with~~within the layers as they increase their distance from the thermocline:

$$K_{z_i} = \begin{cases} 0 & h_i \geq (h_{top} - z_{mix}) \\ K_z \ exp\left[\frac{-(h_{top} - z_{mix} - h_i)^2}{\sigma}\right] & h_i < (h_{top} - z_{mix}) \end{cases} D_{Z_i} \quad (43\text{–}53)$$

$$= \begin{cases} 0 & h_i \geq (h_s - z_{sml}) \\ D_z \ exp\left[\frac{-(h_s - z_{sml} - h_i)^2}{\sigma}\right] & h_i < (h_s - z_{sml}) \end{cases}$$

where $\sigma$ is the variance of the $N^2$ distribution below ~~$h_{mix}$~~the bottom of the mixed layer, $h_s - z_{sml}$, and this scales ~~with~~ the depth over which the mixing ~~decays~~is assumed to decay.

Once the diffusivity is approximated (for either model 1 or 2 ~~in Eq. 43~~), the diffusion of any scalar, $C$, (including salinity), between two layers is numerically accounted for by the following mass transfer expressions:

$$C_{i+1} = \bar{C} + \frac{exp(-f)\Delta z_i \Delta C}{(\Delta z_{i+1} + \Delta z_i)} e^{-f} \frac{\Delta z_i \Delta C}{(\Delta z_{i+1} + \Delta z_i)} \quad (44\text{–}54\text{a,b})$$

$$C_i = \bar{C} - \frac{exp(-f)\Delta z_{i+1} \Delta C}{(\Delta z_{i+1} + \Delta z_i)} e^{-f} \frac{\Delta z_{i+1} \Delta C}{(\Delta z_{i+1} + \Delta z_i)}$$

where $\bar{C}$ is the weighted mean concentration of $C$ for the two layers, and $\Delta C$ is the concentration difference between them. ~~$f$~~ The smoothing function, $f_{dif}$, is related to the diffusivity according to:

$$f = \frac{K_{z_{i+1}} + K_{z_i}}{(\Delta z_{i+1} + \Delta z_i)^2} \Delta t \quad f_{dif} = \frac{D_{Z_{i+1}} + D_{Z_i}}{(\Delta z_{i+1} + \Delta z_i)^2} \Delta t \quad (45\text{–}55)$$

~~The~~and the above diffusion algorithm is run once up the water column and once down the water column as a simple explicit method for capturing diffusion of mass to both the upper and lower layers. An example of the effect of hypolimnetic mixing on a hypothetical scalar concentration released into the hypolimnion is shown in Figure 9.

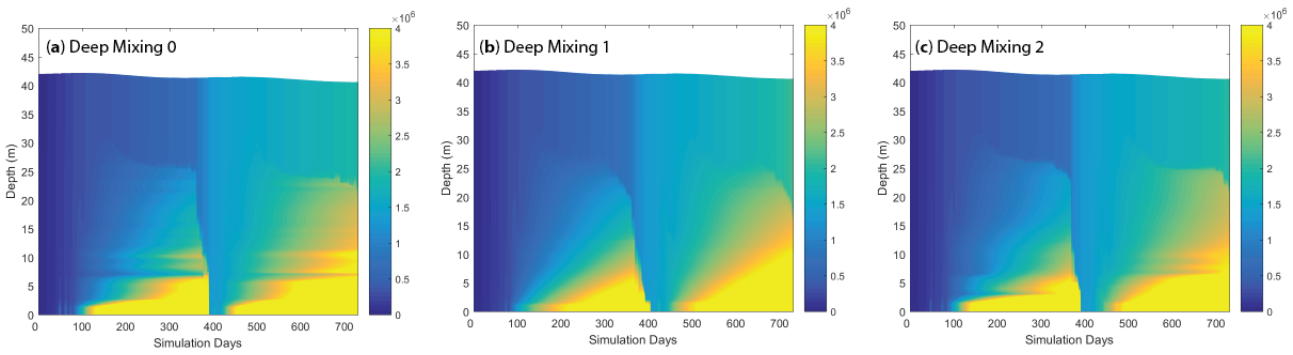

Geosci. Model Dev. Discuss., https://doi.org/10.5194/gmd-2017-257
Manuscript under review for journal Geosci. Model Dev.
Discussion started: 20 November 2017


Geoscientific Model Development Discussions



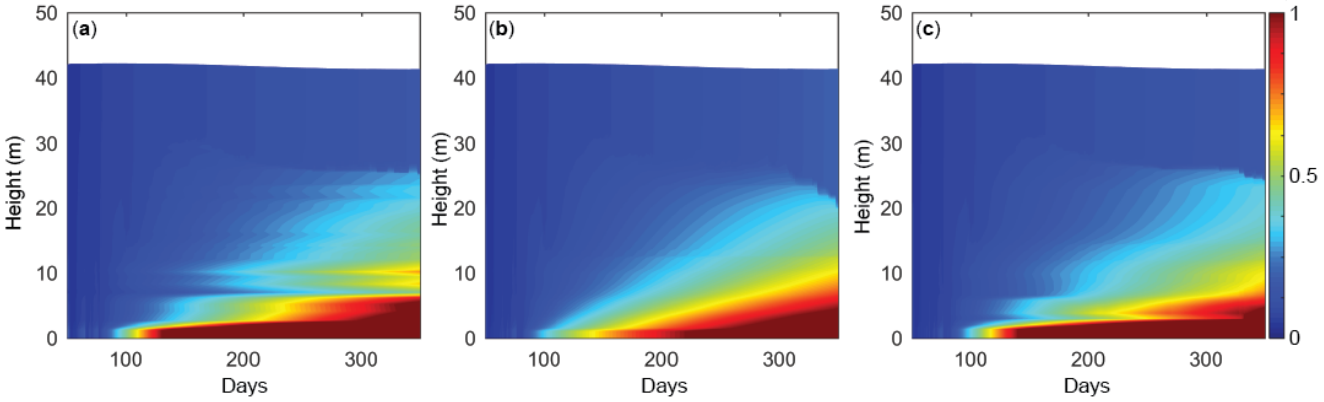


**Figure 9: ~~Simulations~~Example simulations for Lake Kinneret showing the hypolimnetic concentration of a passive tracer (normalised units) released from the ~~bottom~~ sediment into the bottom layer at a constant rate for the case: a) without deep mixing, b) constant vertical diffusivity, $D_z = 2\times10^{-6}$ m$^2$ s$^{-1}$, and c) calculated vertical diffusivity (Eq. ~~38). For~~48). The thermal structure ~~of~~for this case ~~refer to~~is in Figure 8c.**

### 2.~~6~~7 Inflows and outflows

Aside from the surface fluxes of water described above, the water balance of a lake is controlled by the specifics of the inflows and outflows. Inflows can be specified as local runoff from the surrounding (dry) lake domain ($Q_R$ described separately above, Eq. ~~5~~7), rivers entering at the surface of the lake that will be buoyant or plunge depending on their momentum and density (~~Sect~~Section 2.6.1), or submerged inflows (including groundwater ~~(Sect 2.6.2). Any number of inflows to the lake body can be specified and these are applied daily.~~ ) that enter at depth (Section 2.6.2). Four options for outflows are included in GLM~~, including~~. These include withdrawals from a specified depth (~~Sect~~Section 2.6.3), adaptive offtake (~~Sect~~Section 2.6.4), vertical groundwater seepage (~~Sect~~Section 2.6.5~~).~~

#### ~~2.6.1 River inflows~~

~~For~~), and river ~~inflows, depending on the density of the river water, the inflow will~~ outflow/overflow from the surface of the lake (Section 2.6.6). Any number of lake inflows and outflows can be specified and, except for the local runoff term, all applied at a daily time step. Depending on the specific settings of each, these water fluxes can impact the volume of the individual layers, $\Delta V_i$, as well as the overall lake volume.

#### 2.7.1 River inflows

As water from an inflowing river connects with a lake or reservoir environment, it will form a positively or negatively buoyant intrusion ~~that will enter the lake and insert at a depth of neutral buoyancy. As the inflow inserts it will entrains water depending on the rate of mixing created by th inflowing water. In GLM, as the inflow crosses layers~~depending on the density of the incoming river water in the context of the water column stratification. As the inflow progresses towards insertion, it will entrain water ~~from each, until it reaches a level of neutral buoyancy and undergoes insertion. Therefore, when it reaches its point of~~

Geosci. Model Dev. Discuss., https://doi.org/10.5194/gmd-2017-257
Manuscript under review for journal Geosci. Model Dev.
Discussion started: 20 November 2017




~~neutral buoyancy a new layer of thickness dependent on the inflow volume at that time (including additions from entrainment) is created. Following insertion, the inflow layer may then amalgamate with adjacent layers depending on numerical criteria within the model for combining or splitting layers.~~

~~The~~ at a rate depending on the turbulence created by the inflowing water mass (Fischer et al., 1979). For each configured inflow the characteristic rate of entrainment of the intrusion, ~~$E$, can be calculated in a number of ways. For simplicity, in GLM the rate has been adapted from the first~~$E_{inf}$, is computed using the approximation given in Fischer et al. (1979):

$$\text{~~}E = 1.6\frac{C_{D_t}^{3/2}}{Ri}\text{~~}E_{inf} = 1.6\frac{C_{D_{inf}}^{3/2}}{Ri_{inf}} \quad (\text{~~}46\text{~~}56)$$

where ~~$C_{D_t}$~~$C_{D_{inf}}$ is the user-specified drag coefficient for the inflow. ~~The Richardson's~~inflow Richardson number ~~is adapted from~~ $Ri_{inf}$, characterises the stability of the water in the context of the inflow channel geometry (Fischer et al. ~~(~~., 1979~~)~~), computed as:

$$\text{~~}Ri = \frac{C_{D_t}\left(1 + 0.21\sqrt{C_{D_t}}\sin\alpha_{inf}\right)}{\sin\alpha_{inf}\tan\phi_{inf}}\text{~~}Ri_{inf} = \frac{C_{D_{inf}}\left(1 + 0.21\sqrt{C_{D_{inf}}}\sin\alpha_{inf}\right)}{\sin\alpha_{inf}\tan\Phi_{inf}} \quad (\text{~~}47\text{~~}57)$$

where $\alpha_{inf}$ is the stream half angle and $\phi_{inf}$ is the tangent of the slope of the inflow, at the point where it meets the water body (Figure 10).

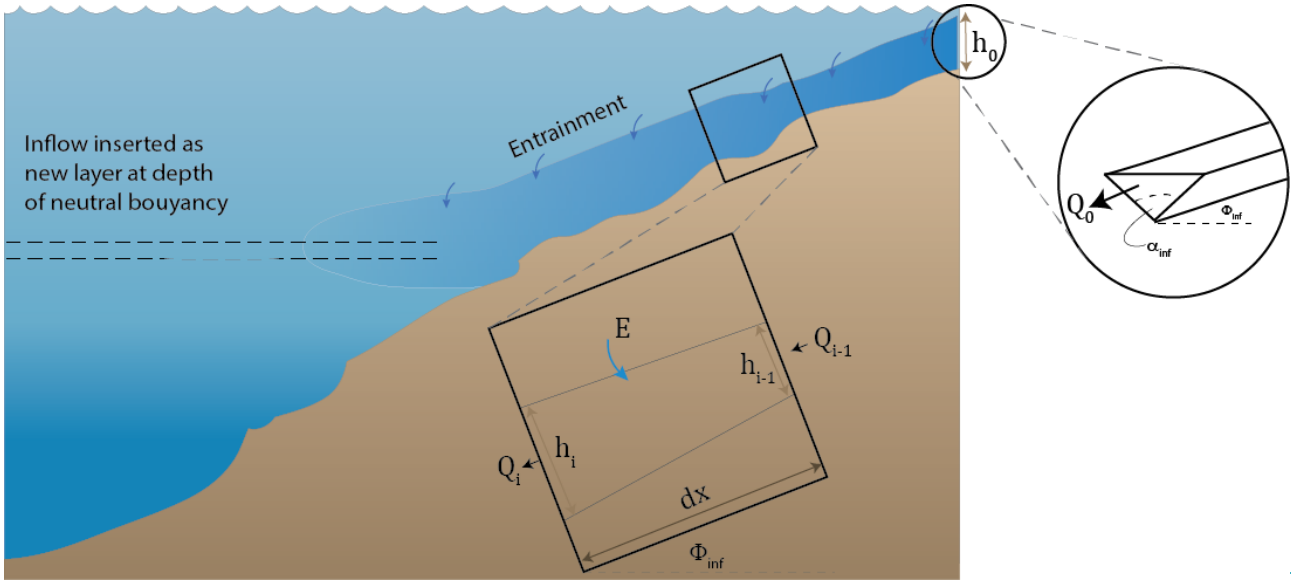

Geosci. Model Dev. Discuss., https://doi.org/10.5194/gmd-2017-257
Manuscript under review for journal Geosci. Model Dev.
Discussion started: 20 November 2017




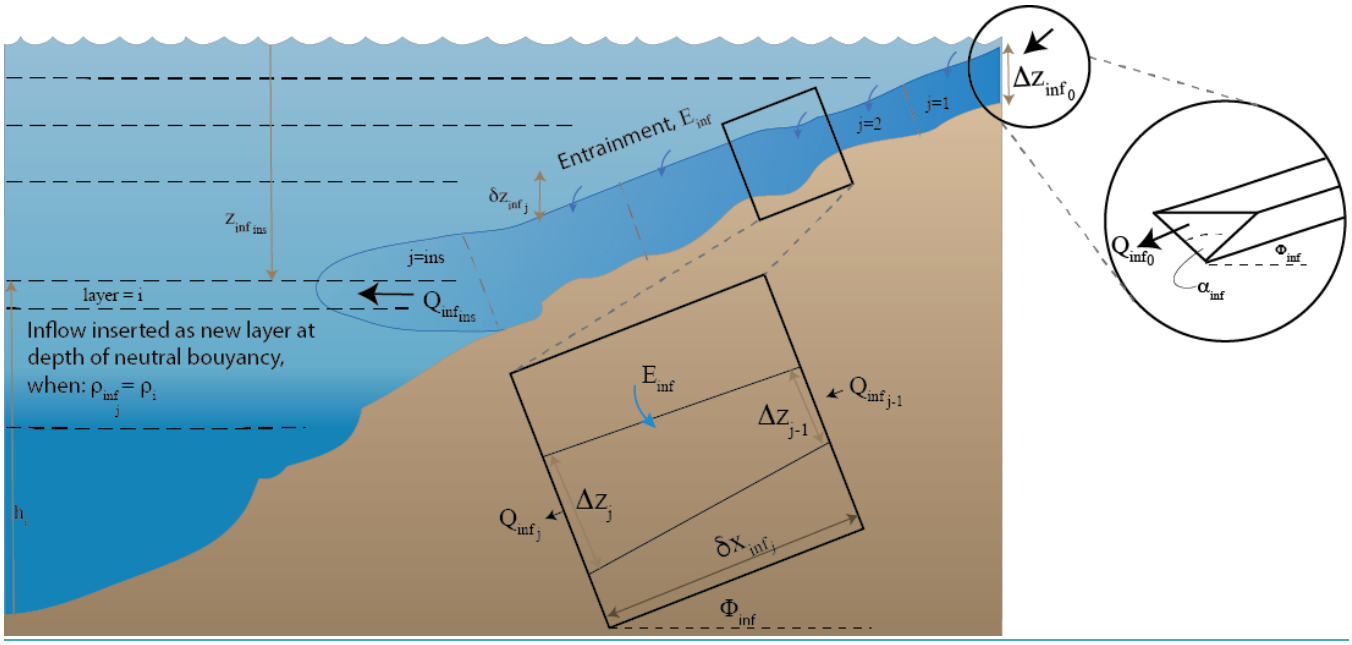


**Figure 10: Schematic showing inflow insertion ~~height~~depth, entrainment, ~~E,~~$E_{inf}$, slope, ~~$\phi_{inf}$~~$\Phi_{inf}$ and half angle, $\alpha_{inf}$ of an inflowing river entering with a ~~user~~ prescribed flow of ~~$Q_{\phi}$~~$Q_{inf_0}$ and estimated starting ~~height~~thickness of ~~$h_{\phi}$~~$\Delta z_{inf_0}$.**

The inflow algorithm captures two phases: first, the inflowing water crosses the layers of the lake until it reaches a level of neutral buoyancy, and second, it then undergoes insertion. In the first part of the algorithm, the daily inflow parcel is tracked down the lake-bed and its mixing with layers is updated until it is deemed ready for insertion. The initial estimate of the intrusion thickness, $\Delta z_{inf_0}$, is computed from Antenucci et al. (2005):

~~As the inflow parcel travels through the layers, the increase in inflow thickness due to entrainment is estimated as:~~

$$~~h_i = 1.2Edx + h_{i-1}~~ \Delta z_{inf_0} = \left( 2 \frac{Ri_{inf}}{g'_{inf}} \left( \frac{Q_{inf_0}}{tan\, \Phi_{inf}} \right)^2 \right)^{1/5} \quad (~~48~~58)$$

~~where $h_i$ is the inflow thickness, $E$ is the entrainment rate and $dx$ is the distance travelled by the inflowing water, calculated from the flow rate and inflow thickness. The initial estimate of the intrusion height is computed from Imberger and Patterson (1981) and Antenucci et al.~~ where $Q_{inf_0} = f_{inf}\, Q_{inf_x}/c_{secday}$ is the inflow discharge entering the domain, based on the data provided as a boundary condition, $Q_{inf_x}$, and $g'$ is the reduced gravity of the inflow as it enters:

~~(2005):~~

$$~~h_0 = \left( 2Q_{inf}^2 \frac{Ri}{g'_{inf}} tan^2 \phi_{inf} \right)^{1/5}~~ g'_{inf} = g \frac{(\rho_{inf} - \rho_s)}{\rho_s} \quad (~~49~~59)$$

~~where $Q_{inf}$ is the inflow discharge provided as a boundary condition and $g'$ is the reduced gravity of the inflow given as:~~

where $\rho_{inf}$ is the density of the inflow, computed from the supplied inflow properties of temperature and salinity ($T_{inf_x}$, $S_{inf_x}$), and $\rho_s$ is the density of the surface layer. If the inflowing water is deemed to be positively buoyant $(\rho_{inf} < \rho_s)$, or the model

Geosci. Model Dev. Discuss., https://doi.org/10.5194/gmd-2017-257
Manuscript under review for journal Geosci. Model Dev.
Discussion started: 20 November 2017




only has one layer ($N_{LEV} = 1$), then the inflow water over the daily time step is added to the surface layer volume ($\Delta V_{N_{LEV}} = Q_{inf_0}\,\Delta t_d$), and $h_s$ is updated accordingly. Otherwise, this inflow volume is treated as a parcel which travels down through the lake layers, and its properties are subsequently incremented over each daily time step, $j$, until it inserts. The thickness of an inflow parcel increases over each increment due to entrainment, assuming:

$$g'_{inf} = g\frac{(\rho_{inf} - \rho_s)}{\rho_s}\Delta z_{inf_j} = 1.2\,E_{inf}\,\Delta x_{inf_j} + \Delta z_{inf_{j-1}} \quad (50\,60)$$

where $\rho_{inf}\Delta z_{inf_j}$ is the density of the inflow thickness and $\rho_s$ the density of the surface layer.$\Delta x_{inf_j}$ is the distance travelled by the inflowing water parcel in the time step. The distance travelled by the inflow aliquot, $dx$, is estimated asbased on the distance travelledchange in the vertical elevation of the inflow, $\delta z$, and the slope of the inflow river, $\phi_{inf}$ and, as given by:

$$dx = \frac{dz}{\sin\phi_{inf}}\Delta x_{inf_j} = \frac{\delta z_{inf_{j-1}}}{\sin\Phi_{inf}} \quad (51\,61)$$

where $dz$, $\delta z_{inf_j} = \left(h_s - z_{inf_j}\right) - h_{i_j-1}$, and the depth of the inflow from the surface is the distance travelled in the vertical.$z_{inf_j} = z_{inf_{j-1}} + \Delta x_{inf_j}\sin\Phi_{inf}$. The average velocity of the inflow aliquotparcel for that dayincrement is then calculated asfrom:

$$u = h_i^2\frac{Q_{inf}}{\tan\alpha}u_{inf_j} = Q_{inf_j}\frac{\tan\alpha_{inf}}{\left(\Delta z_{inf_j}\right)^2} \quad (52\,62)$$

where the numerator links the relationship between inflow height and channel width in order to define the cross-sectional area of the flow. This velocity is used to estimate the time scale of transport of the parcel ($\delta t_d = \Delta x_{inf_j}/u_{inf_j}$). Following conservation of mass, the flow is estimated to increase according to Fischer et al. (1979), as in) (see also Antenucci et al. (2005):

$$Q_i = Q_{i-1}\left[\left(\frac{h_i}{h_{i-1}}\right)^{5/3} - 1\right]\Delta Q_{inf_j} = Q_{inf_{j-1}}\left[\left(\frac{\Delta z_{inf_j}}{\Delta z_{inf_{j-1}}}\right)^{5/3} - 1\right] \quad (53\,63)$$

The above entrainment and insertion algorithm is repeated for each inflow.

whereby $\Delta Q_{inf_j}$ is removed from the volume of the corresponding layer, $i_j$, and added to the previous time-step inflow $Q_{inf_{j-1}}$ to capture the entrainment effect on the inflow. The inflow travel algorithm (Eq. 63) increments through $j$ until the density of the inflow reaches its depth of neutral buoyancy: $\rho_{inf_j} \leq \rho_{i_j}$. Once this condition is met, the second part of the algorithm creates a new layer of thickness dependent on the inflow volume at that time (including the successive additions from entrainment; Eq. 60).

Note that a new inflow parcel is created each day, and the user may configure multiple inflows, $N_{INF}$, creating a complex set of parcels being tracked via Eqs 56-63, and a queue of new layers to be inserted. Following creation of a new layer for the inflow parcel, $N_{LEV}$ is incremented and all layer heights are updated. The new inflow layer is then subject to the thickness



limits criteria within the layer limit checking routine and may amalgamate with adjacent layers for combining or splitting layers.

Aside from importing mass into the lake, river inflows also contribute turbulent kinetic energy to the hypolimnion, as discussed in ~~the~~ Sect 2.5.2 (e.g., see Eq. ~~42~~49), and contribute to the scalar transport in the water column by adding mass and contributing to mixing (Figure 11a).

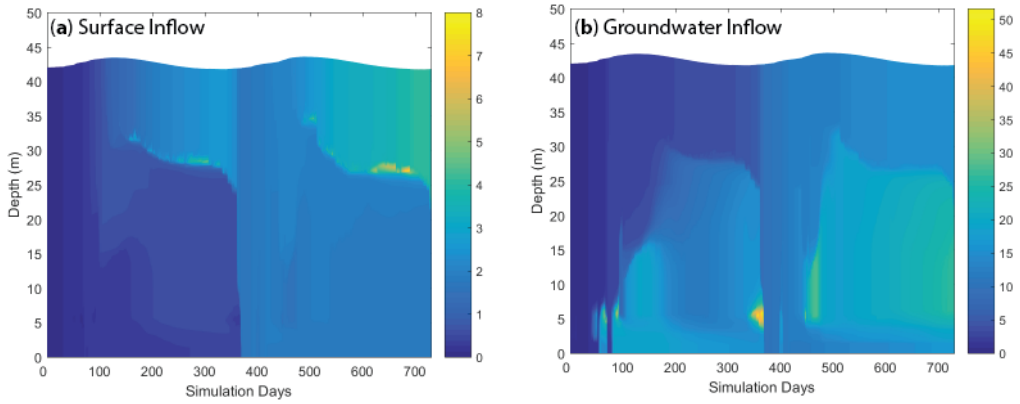


~~**Figure 11: Simulation showing inflow tracer insertion example for the case where a) the inflow was set as a surface river inflow, and b) the inflow was set as a submerged inflow at a specified height (h=5m). After input the tracer is subject to mixing during inflow entrainment and by surface and deep mixing once inserted.**~~

### 2.~~6~~7.2 Submerged inflows

Submerged inflows are inserted at the user-specified depth with zero entrainment~~.~~ by utilising the second part of the algorithm described in Section 2.6.1. The submerged inflow volume is added as a new layer which may then be mixed with adjacent layers (above or below) depending on the density difference~~, until neutral buoyancy is attained~~ and layer thickness criteria (Figure 11b). This option can be used across one or more ~~layers~~inflow elevations to account for groundwater ~~inputs~~input to a lake, or for capturing a piped inflow, for example.

Geosci. Model Dev. Discuss., https://doi.org/10.5194/gmd-2017-257
Manuscript under review for journal Geosci. Model Dev.
Discussion started: 20 November 2017


Geoscientific Model Development Discussions
Open Access
EGU

Revision 8 Mar 2018

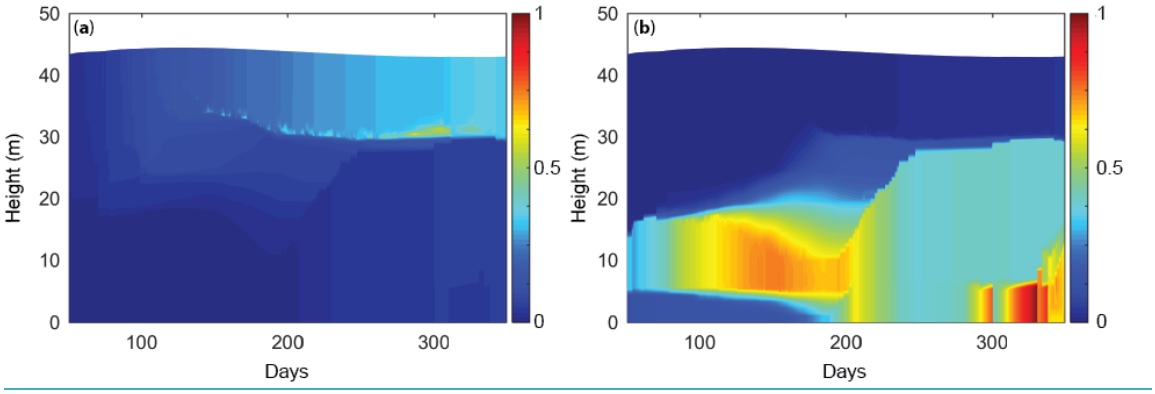


**Figure 11: Example simulations demonstrating inflow insertion example for the case where a) the inflow was set as a surface river inflow and subject to the insertion algorithm (Eqs 56-63) prior to insertion, and b) the inflow was set as a submerged inflow at a specified height ($h_{inf}$ = 5m). Once entering the water column, the tracer, $C$, is subject to mixing during inflow entrainment in case (a), and by surface and/or deep mixing once inserted, for both cases (a) and (b). The colour scale represents an arbitrary inflow concentration which entered with a value of 1.**

### 2.67.3 Withdrawals

Outflows from a specific depth can ~~be accommodated including~~include outlets from a dam wall offtake~~,~~ or other piped withdrawal, or ~~for removing~~removal of water that may be lost due to groundwater ~~discharge~~recharge or seepage to an outflow. For a stratified water column, the water will be removed from the layer corresponding to the specified withdrawal ~~depth,~~height, $h_{outf}$, as well as layers above or below, depending on the strength of discharge and stability of the water column. Accordingly, the model assumes ~~a line sink~~an algorithm where the thickness of the withdrawal layer is dependent on the internal Froude ($Fr$) and Grashof ($Gr$) numbers, and the parameter, $R$ (see Fischer et al., 1979; Imberger and Patterson, 1981):

$$Fr = \frac{Q_{outf}}{N_{outf}^2 W_{outf} L_{outf}^2} \quad Fr = \frac{f_{outf}\ Q_{outf_x}/c_{secday}}{N_{outf}\ W_{outf}\ L_{outf}^2} \tag{5464}$$

$$Gr = \frac{N_{outf}^2 A_{outf}^2}{\nu_{outf}^2} \quad Gr = \frac{N_{outf}^2 A_{outf}^2}{D_{outf}^2} \tag{5565}$$

$$R = FrGr^{1/3} \tag{5666}$$

where $W_{outf}$, $L_{outf}$ and $A_{outf}$ are the width, length and area of the lake at the outlet elevation, and $\nu_{outf}^2 D_{outf}^2$ is the vertical ~~diffusion coefficient~~diffusivity averaged over the layers corresponding to the withdrawal ~~layer. The Brunt- Väisälä frequency averaged over the~~ thickness ~~of the withdrawal layer, $N_{outf}^2$, is calculated as:~~

$$N_{outf}^2 = \frac{g}{dz}\frac{\rho_{outf} - \rho_t}{\rho_{outf}} \tag{57}$$

~~where $dz$ is the thickness of the withdrawal layer, $\rho_{outf}$ is the density of the lake at the height of withdrawal and $\rho_t$ is the density of the lake at the edge of the withdrawal layer. The thickness of the withdrawal layer is then,~~ $\delta_{outf}$ (described ~~calculated depending on the value of $R$ (Fischer et al. 1978), such that:~~

Geosci. Model Dev. Discuss., https://doi.org/10.5194/gmd-2017-257
Manuscript under review for journal Geosci. Model Dev.
Discussion started: 20 November 2017






~~$$\delta_{outf} = \begin{cases} 2L_{outf} Gr^{-1/6} & R \leq 1 \\ 2L_{outf} Fr^{1/2} & R > 1 \end{cases}$$~~ ~~(58)~~

~~The proportion of fluid withdrawn from each layer either above or~~ below ~~the layer of the outlet elevation is determined using a curve that fits the region of fluid drawn in a given time.~~). To calculate the width and length of the lake at the height of the outflow, it is assumed, firstly, that the lake shape can be approximated as an ellipse, and secondly, that the ratio of length to width at the height of the outflow is the same as that at the lake crest. The length of the lake at the outflow height, $L_{outf}$ and the lake width, $W_{outf}$ are given by:

$$L_{outf} = \sqrt{A_{outf} \frac{4}{\pi} \frac{L_{crest}}{W_{crest}}} \quad (59a67)$$

$$W_{outf} = L_{outf} \frac{W_{crest}}{L_{crest}} \quad (59b68)$$

where $A_{outf}$ is the area of the lake at the outflow height, $L_{crest}$ is the length and $W_{crest}$ the width of the lake at the crest height. ~~Depending on the layer(s) the water is withdrawn from, the water taken will have the associated scalar concentrations.~~

The thickness of the withdrawal layer is calculated depending on the value of $R$ (Fischer et al. 1978), such that:

~~2.6~~

$$\delta_{outf} = \begin{cases} 2L_{outf}\, Gr^{-1/6} & R \leq 1 \\ 2L_{outf}\, Fr^{1/2} & R > 1 \end{cases} \quad (69)$$

If stratification is apparent near $h_{outf}$, either above or below this elevation, then the thickness computed in Eq 69 may not be symmetric about the offtake level (Imberger and Patterson, 1981); therefore the algorithm separately computes the thickness of the withdrawal layer above and below, denoted $\delta_{outf_{top}}$ and $\delta_{outf_{bot}}$, respectively. The Brunt-Väisälä frequency is averaged over the relevant thickness, $N^2_{outf}$, and calculated as:

$$N^2_{outf} = \frac{g}{\delta_{outf}} \frac{\rho_{outf} - \rho_i}{\rho_{outf}} \quad (70)$$

where $\rho_{outf}$ is the density of the layer corresponding to the height of the withdrawal, $i_{outf}$, and $\rho_i$ is the density of the water column at the edge of the withdrawal layer, as determined below. The proportion of water withdrawn from each layer, $Q_{outf_i}$, either above or below the layer of the outlet elevation, requires identification of the upper and lower-most layer indices influenced by the outflow, denoted $i_{top}$ and $i_{bot}$. Once the layer range is defined, $Q_{outf_i}$ is computed for the layers between $i_{outf}$ and $i_{top}$, and $i_{outf}$ and $i_{bot}$, by partitioning the total outflow using a function to calculate the proportion of water withdrawn from any layer that fits the region of water drawn in a given time ($Q_{outf_i} = f\left[f_{outf}\, Q_{outf_x}/c_{secday}, h_i, h_{i-1}, h_{outf}, \delta_{outf_{bot}}, \delta_{outf_{top}}\right]$; see Imberger and Patterson, 1981, Eq 65). Given that users configure any height for a withdrawal outlet and flow rates of variable strength, the upper ($h_{outf} + \delta_{outf_{top}}$) and lower ($h_{outf} - \delta_{outf_{bot}}$) elevation limits computed by the algorithm are limited to the lake surface layer or bottom layer. Once computed, the volumes are removed from the identified layer set, and their height and volumes updated accordingly. $Q_{outf_i}$ is constrained within the model to ensure no more than 90% of a layer can be removed in a single time step. Depending on the



fractional contribution from each of the layers the water is withdrawn from, the water taken will have the associated weighted average of the relevant scalar concentrations (heat, salinity and water quality) which are reported in the outlet file for the particular withdrawal. This routine is repeated for each withdrawal considered, denoted $O$, and the model optionally produces a summary file of all the outflow water and its properties.

### 2.7.4 Adaptive offtake dynamics

For reservoir applications, a special outflow option has been implemented that extends the dynamics in ~~Sect.~~Section 2.6.3 to simulate an adaptive offtake or selective withdrawal. This approach is used for accommodating flexible reservoir withdrawal regimes and their effects on the thermal structure within a reservoir. For this option, a target temperature is specified by the user and GLM ~~estimates~~identifies the corresponding withdrawal height within a predefined (facility) range to meet this target temperature during the runtime of the simulation, i.e., the withdrawal height adaptively follows the thermal stratification in the reservoir. The target temperature can be defined as a constant temperature (e.g., 14 °C) or a time~~-~~ series (via a *.csv file), such as a measured water temperature from an upstream river ~~(via a *.csv file). The~~that could be used to plan environmental releases from the reservoir to the downstream river. The selected height of the adaptive offtake is printed out in a *.txt file ~~and may be used~~ for assisting reservoir operation. In addition to the basic adaptive offtake function, GLM can also simulate withdrawal mixing, i.e., water from the adaptive offtake is mixed with water from another predefined height (e.g., the bottom outlet). For this option, the discharges at both locations need to be predefined by the user (via the standard outflow *.csv ~~file~~files) and GLM chooses the adaptive withdrawal from a height, where the water temperature is such that the resulting mixing temperature meets the target temperature. This withdrawal mixing is a common strategy in reservoir operation where deep water withdrawal and temperature control are required simultaneously to prevent deleterious downstream impacts.

An example of the adaptive offtake function with and without withdrawal mixing, assuming a constant water temperature of 14 °C for the outflow water, shows that GLM is able to deliver a constant outflow temperature of 14 °C during the stratified period (Figure 12). In winter, when the water column is cooler than 14 °C, the model withdraws surface water. The adaptive offtake functionality can be used in a stand-alone mode or ~~coupled~~also linked to the dissolved oxygen concentration (~~via~~when operated with the coupled water quality model AED2, see Section 4). In the latter case, the effect of the withdrawal regime on the oxygen dynamics in the hypolimnion can be simulated (see Weber et al., 2017). In this setting, the simulated hypolimnetic dissolved oxygen concentration at a specified height is checked against a user-defined critical threshold. If the hypolimnetic oxygen falls below the critical threshold, the height of the adaptive offtake will be automatically switched to a defined height (usually deep outlets in order to ~~get rid of~~remove the oxygen-depleted water) to withdraw water from this layer, until the oxygen concentrations have recovered.

~~(a)~~ ~~(b)~~

Geosci. Model Dev. Discuss., https://doi.org/10.5194/gmd-2017-257
Manuscript under review for journal Geosci. Model Dev.
Discussion started: 20 November 2017






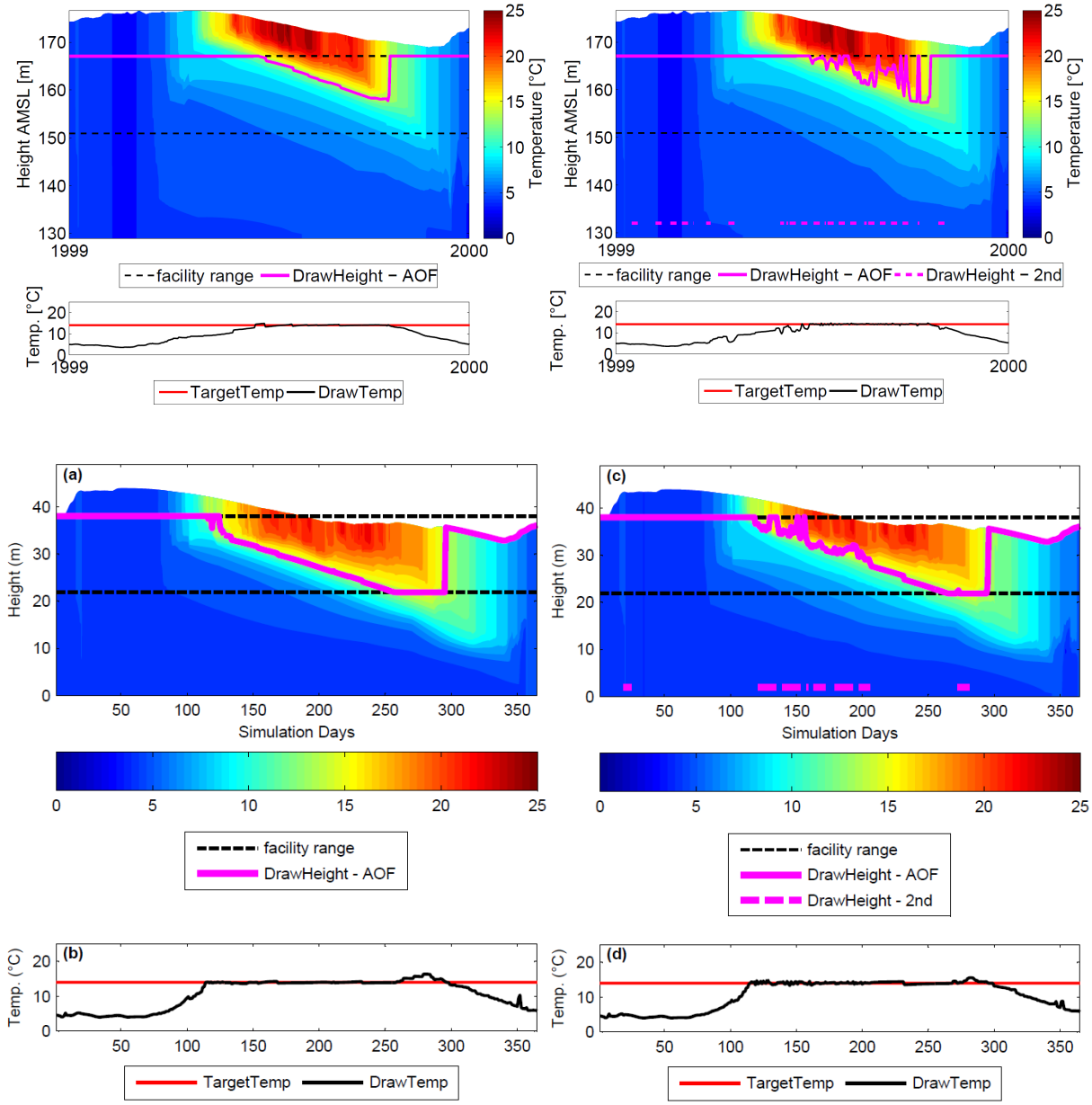


**Figure 12: Adaptive offtake reservoir simulation; water temperatures of the adaptive offtake model assuming a constant target temperature of 14 °C (a,b) without ~~(a)~~ and (c,d) with ~~(b)~~ mixing with the bottom outlet withdrawal. The black dashed line (a,c) represents the height range of the variable withdrawal facility (AOF) and the magenta lines the adaptive offtake and second withdrawal height. Panels (b) and (d) indicate where the actual withdrawal temp (DrawTemp) was able to meet the target (TargetTemp).**

### 2.~~6~~7.5 Seepage

Seepage of water from the ~~bottom layer is~~lake can also be configured~~configurable~~ within the model, for example, as might be required in a wetland simulation or for small reservoirs perched above the water table that experience leakage to the soil below.

Geosci. Model Dev. Discuss., https://doi.org/10.5194/gmd-2017-257
Manuscript under review for journal Geosci. Model Dev.
Discussion started: 20 November 2017






~~Seepage is configured to leave the lake at a constant rate~~The seepage rate, $Q_{seepage}$, can be assumed constant or dependent on the overlying lake head:

$$\frac{dh_B}{dt} = -GQ_{seepage} \qquad (60\,71)$$

$$= \begin{cases} -GA_s/c_{secday}, & \text{Option 1: constant rate} \\ -\left(\frac{K_{seep}}{\Delta z_{soil}}\right) A_s\, h_s/(c_{secday}), & \text{Option 2: Darcy flux based on water height} \end{cases}$$

where ~~$h_B$ is the depth of the bottom-most layer at any time, and~~ $G$ is the seepage rate (m day$^{-1}$~~). $G$~~) and $K_{seep}$ is the soil hydraulic conductivity (m day$^{-1}$) and $\Delta z_{soil}$ is an assumed soil thickness over which the seepage is assumed to occur. The water leaving the lake is treated as a "vertical withdrawal" whereby the water exits via the bottom-most layer(s), and the amount $\Delta V_G = Q_{seepage}\Delta t_d$, is generally all taken from the bottom-most layer ($i = 1$), however, it is constrained within the model to ensure no more than ~~50~~90% of the layer can be reduced in any one time- step~~. Note that in shallow lake or wetland simulations, the layer structure may simplify to a single~~; where $\Delta V_G > 0.9V_{i=1}$ then the routine sequentially loops up through the above layers until enough lake volume has been identified to cover the seepage demand. Once the individual layer~~, in which case the surface and bottom layer~~ volumes are ~~the same, and Eqs. 4 and 60~~incremented due to the seepage flux, $\Delta V_{G_i}$, the heights of all layers ($h_1$: $h_s$) are ~~effectively combined.~~re-computed based on the hypsographic curve using $h_i = f[V_i]$. Where seepage reduces the lake below 0.05 m, the lake becomes dry until new inputs from rain or inflows (e.g., Figure 8a).

### 2.7.6 Overflows

Once the lake volume exceeds the maximum volume, the excess water is assumed to leave the domain as an overflow. The flow rate, $Q_{ovfl}$, is computed based on the interim volume, $V_S^*$, prior to the end of the daily time-step, where $V_S^* = V_S^t + \Delta h_s A_s + \Delta t\left(\sum_I^{N_{INF}} Q_{inf_{0_I}} - \sum_O^{N_{OUT}} Q_{outf_O} - Q_{seepage}\right)$. Users can optionally also specify a crest elevation which sits below the elevation of maximum lake volume, and support a rating curve linking the height of water above the crest level with the overflow volume:

$$Q_{weir} = \begin{cases} 0, & V_S^* \le V_{crest} \\ \frac{2}{3} C_{D_{weir}} \sqrt{2g}\; b\; (h_S^* - h_{crest})^{3/2}, & V_S^* > V_{crest} \end{cases} \qquad (72)$$

where $h_S^*$ is the interim update to the water surface height, $C_{D_{weir}}$ is a coefficient related to the drag of the weir, $b$ is the width of the crest and $h_{crest}$ is the height of the crest level. The overflow rate is then computed as the sum of the flow over the weir crest and the volume of water exceeding the volume of the domain:

$$Q_{ovfl} = \begin{cases} Q_{weir}, & V_S^* \le V_{max} \\ Q_{weir} + (V_S^* - V_{max})/\Delta t_d, & V_S^* > V_{max} \end{cases} \qquad (73)$$

Geosci. Model Dev. Discuss., https://doi.org/10.5194/gmd-2017-257
Manuscript under review for journal Geosci. Model Dev.
Discussion started: 20 November 2017




### 2.8 Wave height and bottom stress

Wind- induced resuspension of sediment from the bed of shallow lakes is sporadic and occurs as the waves ~~created~~ at the water surface create oscillatory currents that propagate down to the lake-bed. GLM does not predict resuspension and sediment concentration directly, but computes the bottom shear stress for later use by sediment and water quality modules. Nonetheless, even without this explicit formulation, the model can identify the areal extent and potential for bed-sediment resuspension by computing the area of the lake over which the bed shear stress exceeds some critical value required for resuspension to occur.

To compute the stress at the lake bottom ~~we estimate~~the model estimates the surface wave conditions using a simple, fetch-based, steady state wave model (Laenen and LeTourneau, 1996; Ji 2008). The wave geometry (wave period, significant wave height and wave length), is predicted based on the wind speed and fetch over which the waves develop (Figure 13~~), calculated as~~). The fetch is approximated from:

$$F = 2\sqrt{A_s/\pi} \qquad (6174)$$

~~Using this model,~~and the wave period, ~~$T$,~~$\delta t_{wave}$, is calculated from fetch as:

$$\cancel{T =}\ \delta t_{wave} = 7.54\left(\frac{\cancel{U_x}}{\cancel{g}}\right)\left(\frac{U_{10}}{g}\right) tanh(\xi)\ tanh\left(\frac{\cancel{0.0379\left[\frac{gF}{U_x^2}\right]^{0.333}}}{\cancel{tanh(\xi)}}\right)\left(\frac{0.0379\left[\frac{gF}{U_{10}^2}\right]^{0.333}}{tanh(\xi)}\right) \qquad (6275)$$

where:

$$\xi = 0.833\frac{\left[\frac{g\cancel{d_{avg}}}{U_x^2}\right]^{\cancel{0.375}}}{}\left[\frac{gz_{avg}}{U_{10}^2}\right]^{0.375} \qquad (6376)$$

and ~~$h_{avg}$~~$z_{avg}$ is the average lake depth. ~~Wave~~The typical wave length is then estimated from:

$$\cancel{L =}\left[\frac{\cancel{gT^2}}{\cancel{2\pi}}\right]\cancel{tanh}\left(\frac{\cancel{2\pi\, d_{avg}}}{\left[\frac{\cancel{gT^2}}{\cancel{2\pi}}\right]}\right)\delta x_{wave} = \left[\frac{g(\delta t_{wave})^2}{2\pi}\right] tanh\left(\frac{2\pi\, z_{avg}}{\left[\frac{g(\delta t_{wave})^2}{2\pi}\right]}\right) \qquad (6477)$$

and the significant wave height from:

$$\cancel{H_s}\delta z_{wave} = 0.283\left(\frac{\cancel{U_x^2}}{\cancel{g}}\right)\left(\frac{U_{10}^2}{g}\right) tanh(\zeta) tanh\left(\frac{\cancel{0.00565\left[\frac{gF}{U_x^2}\right]^{0.5}}}{\cancel{tanh(\zeta)}}\right)\left(\frac{0.00565\left[\frac{gF}{U_{10}^2}\right]^{0.5}}{tanh(\zeta)}\right) \qquad (6578)$$

where

$$\zeta = 0.53\frac{\left[\frac{g\cancel{d_{avg}}}{U_x^2}\right]^{\cancel{0.75}}}{}\left[\frac{gz_{avg}}{U_{10}^2}\right]^{0.75} \qquad (6679)$$

Based on these properties the orbital wave velocity at depth (in the $i^{th}$ layer) is calculated as:

Geosci. Model Dev. Discuss., https://doi.org/10.5194/gmd-2017-257
Manuscript under review for journal Geosci. Model Dev.
Discussion started: 20 November 2017




$$U_{orb_i} = \frac{\pi H_s}{T \sinh\left[\frac{2\pi d_i}{L}\right]} \frac{\pi\, \delta z_{wave}}{\delta t_{wave}\, \sinh\left[\frac{2\pi\, z_{i-1}}{\delta x_{wave}}\right]} \quad (6780)$$

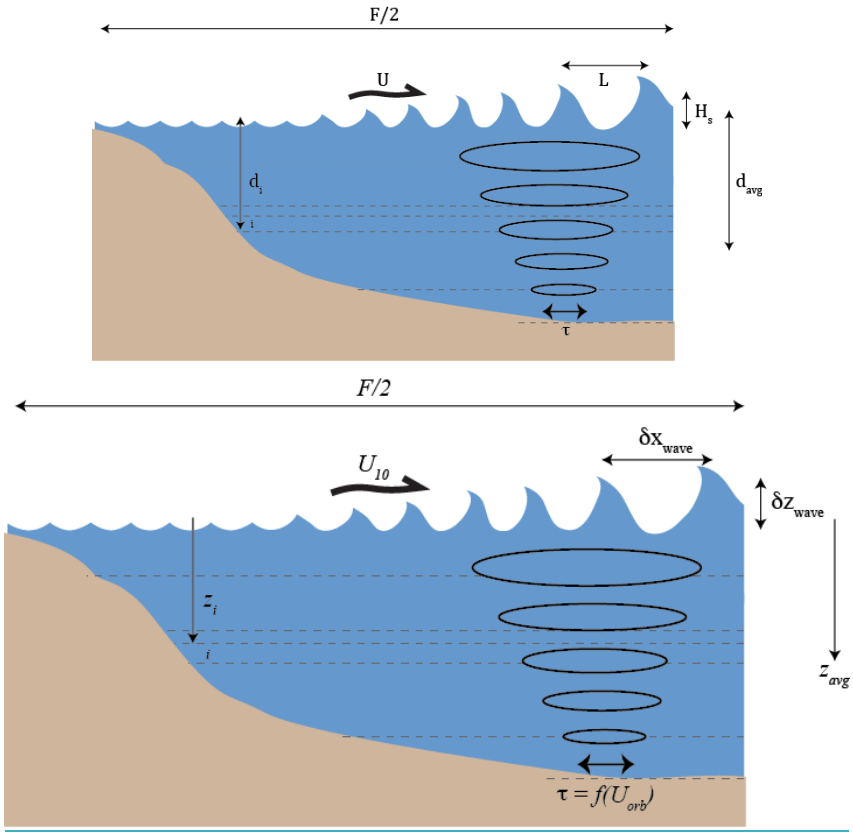


**Figure 13: Schematic of the wave estimation approach depicting the lake fetch, surface wind speed, wave height ~~and~~, wavelength~~,~~ and bottom stress created by the orbital velocity.**

~~The~~ For each layer, the total shear stress experienced at the lake bed portion of that layer (equivalent in area to $A_i - A_{i-1}$) is calculated ~~as~~from:

$$\tau_i = \frac{1}{2} \rho_w \left[ f_w\, U_{orb_i}^{\ 2} + f_c\, U_{m_i}^{\ 2} \right] \rho_i \left[ f_w\, U_{orb_i}^{\ 2} + f_c\, U_{m_i}^{\ 2} \right] \quad (6881)$$

where $U_m$ is the mean layer velocity ~~of~~, which for simplicity is assumed based on the ~~layer, computed~~velocity estimate made during the mixing calculations (Eq. ~~33). The friction factors use $D$ (a typical particle diameter). For~~40) in the ~~current stress we compute $f_w = 0.24/\log(12 d_{avg}/2.5D)$ and for waves:~~surface mixed layer, such that:

$$f_w = \exp\left[-5.977 + 5.213\left(\frac{a}{2.5D}\right)^{-0.19}\right] \quad \text{Option 1 : Laenen and LeTourneau, 1996} \quad (6982)$$

$$f_w = 0.00251 \exp\left[5.213\left(\frac{U_{orb}\, T}{4\pi D}\right)^{-0.19}\right] \quad \text{Option 3 : Kleinhans \& Grasmeijer (2006)}$$

Geosci. Model Dev. Discuss., https://doi.org/10.5194/gmd-2017-257
Manuscript under review for journal Geosci. Model Dev.
Discussion started: 20 November 2017




~~$f_w = \frac{2\beta g \rho_B D}{U^2 \rho_w}$~~ ~~Option 3 : Le Roux (2007)~~ $U_{m_i} = \begin{cases} u_*, & i \geq k \\ 0, & i < k \end{cases}$

~~Figure 14 demonstrates wave-related outputs from a shallow lake.~~

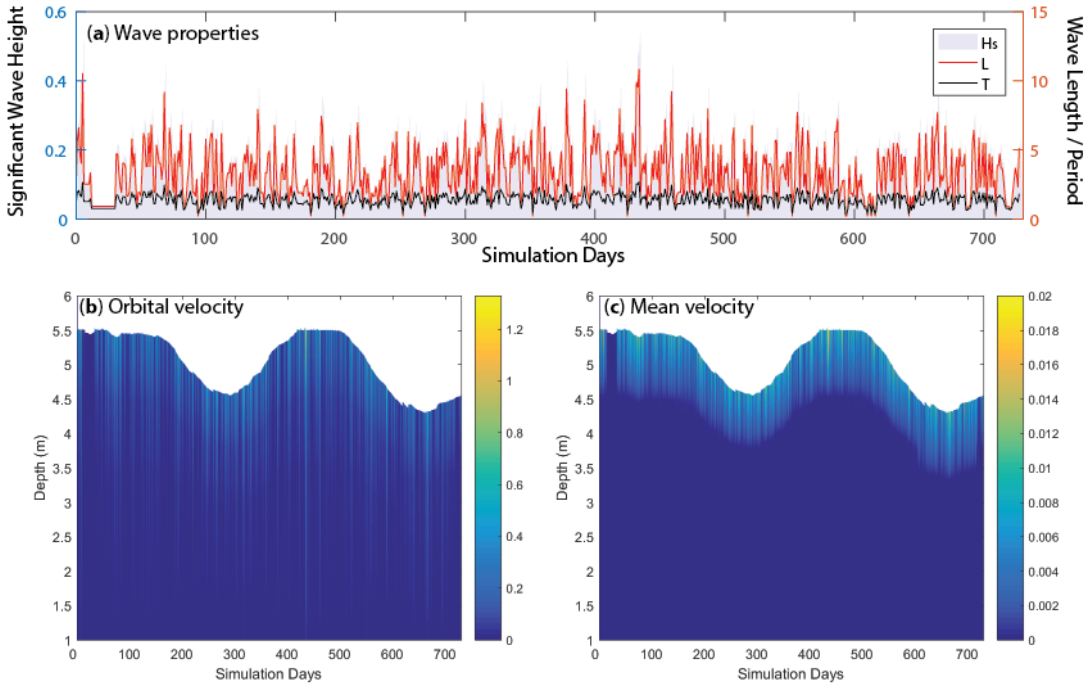


The friction factors depend upon the characteristic particle diameter of the lake bottom sediments, $\delta_{ss}$ and the fluid velocity. For the current induced stress, we compute $f_c = 0.24/\log\left(12z_{avg}/2.5\delta_{ss_{z_i}}\right)$, and for waves (Kleinhans and Grasmeijer, 2006):

$$f_w = \exp\left[-5.977 + 5.213\left(\frac{U_{orb_i}\ \delta t_{wave}}{5\pi\ \delta_{ss_{z_i}}}\right)^{-0.194}\right] \quad (83)$$

where $\delta_{ss_{z_i}}$ is specific for each layer $i$, depending on which sediment zone it overlays (see Section 4). The current and wave induced stresses at the lake bottom manifest differently within the lake, as demonstrated in Figure 14 for a shallow lake.

Geosci. Model Dev. Discuss., https://doi.org/10.5194/gmd-2017-257
Manuscript under review for journal Geosci. Model Dev.
Discussion started: 20 November 2017


Geoscientific Model Development Discussions
Open Access
EGU

Revision 8 Mar 2018

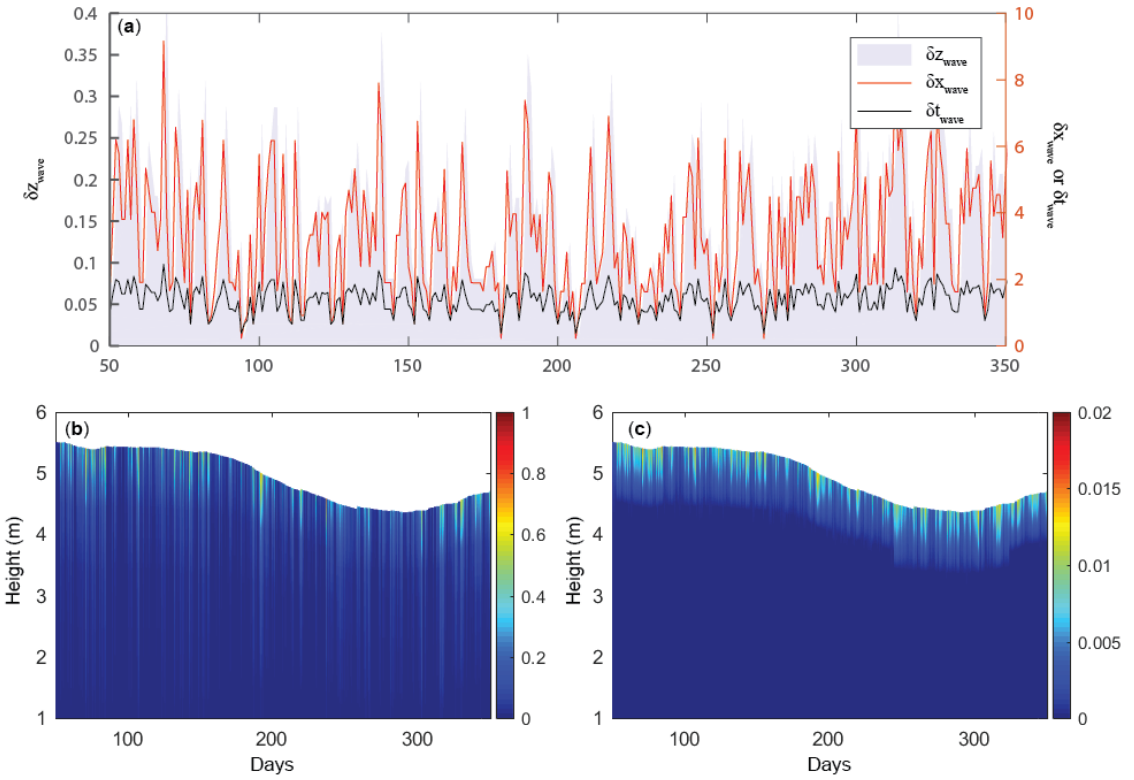


**Figure 14: Simulation from Woods Lake, Australia, showing a) time- series of surface wave properties (Hs~~,~~ = $\delta z_{wave}$, L= $\delta x_{wave}$ and T~~),~~= $\delta t_{wave}$), b) orbital velocity, $U_{orb}$, ~~changes over time~~ (m/ s$^{-1}$), and c) comparison with the layer mean ~~velocity~~velocities, $U_m$ (m/ s$^{-1}$).**

## 3 Code organization and model operation

Aside from the core water balance and mixing functionality, the model features numerous options and extensions in order to make it a fast and easy-to-use package suitable for a wide range of contemporary applications. Accommodating these requirements has led to the modular code structure outlined in Figure 15. The model is written in C, with a Fortran-based interface module to link with Fortran-based water quality modelling libraries described in ~~Sect.~~Section 4. The model compiles with gcc, and gfortran, and commercial compilers, with support for Windows, OS X and Linux.

Geosci. Model Dev. Discuss., https://doi.org/10.5194/gmd-2017-257
Manuscript under review for journal Geosci. Model Dev.
Discussion started: 20 November 2017




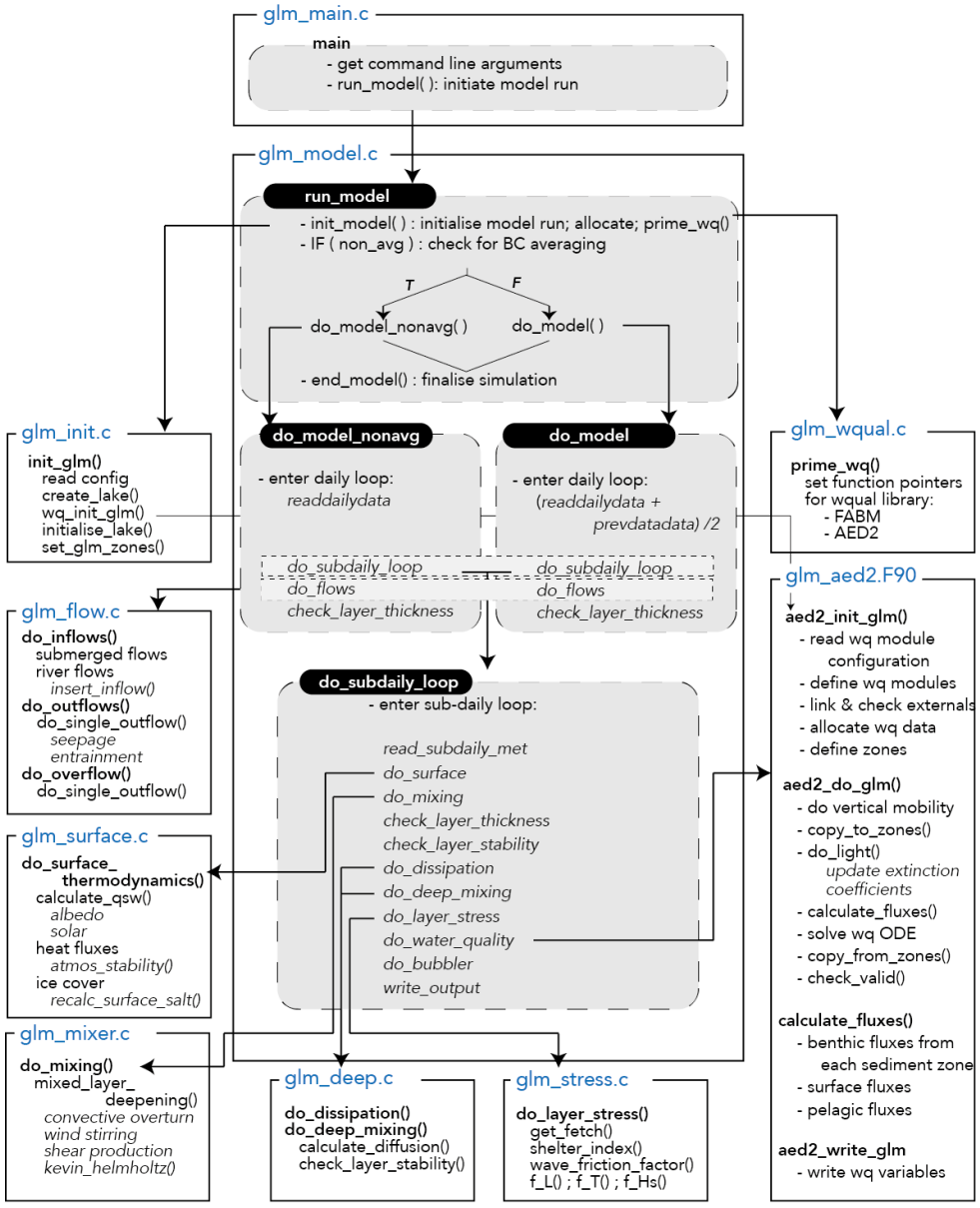


**Figure 15: GLM code structure and logic flow. Each module is depicted as a box with the main routines and functions summarised.**

The model may also be compiled as a library, termed libGLM, that can be called as a plugin into other models (e.g., see Section 5.4). Whilst the model is not object-oriented, users may easily customise specific modules described in Section 2 by adding or extending options for alternate schemes or functions.

To facilitate the use of the model in teaching environments and for users with limited technical support, ~~the model~~iti may be operated without any third party software, as the input files consist of "namelist" (`nml`) text files for configuration and csv files for meteorological and flow time- series data (Figure 16). The outputs from predictions are stored into a structured ~~netcdf~~netCDF file, ~~and this~~which can be visualised in real-time through the simple inbuilt plotting library (libplot~~),~~) or may be



opened for post-processing in MATLAB, R, or ~~R~~any other tool supporting the open netCDF format (see ~~Sect.~~Section 5.1). Parameters and configuration details are input through the main `glm.nml` text file (Figure 16) and default parameters and their associated ~~description~~descriptions are outlined in Table 1.

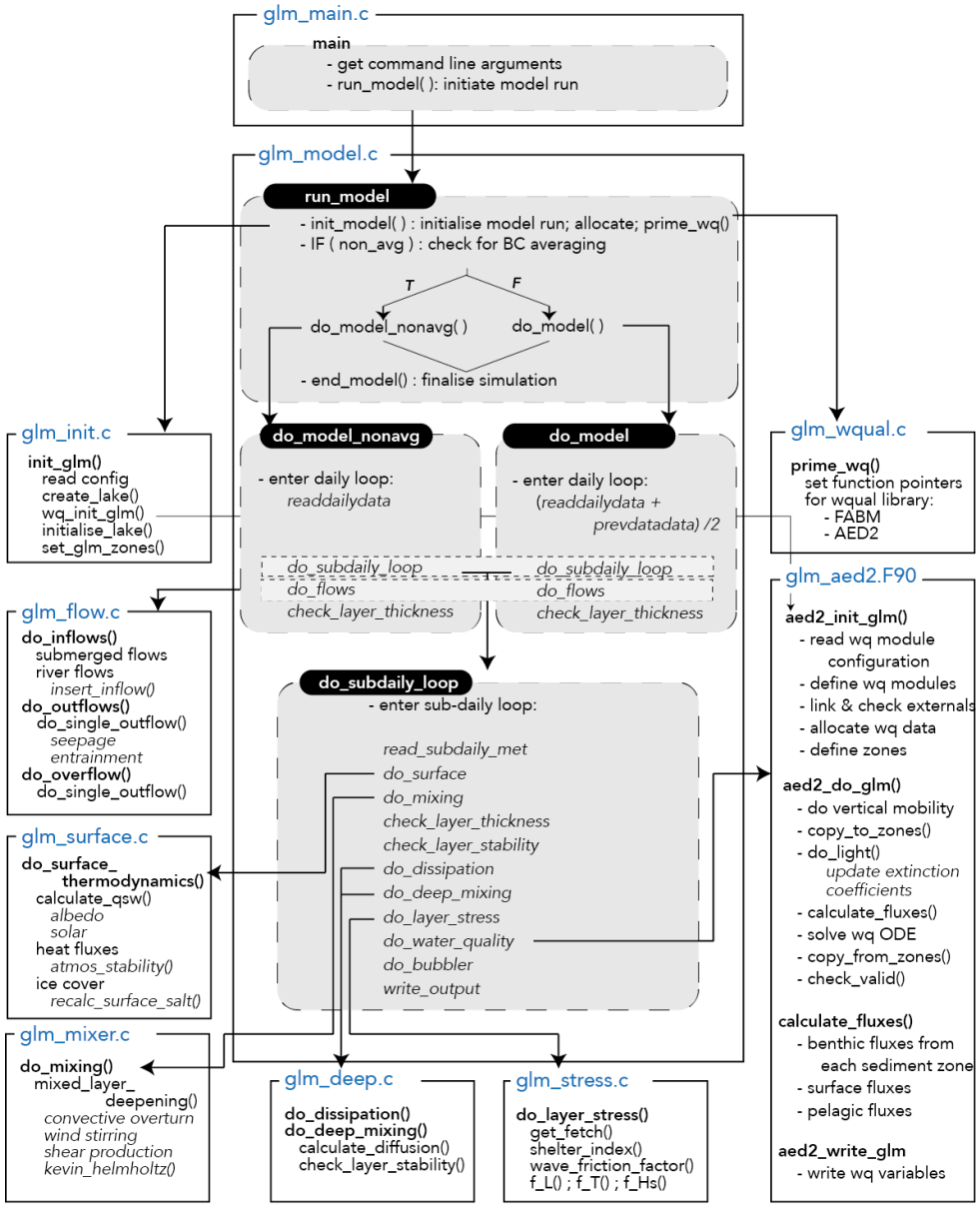


~~Figure 15: GLM code structure and logic flow. Each module is depicted as a box with the main routines and functions summarised.~~

Geosci. Model Dev. Discuss., https://doi.org/10.5194/gmd-2017-257
Manuscript under review for journal Geosci. Model Dev.
Discussion started: 20 November 2017






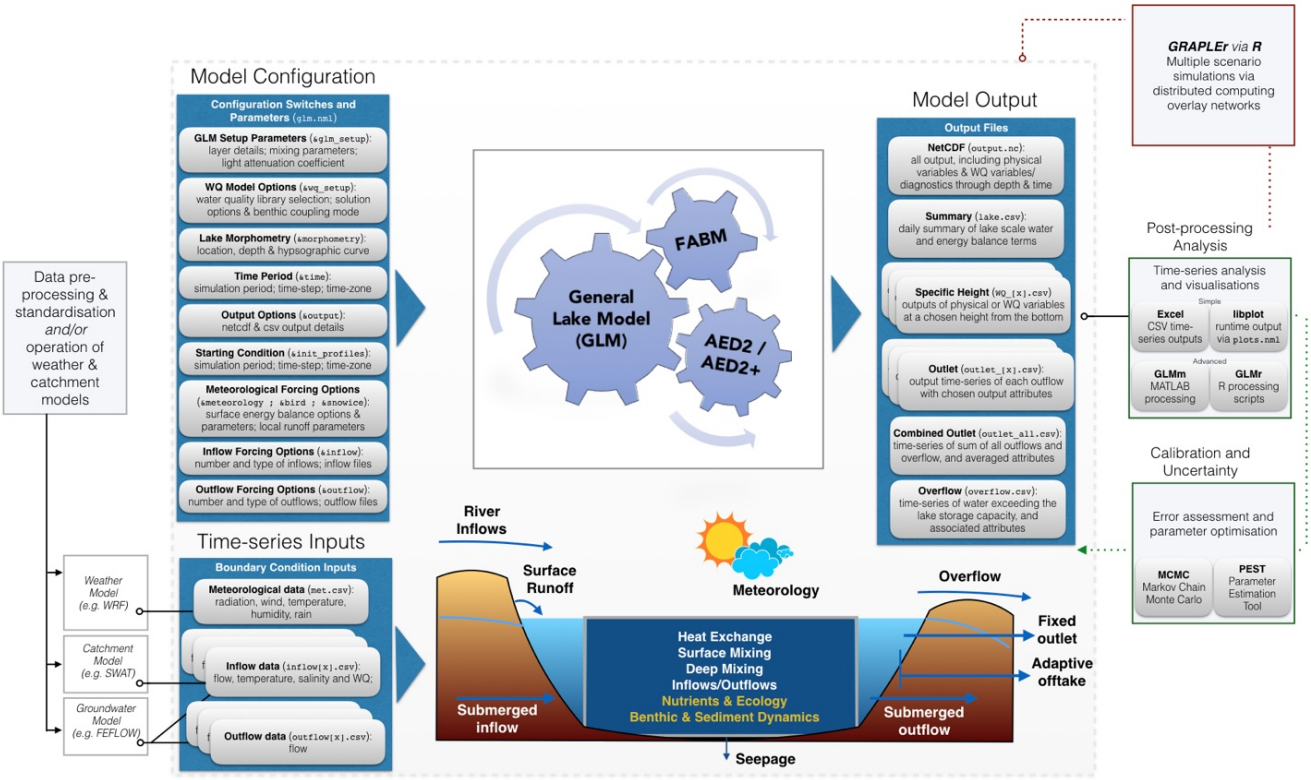

Geosci. Model Dev. Discuss., https://doi.org/10.5194/gmd-2017-257
Manuscript under review for journal Geosci. Model Dev.
Discussion started: 20 November 2017


Geoscientific Model Development Discussions
Open Access
EGU



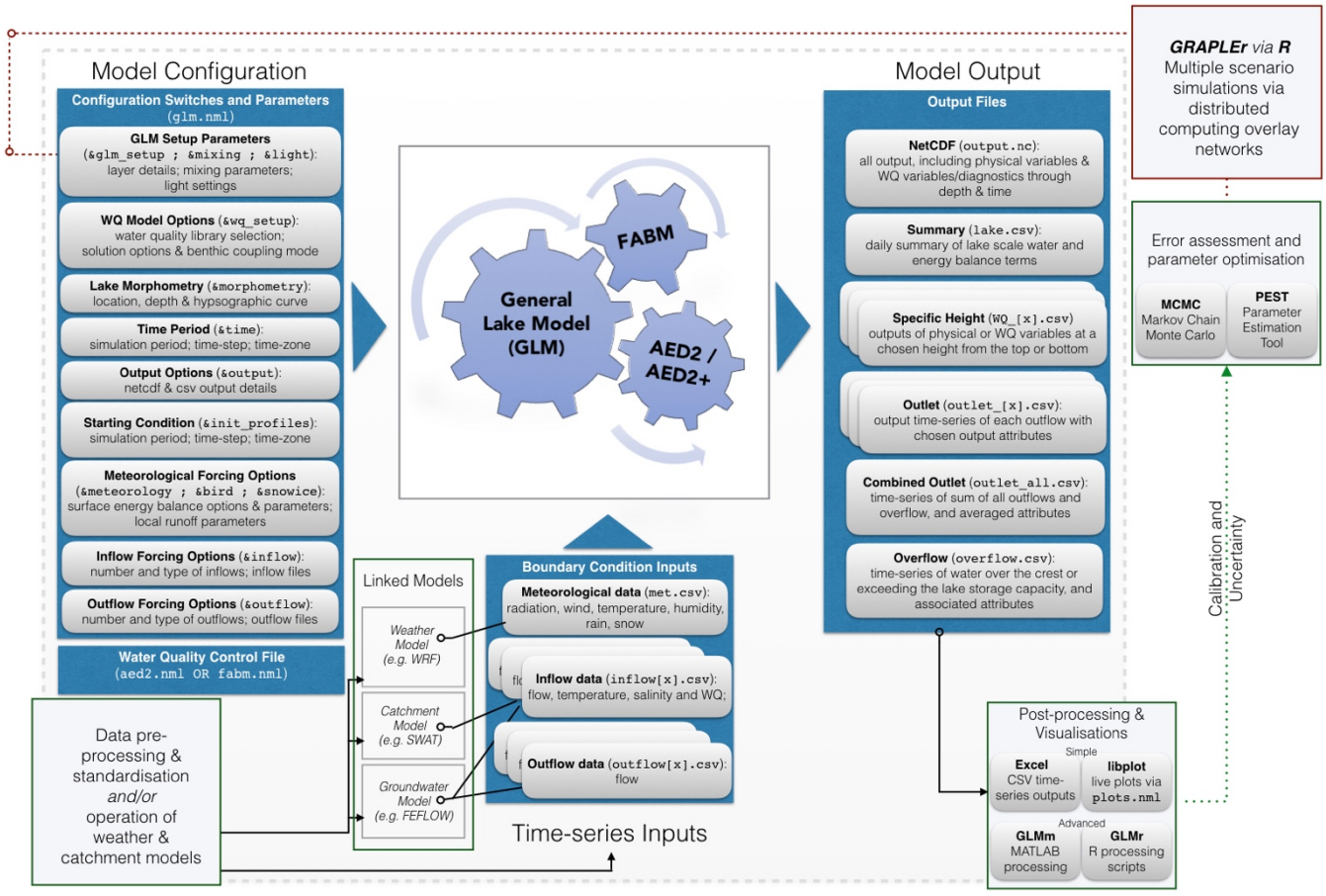


**Figure 16: Flow diagram showing the input information required for operation of the model, ~~and~~the outputs, and analysis pathways.**

## 4 Dynamic coupling with biogeochemical and ecological model libraries

Beyond modelling the vertical temperature distribution, the water, ice and heat balance, as well as the transport and mixing in a lake, the model has been designed to couple with biogeochemical and ecological model libraries. Currently the model is distributed pre-linked with the AED2 simulation library (Hipsey et al., 2013) and the Framework for Aquatic Biogeochemical Models (FABM; Bruggeman and Bolding, 2014). Through connection with these libraries, GLM can simulate the seasonal changes in vertical profiles of turbidity, oxygen, nutrients, phytoplankton, zooplankton, pathogens and other water quality variables of interest. Documentation of these models is beyond the scope of the present paper, however, two features are highlighted here as being relevant to managing physical-ecological interactions.

Firstly, the model is designed to allow a user- defined number of sediment zones that span the depth of the lake. Using this approach, the current setup allows for depth-dependent sediment properties, both for physical properties such as roughness or sediment heat flux, (as outlined in previous sections), and also biogeochemical properties such as sediment nutrient fluxes and



benthic ecological interactions. Since the GLM layer structure is flexible over time (i.e., layer depths are not fixed), any interactions between the water and sediment/benthos must be managed at each time-_step. The model therefore supports disaggregation and/or aggregation of layer properties, for mapping individual water layers to one or more sediment zones (Figure 17). The weightings provided by each layer to the sediment are based on the relative depth overlap of a layer with the depth range of the sediment zone. This approach makes the model suitable for long-term assessments of wetland, lake and reservoir biogeochemical budgets, including for C, N and other attribute balances as required (Stepanenko et al., 2016).

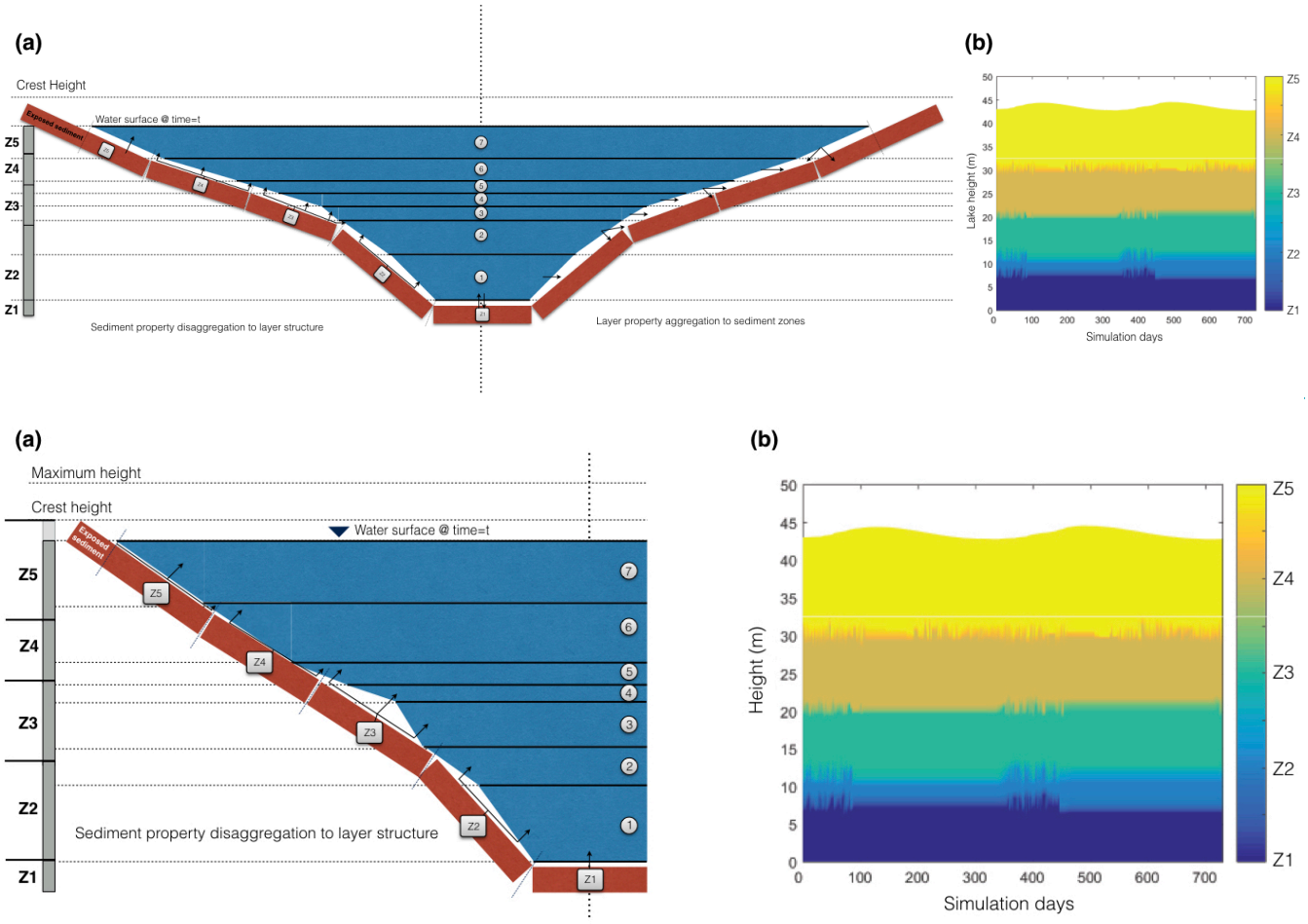


**Figure 17: a) Schematic of a lake model layer structure (indicated by layers 1-7), in conjunction with five sediment "zones" (Z1-Z5) activated when `benthic_mode` = 2. The dynamically varying layer structure is re-mapped to the fixed sediment zone locations at each time step in order for the sediment zone to receive the average overlying water properties, and for the water to receive the appropriate information from benthic/sediment variables. b) example of GLM output showing the sediment zone each water layer is mapped to.**

Secondly, the water quality modules feed back to GLM properties related to the water and/or heat balance. Feedback options include water density additions, bottom ~~drag~~friction, $f_w$, the light attenuation coefficient, $K_w$, solar shading $f_{SR}$, and rainfall interception, $f_R$.

Geosci. Model Dev. Discuss., https://doi.org/10.5194/gmd-2017-257
Manuscript under review for journal Geosci. Model Dev.
Discussion started: 20 November 2017


Geoscientific Model Development Discussions



## 5 Workflow tools for integrating GLM with sensor data and supporting models

The GLM model has been designed to support integration of large volumes of data coming from instrumented lakes, including many GLEON sites ~~(cite ref, e.g., Weathers, Hanson, etc.).~~ These data consist of high-frequency and discrete time~~-~~ series observations of hydrologic fluxes, meteorology, temperature, and water quality (e.g., Hamilton et al. 2014). To facilitate research that requires running the model using these data sources, we have created GLM interfaces in the R and MATLAB analysis environments. These tools support user-friendly access to the model and include routines that streamline the process of calibrating models or running various scenarios. ~~-~~In addition, for assessment of lake dynamics in response to catchment or climatic forcing, it is desirable to be able to connect GLM with other model platforms associated with surface and groundwater simulation, and weather prediction (Read et al., 2016).

### 5.1 R and MATLAB libraries for model setup and post-processing

The R and MATLAB scientific languages are commonly used in aquatic research, often as part of automated modelling and analysis workflows. GLM has a client library for both, and these tools are shared freely online. The R package is called "`glmtools`" (https://github.com/~~GLEON~~USGS-R/glmtools) and the MATLAB library is called "`GLMm`" (https://github.com/AquaticEcoDynamics/GLMm). Both tools have utilities for model output pre- and post-processing. The pre-processing components can be used to format and modify data inputs and configuration files, and define options for how GLM executes. Post-processing tools include visualizations of simulation results (as shown in the results figures above), comparisons to field observations, and various evaluations of model performance.

### 5.2 Utilities for assessing model performance, parameter identification and uncertainty analysis

In order to compare the performance of the model for ~~varied~~various types of lakes, numerous ~~different~~ metrics of model performance are relevant. These include simple measures like surface or bottom temperature, or ice thickness~~, however, it~~. It is also possible to ~~compare~~assess the model's performance in capturing higher-order metrics relevant to lake dynamics, including Schmidt Stability, thermocline depth, ice on/off dates (see also Bruce et al., ~~2017~~2018, for a detailed assessment of the model's accuracy across a wide diversity of lakes across the globe). With particular interest in the model's ability to interface with high frequency sensor data for calculation of key lake stability metrics (Read et al., 2011), ~~then~~ continuous wavelet transform comparisons are also possible (Kara et al., 2012), allowing assessment of the time~~-~~ scales over which the model is able to capture the observed variability within the data.

As part of the modelling process, it is common to adjust parameters to get the best fit with available field data and, as such, the use of a Bayesian Hierarchical Framework in the aquatic ecosystem modelling community has become increasingly useful (e.g., Zhang and Arhonditsis, 2009; Romarheim et al., 2015). Many parameters described throughout ~~Sect.~~Section 2 are attempts at physically based descriptions where there is relatively little variation (Bruce et al., ~~2017~~2018), thereby reducing the number of parameters that remain uncertain. For others, however, ~~for others~~ their variation reflects imperfect formulation of some processes that are not ~~fully considered~~completely described numerically. Therefore, within MATLAB, support scripts for GLM to work with the Markov Chain Monte Carlo (MCMC) code outlined in Haario et al. (2006) can be used to provide

Geosci. Model Dev. Discuss., https://doi.org/10.5194/gmd-2017-257
Manuscript under review for journal Geosci. Model Dev.
Discussion started: 20 November 2017




improved parameter estimates and uncertainty assessment (Figure 18). ~~Wrappers and examples~~Example setups for use of GLM within the ~~openDA framework and~~ PEST ~~are~~(Parameter Estimation Tool) have also ~~being tested~~been developed, giving users access to a wide range of ~~uncertainty~~ assessment ~~and data assimilation algorithms.~~methodologies. The PEST framework allows for calibration of complex ~~model~~models using highly-parameterised regularisation with pilot-points (Doherty, 2015~~), and sensitivity~~). Sensitivity matrices derived from the calibration process can also be utilised in linear and non-linear uncertainty analysis.

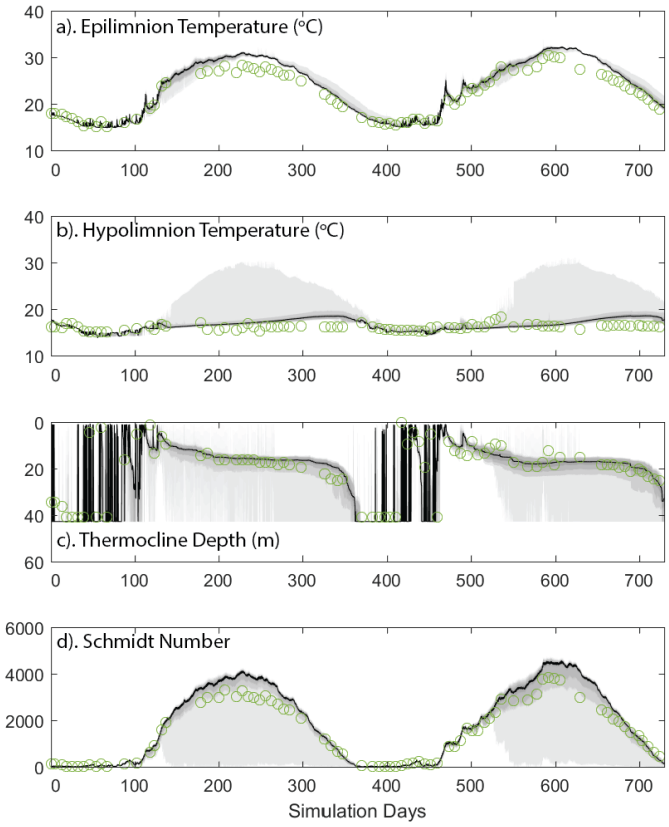


**Figure 18: Depiction of parameter uncertainty for a GLM simulation of Lake Kinneret, Israel, following calibration against observations (green circles) via MCMC for a) epilimnion temperature, b) hypolimnion temperature, c) thermocline depth, and d) Schmidt number. The black line indicates the ~~mean~~50th-percentile likelihood of the prediction, and the grey bands depict the 40$^{th}$, 60$^{th}$ and 80$^{th}$ percentile.**

### 5.3 Operation in the cloud: GRAPLEr

Questions relevant to land use and climate change are driving scientists to develop numerous scenarios for how lake ~~ecosystem services~~ecosystems might respond to changing exogenous drivers. An important approach to addressing these questions is to simulate lake or reservoir physical-biological interactions in response to changing hydrology, nutrient loads or meteorology, and then infer consequences from the emergent properties of the simulation, such as changes in water clarity, extent of anoxia,



mixing regime, or habitability to fishes (Hipsey et al., 2015). Often, it takes years or even decades for lakes to respond fully to changes in exogenous drivers, requiring simulations to recreate lake behavior over extended periods. While most desktop computers can run a decade-long, low-resolution simulation in less than one minute, high-resolution simulations of the same extent may require minutes to hours of processor time. When questions demand hundreds, thousands or even millions of simulations, the desktop approach is no longer suitable.

Through access to distributed computing resources, modellers can run thousands of GLM simulations in the time it takes to run a few simulations on a desktop computer. Collaborations between computer scientists in the Pacific Rim Applications and Grid Middleware Assembly (PRAGMA) and GLEON have led to the development of GRAPLEr (GLEON Research and PRAGMA Lake Expedition in R), software, written in R, that enables modellers to distribute batches of GLM simulations to pools of computers (Subratie et al., 2017). Modellers use GRAPLEr in two ways: by submitting a single simulation to the GRAPLEr Web service, along with instructions for running that simulation under different climate scenarios, or by configuring many simulations on the user's desktop computer, and then submitting them as a batch to the Web service. The first approach provides a high degree of automation that is well suited to training and instruction, and the second approach has the full flexibility often needed for research projects. In all approaches, GRAPLEr converts the submitted job to a script that is used by the scheduling program HTCondor (Thain et al., 2005) to distribute and manage jobs among the computer pool and ensure that all simulations run and return results. An iPOP overlay network (Ganguly et al., 2006) allows the compute services to include resources from multiple institutions, as well as cloud computing services.

GRAPLEr's Web service front-end shields the modeller from the compute environment, greatly reducing the need for modellers to understand distributed computing; they therefore only need to install the R package, know the URL of the GRAPLEr Web service, and decide how the simulations should be setup.

### 5.4 Integration with catchment and climate models

GLM simulations may be coupled with catchment models, such as the Soil Water Assessment Tool (SWAT) or similar catchment models, simply by converting the catchment model output into the inflow file format via conversion scripts. Similarly, scripts exist for coupling GLM with the Weather Research Forecasting (WRF) model, or similar climate models, for specification of the meteorological input file from weather prediction simulations.

The above coupling approaches require the models to be run in sequence~~, however, for~~. For the simulation of lake-wetland-groundwater systems, however, two-way coupling is required to account for the flow of water into and out of the lake throughout the simulation. For these applications, the interaction can be simulated using GLM coupled with the 3D groundwater flow model, FEFLOW (https://www.mikepoweredbydhi.com/products/feflow). For this case, the GLM code is compiled as a Dynamic Link Library (DLL) termed libGLM and loaded into FEFLOW as a plug-in module. The coupling between GLM and FEFLOW is implemented using a one-step lag between the respective solutions of the groundwater and

lake models. This approach, in most simulations, does not introduce a significant error, however, error can be assessed and reduced using smaller time step lengths. ~~FEFLOW models can be simulated for flow only, or including heat and/or solute transport. Depending on the simulation mode, GLM accounts for the different process variables, assigning boundaries for lake level, salinity and temperature accordingly.~~

The GLM module was designed to accommodate situations of variable lake geometry, by using a dry-lake/wet-lake approach. In this approach, dry-lake areas are defined as those above the current lake level and wet-lake areas as below the current lake level. Different boundary types in FEFLOW are assigned to dry-lake and wet-lake areas (Figure 19). The calibration of such coupled models is often complex, given the large number of parameters and sensitivities when different sources of information are utilised (for example flow and water level measurements). The FEFLOW-GLM coupling structure allows for a relatively straightforward integration with PEST (Doherty, 2015), based on existing FEFLOW workflows.

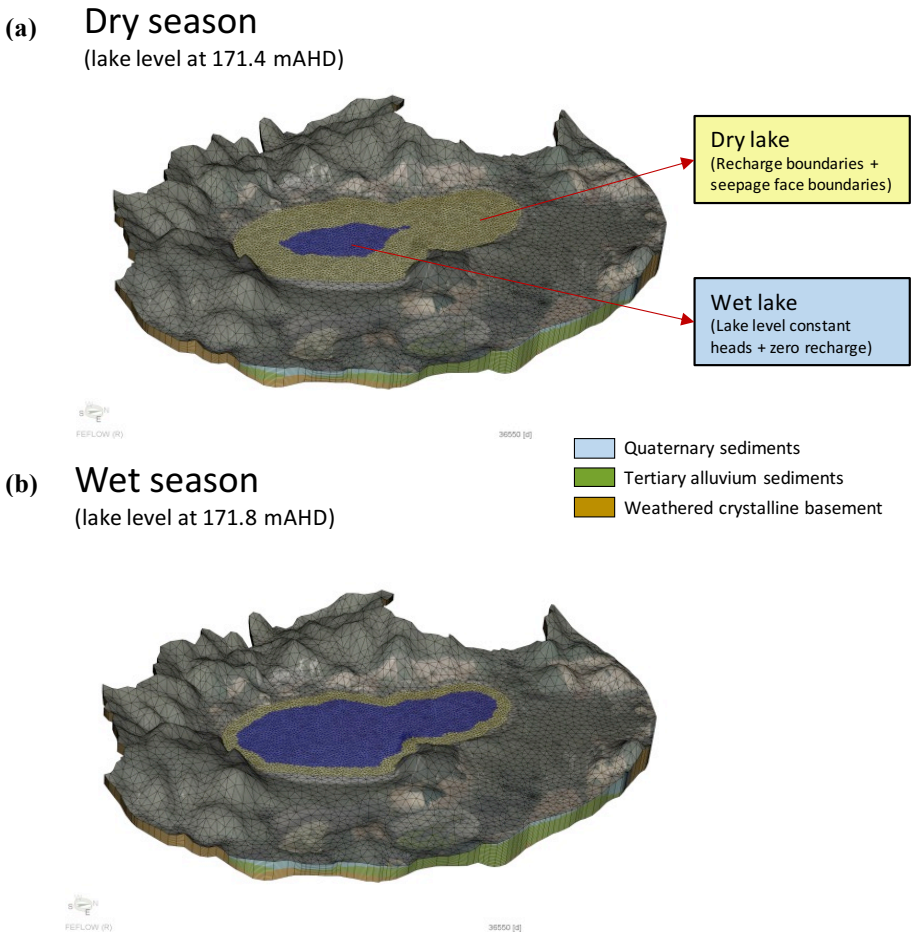


**Figure 19: Example of lake boundary changes during wet and dry cycles from Lake Muir, Australia. GLM water level is communicated to FEFLOW to each time- step and used as a constant head boundary condition for all wet cells.**

Geosci. Model Dev. Discuss., https://doi.org/10.5194/gmd-2017-257
Manuscript under review for journal Geosci. Model Dev.
Discussion started: 20 November 2017




## 6 GLM as a tool for teaching environmental science and ecology

Environmental modelling is integral for understanding complex ecosystem responses to anthropogenic and natural drivers, and also provides a valuable tool for engaging students learning environmental science (Carey and Gougis, 2017). Previous pedagogical studies have demonstrated that engaging students in modelling provides cognitive benefits, enabling them to build new scientific knowledge and conceptual ~~development~~understanding (Stewart et al., 2005; Zohar and Dori 2011). For example, modelling forces students to analyze patterns in data, create evidence-based hypotheses for those patterns and make their hypotheses explicit, and develop predictions of future conditions (Stewart et al., 2005). As a result, the U.S. National Research Council has recently integrated modelling into the *Next Generation Science Standards*, which provide recommendations for primary and secondary school science pedagogy in the United States (NRC, 2013). However, it remains rare for undergraduate and graduate science courses to include the computer-based modelling that environmental scientists need to manage natural ecosystems.

A teaching module for the use of GLM within undergraduate and graduate classrooms has been developed to explore lake responses to climate change (Carey and Gougis, 2017). The GLM module, called the "Climate Change Effects on Lake Temperatures", teaches students how to set up a simulation for a model lake within R. After they are able to successfully run their lake simulations, they force the simulation with climate scenarios of their own design to examine how lakes may change in the future. To improve computational efficiency, students also learn how to submit, retrieve, and analyze hundreds of model simulations through distributed computing overlay networks embedded via the GRAPLEr interface~~, described above.~~ (Section 5.3). Hence, students participating in the module learn computing and quantitative skills in addition to improving their understanding of how climate change ~~is affecting~~affects lake ecosystems.

Initial experiences teaching GLM as well as pre- and post-assessments indicate that participation in the module improves students' understanding of lake responses to climate change (Carey and Gougis, 2017). By modifying GLM boundary condition data and exploring model output, students are able to better understand the processes that control lake responses to altered climate, and improve their predictions of future lake change. Moreover, the module exposes students to computing and modelling tools not commonly experienced in most university classrooms, building competence with manipulating data files, scripting, creating figures and other visualizations, and statistical and time series analysis; all skills that are transferrable for many other applications. ~~Thus, following previous studies (Schwarz and White 2005, Schwarz et al. 2009), we predict that increased experience with GLM modelling will not only build students' understanding of lake ecosystem concepts but also their ability to interpret natural phenomena and generate new scientific knowledge.~~

## 7 Conclusions

As part of GLEON activities, the emergence of complex questions about how different lake types across the world are responding to climate change and land-use change has created the need for a robust, accessible community code suitable for a diverse range of lake types and simulation contexts. Here, GLM is presented as a tool that meets many of the needs of network



participants for their individual lake simulation requirements, in addition to being suitable for application in a distributed way across tens to thousands of lakes for regional and global scale assessments. Recent examples include an application of the model for assessing how the diversity of >2000 lakes in the lake-rich landscape in Wisconsin respond to ~~meteorological conditions and~~climate including projected warming (Read et al., 2014~~), and given~~; Winslow et al., 2017). Given its computationally efficient nature, it is envisioned ~~to~~that GLM can be made available as a library for use within in land-surface models (e.g., the Community Land Model, CLM), allowing improved representation of lake dynamics in regional hydrological or climate assessments. With further advances in the degree of resolution and scope of earth system models, we further envisage GLM as an option suitable to be embedded within these models to better allow the simulation of lake stratification, air-water interaction of momentum and heat, and also biogeochemically relevant variables associated with contemporary questions about greenhouse gases emissions such as $CO_2$, $CH_4$, and $N_2O$.

Since the model is one-dimensional, it assumes no horizontal variability in the simulated water layers and users must therefore ensure their application of the model is suited to this simplifying assumption. For stratified systems, the parameterization of mixing due to internal wave and inflow intrusion dynamics is relatively simple, making the model ideally suited to longer-term investigations ranging from weeks to decades (depending on the domain size), and for coupling with biogeochemical models to explore the role that stratification and vertical mixing play on lake ecosystem dynamics. However, the model can also be used for shallow lakes, ponds and wetland environments where the water column is relatively well mixed. ~~In order to better define the typical level of model performance across these diverse lake types, a companion paper by Bruce et al. (2017), has undertaken a systematic assessment of the model's error structure against 31 lakes from across GLEON, to which readers can refer to for further guidance.~~ In cases where the assumption of one-dimensionality is not met for a particular lake application, ~~then it is possible for users to apply~~a two or three dimensional ~~models; potentially these can~~model may be ~~temporally nested within a longer term GLM simulation~~preferred.

This paper has focused on description of the hydrodynamic model, but we highlight that the model is a platform for coupling with advanced biogeochemical and ecological simulation libraries for water quality prediction and integrated ecosystem assessments. As with most coupled hydrodynamic-ecological modelling platforms, GLM handles the boundary conditions and transport of variables simulated within these libraries, including the effects of inflows, vertical mixing, and evapo-concentration. Whilst the interface to these libraries is straightforward, the Lagrangian approach adopted within GLM for simulation of the water column necessitates the adoption of sediment zones on a static grid that is independent from the water column numerical grid.

More advanced workflows for operation of the model within distributed computing environments and with data assimilation algorithms is an important application when used within GLEON capabilities related to high frequency data and its interpretation. The 1D nature of the model makes the run-times modest and therefore the model ~~is~~ suitable for application within more intensive parameter identification and uncertainty assessment procedures. This is particularly relevant as the needs for network participants to expand model configurations to further include biogeochemical and ecological state variables. It is



envisioned that continued application of the model ~~to lakes of GLEON~~ will allow us to improve parameter estimates and ranges, and this will ultimately support other users of the model in identifying parameter values, and assigning parameter prior distributions. Since many of the users the model is intended for may not have access to the necessary cyberinfrastructure, the use of GLM with the open-source GRAPLEr software in the R environment provides access to otherwise unavailable distributed computing resources. This has the potential to allow non-expert modellers within the science community to apply good modelling practices by automating boundary condition and parameter sensitivity assessments, with technical aspects of simulation management abstracted from the user.

Finally, the role of models in informing and educating members of the network and the next generation of hydrologic and ecosystem modellers has been identified as a critical element of synthesis activities and supporting cross-disciplinary collaboration (Weathers et al., 2017). Initial use of GLM within the classroom has found that teaching modules integrating GLM into classes improves students' understanding of ~~how climate change is altering~~ lake ecosystems.

**Code availability**

The GLM code is provided as open-source under the GNU GPL3 license, and version controlled via the GitHub repository: https://github.com/AquaticEcoDynamics/GLM. *[Code DOI to be inserted here on final acceptance]*

**Data availability**

The five example lakes used to demonstrate the model operation are described along with model input files (and associated hydrologic and meteorological forcing data) within the GitHub repository:
https://github.com/AquaticEcoDynamics/GLM/tree/master/Examples/2.4.0
*[Examples DOI to be inserted here on final acceptance]*

**Acknowledgments**

The primary code of GLM has been developed by MH, LB, CB, BB and DH at The University of Western Australia in collaboration with researchers participating in GLEON ~~and benefited directly from~~, with support provided by ~~the~~ a National Science Foundation (NSF) (USA) Research Coordination Network Award. Whilst GLM is a new code, it is based on the large body of historical research and publications produced by the Centre for Water Research at the University of Western Australia, which we acknowledge for the inspiration, development and testing of several of the model algorithms that have been adopted. Funding for initial development of the GLM code was from the U.S. NSF Cyber-enabled Discovery and Innovation grant awarded to PH (lead investigator) and colleagues from 2009-2014 (NSF CDI-0941510), and subsequent development was supported by the Australian Research Council projects awarded to MH and colleagues (ARC projects LP0990428, LP130100756 and DP130104087). Funding for the optimization and improvement of the snow and ice model was provided by NSF MSB-1638704. Funding for development of the GLM teaching module and GRAPLEr was ~~sup ported~~supported from

Geosci. Model Dev. Discuss., https://doi.org/10.5194/gmd-2017-257
Manuscript under review for journal Geosci. Model Dev.
Discussion started: 20 November 2017


Geoscientific Model Development Discussions

Revision 8 Mar 2018

NSF ACI-1234983 and NSF EF-1702506 awarded to CC. Provision of the environmental symbols used for the GLM scientific diagrams are courtesy of the Integration and Application Network, University of Maryland Center for Environmental Science. Joanne Moo and Aditya Singh also provided support in model setup and testing.



**References**

Ashton, G.D. (ed.), 1986. River and lake ice engineering. Water Resources Publications, Littleton, Colorado, U.S.A.

Antenucci, J.P., Brookes, J.D. and Hipsey, M.R., 2005. A simple model for quantifying" Cryptosporidium" transport, dilution, and potential risk in reservoirs. *Journal of the American Water Works Association*, 97(1): 86-93.

Babanin, A.V. and Makin, V.K., 2008. Effects of wind trend and gustiness on the sea drag: Lake George study. *Journal of Geophysical Research: Oceans,* 113(C2).

Bird, R.E., 1984. A simple, solar spectral model for direct-normal and diffuse horizontal irradiance. *Solar ~~energy~~Energy*, 32: 461-471.

Briegleb, B.P., Minnis, P., Ramanathan, V. and Harrison, E., 1986. Comparison of regional clear-sky albedos inferred from satellite observations and model computations. *Journal of Climate and Applied Meteorology*, 25(2): 214-226.

Bruce, L.C., Frassl, M.A., Arhonditsis, G.B., Gal, G., Hamilton, D.P., Hanson, P.C., et al., ~~2017~~2018. A multi-lake comparative analysis of the General Lake Model (GLM): Stress-testing across a global observatory network. *Environmental Modelling ~~&~~and Software*, ~~accepted pending final revision~~102: 274-291.

Bruggeman, J. and Bolding, K., 2014. A general framework for aquatic biogeochemical models. *Environmental Modelling ~~&~~and Software*, 61: 249-265.

Brutsaert, W., 1975. On a derivable formula for long-wave radiation from clear skies, *Water Resources Research*, 11(5): 742–744.

Bueche, T., Hamilton, D.P. and Vetter, M., 2017. Using the General Lake Model (GLM) to simulate water temperatures and ice cover of a medium-sized lake: a case study of Lake Ammersee, Germany. *Environmental Earth Sciences*, *76*(13~~), p.461. doi.org/10.1007/s12665-017-6790-7~~): 461.

Businger, J.A., Wyngaard, J.C., Izumi, Y. and Bradley, E.F., 1971. Flux profile relationships in the atmospheric surface layer. *Journal of Atmospheric Sciences*, 28: 181-189.

Carey, C.C. and Gougis, R.D., 2017. Simulation modeling of lakes in undergraduate and graduate classrooms increases comprehension of climate change concepts and experience with computational tools. *Journal of Science Education and Technology*, 26: 1-11.

Cengel, Y.A. and Ozisk, M.N., 1984. Solar radiation absorption in solar ponds. *Solar Energy,* 33(6): 581-591.

Chung, E. G., Schladow, S. G., Perez-Losada, J., and Robertson, D. M., 2008. A linked hydrodynamic and water quality model for the Salton Sea. *Hydrobiologia*, 604:57–75.

Chung, S.W., Imberger, J., Hipsey, M.R. and Lee, H.S., 2014. The influence of physical and physiological processes on the spatial heterogeneity of a Microcystis bloom in a stratified reservoir. *Ecological Modelling*, *289*, pp.133-149.



Cole, J.J., Prairie, Y.T., Caraco, N.F., McDowell, W.H., Tranvik, L.J., Striegl, R.G., Duarte, C.M., Kortelainen, P., Downing, J.A., Middelburg, J.J. and Melack, J., 2007. Plumbing the Global Carbon Cycle: Integrating Inland Waters into the Terrestrial Carbon Budget. *Ecosystems*, 10: 172–185.

Doherty, J., 2015. Calibration and Uncertainty Analysis for Complex Environmental Models. Watermark Numerical Computing, Brisbane, Australia. ISBN: 978-0-9943786-0-6

Dyer, A.J., 1974. A review of flux-profile relationships. *Boundary- Layer Meteorology*, *7*: 363-372.

Fischer, H.B., List, E.G., Koh, R.C.Y., Imberger, J. and Brooks, N.H., 1979. Mixing in Inland and Coastal Waters. Academic Press. New York, NY, 483 pp.

Flerchinger, G.N., Xaio, W., Marks, D., Sauer, T.J. and Yu, Q., 2009. Comparison of algorithms for incoming atmospheric long-wave radiation, *Water Resources Research*, 45: W03423.

Francey, R.J. and Garratt, J.R., 1978. Eddy flux measurements over the ocean and related transfer coefficients. ~~*Boundary-Layer*~~*BoundaryLayer Meteorology*, 14: 153-166.

Gal, G., Imberger, J., Zohary, T., Antenucci, J., Anis, A. and Rosenberg, T., 2003. Simulating the thermal dynamics of Lake Kinneret. *Ecological Modelling*, 162: 69-86.

Gal, G., Hipsey, M.R., Parparov, A., Wagner, U., Makler, V. and Zohary, T., 2009. Implementation of ecological modeling as an effective management and investigation tool: Lake Kinneret as a case study. *Ecological Modelling*, 220(13~~), pp.~~): 1697-1718.

Ganguly, A., Agrawal, A., Boykin, P. O. and Figueiredo, R., 2006. IP over P2P: Enabling self-configuring virtual IP networks for grid computing. In International Parallel and Distributed Processing Symposium.

Gill, A.E., 1982. Atmosphere-ocean dynamics (Vol. 30). Academic ~~press~~Press.

Gu, R. and Stefan, H.G., 1993. Validation of cold climate lake temperature simulation. *Cold ~~regions science~~Regions Science and ~~technology~~Technology*, 22: 99-104.

Haario, H., Laine, M., Mira, A. and Saksman, E., 2006. DRAM: Efficient adaptive MCMC, *Statistics and Computing,* 16: 339-354.

Hamilton, D.P. and Schladow, S.G. 1997. Water quality in lakes and reservoirs. Part I Model description. *Ecological Modelling*, 96: 91–110.

Hamilton, D.P., Carey, C.C., Arvola, L., Arzberger, P., Brewer, C., Cole, J.J., Gaiser, E., Hanson, P.C., Ibelings, B.W., Jennings, E. and Kratz, T.K., 2015. A Global Lake Ecological Observatory Network (GLEON) for synthesising high-frequency sensor data for validation of deterministic ecological models. *Inland Waters*, 5(1): 49-56.



Hanson, P.C., Weathers, K.C. and Kratz, T.K., 2016. Networked lake science: how the Global Lake Ecological Observatory Network (GLEON) works to understand, predict, and communicate lake ecosystem response to global change. *Inland Waters*, 6(4): 543-554.

Harvey, L.D.D., 1990. Testing alternative parameterizations of lateral melting and upward basal heat flux in a thermodynamic sea ice model. *Journal of Geophysical Research,* 95: 7359-7365.

Henderson-Sellers, B., 1986. Calculating the surface energy balance for lake and reservoir modeling: A review. *Reviews of Geophysics*, 24(3): 625-649.

Hicks, B.B., 1975. A procedure for the formulation of bulk transfer coefficients over water. *Boundary Layer Meteorology*, 8: 515-524.

Hicks, B.B., 1972. Some evaluations of drag and bulk transfer coefficients over water. *Boundary Layer Meteorology*, 3: 201:213.

Hipsey, M.R. and Sivapalan, M., 2003. Parameterizing the effect of a wind-shelter on evaporation from small waterbodies. *Water Resources Research*, 39(12): 1339.

Hipsey, M.R., Bruce, L.C. and Hamilton, D.P., 2013. Aquatic EcoDynamics (AED) Model Library Science Manual. The University of Western Australia Technical Manual, Perth, Australia, ~~p.34~~34pp.

Hipsey, M.R., Hamilton, D.P., Hanson, P.C., Carey, C.C., Coletti, J.Z., Read, J.S., Ibelings, B.W., Valesini, F.J. and Brookes, J.D., 2015. Predicting the resilience and recovery of aquatic systems: A framework for model evolution within environmental observatories. *Water Resources Research*, 51(9): 7023-7043.

Hocking, G.C. and Patterson, J.C., 1991. Quasi-two-dimensional reservoir simulation model. *Journal of Environmental Engineering*, 117: 595-613.

Hu, F., Bolding, K., Bruggeman, J., Jeppesen, E., Flindt, M., van Gerven, L.P.A., Janse, J.H., Janssen, A.B.G., Kuiper, J.J., Mooij, W.M. and Trolle, D. 2016. FABM-PCLake - Linking aquatic ecology with hydrodynamics. *Geoscientific Model Development*, 9: 2271-2278

Idso, S.B. and Jackson, R.D., 1969. Thermal radiation from the atmosphere. *Journal of Geophysical Research*, 74: 5397-5403.

Imberger, J., Patterson, J., Hebbert, B. and Loh, I., 1978. Dynamics of reservoir of medium size. *Journal of the Hydraulics Division - ASCE*, 104 No HY5: 725-743.

Imberger, J. and Patterson, J.C., 1981. *A dynamic reservoir simulation model-DYRESM:5*. In: H.B. Fischer (ed.), Transport Models for Inland and Coastal Waters. Academic Press, New York: 310-361.

Imberger, J. and Patterson, J.C., 1990. *Physical Limnology*. In: T. Wu (ed.), Advances in applied mechanics 27. Academic Press. Boston. U.S.A.



Imboden, D.M. and Wüest, A., 1995. *Mixing Mechanisms in Lakes*, p. 83-138. In: A. Lerman, D.M. Imboden and J.R. Gat (eds.), Physics and Chemistry of Lakes. Springer-Verlag.

Janssen, A.B.G., Arhonditsis, G.B., Beusen, A., Bolding, K., Bruce, L., Bruggeman, J., Couture, R.M., Downing, A.S., Elliott, J.A., Frassl, M.A., Gal, G., Gerla, D.J., Hipsey, M.R., Hu, F., Ives, S.C., Janse, J., Jeppesen, E., Jöhnk, K.D., Kneis, D., Kong, X., Kuiper, J.K., Lehmann, M., Lemmen, C., Ozkundakci, D., Petzoldt, T., Rinke, K., Robson, B.J., Sachse, R., Schep, S., Schmid, M., Scholten, H., Teurlincx, S., Trolle, D., Troost, T.A., Van Dam, A., Van Gerven, L.A., Weijerman, M., Wells S.A. and Mooij, W.M., 2015. Exploring, exploiting and evolving diversity of aquatic ecosystem models: a community perspective. *Aquatic ~~ecology~~Ecology*, 49(4): 513-548.

Jellison, R. and Melack, J.M., 1993. Meromixis and vertical diffusivities in hypersaline Mono Lake, California. *Limnology and Oceanography*, 38: 1008–1019.

Ji, Z.G., 2008. Hydrodynamics and water quality: modeling rivers, lakes, and estuaries. John Wiley & Sons.

Kara, E.L., Hanson, P., Hamilton, D., Hipsey, M.R., McMahon, K.D., Read, J.S., Winslow, L., Dedrick, J., Rose, K., Carey, C.C. and Bertilsson, S., 2012. Time-scale dependence in numerical simulations: assessment of physical, chemical, and biological predictions in a stratified lake at temporal scales of hours to months. *Environmental Modelling ~~&~~and Software*, *35~~,~~ ~~pp.~~:* 104-121.

Kim, J-W., 1976. A generalized bulk model of the oceanic mixed layer. *Journal of Physical Oceanography*, 6: 686-695.

Kirk, J.T.O., 1994. Light and photosynthesis in aquatic ecosystems. Cambridge University Press.

Kirillin, G., Hochschild, J., Mironov, D., Terzhevik, A., Golosov, S. and Nützmann, G., 2011. FLake-Global: Online lake model with worldwide coverage. *Environmental Modelling ~~&~~and Software*, 26(5~~), pp.~~): 683-684.

Kleinhans, M.G. and Grasmeijer, B.T., 2006. Bed load transport on the shoreface by currents and waves. *Coastal Engineering*, 53: 983-996.

Klug, J.L., Richardson, D.C., Ewing, H.A., Hargreaves, B.R., Samal, N.R., Vachon, D., Pierson, D.C., Lindsey, A.M., O'Donnell, D.M., Effler, S.W. and Weathers, K.C., 2012. Ecosystem Effects of a Tropical Cyclone on a Network of Lakes in Northeastern North America. *Environmental Science ~~&~~and Technology*, 46 (21): 11693-11701.

Kraus, E.B. and Turner, J.S., 1967. A one-dimensional model of the seasonal thermocline: II The general theory and its consequences. *Tellus*, 19: 98-106.

Laenen A. and LeTourneau A.P., 1996. Upper Klamath Lake nutrient loading study – Estimate of wind-induced resuspension of bed sediment during periods of low lake elevation. *US Geological Survey Open-File Report, 95-414*, 11 pp

Launiainen, J., 1995. Derivation of the relationship between the Obukhov stability parameter and the bulk Richardson number for flux-profile studies. *Boundary Layer Meteorology*, 76: 165-179.

Launiainen, J. and Cheng, B., 1998. Modelling of ice thermodynamics in natural water bodies. *Cold Region Science and Technology*, 27: 153-178.



Launiainen, J. and Vihma, T., 1990. Derivation of turbulent surface fluxes—An iterative flux-profile method allowing arbitrary observing heights. *Environmental Software*, 5: 113-124.

~~Le Roux, J.P., 2007. A simple method to determine breaker height and depth for different deepwater wave height/length ratios and sea floor slopes. *Coastal Engineering*, 54: 271-277.~~

Luo, L., Hamilton, D.P. and Han, B., 2010. Estimation of total cloud cover from solar radiation observations at Lake Rotorua, New Zealand. *Solar Energy*, 84: 501-506.

Magee, M.R., Wu, C.H., Robertson, D.M., Lathrop, R.C. and Hamilton, D.P., 2016. Trends and abrupt changes in 104 years of ice cover and water temperature in a dimictic lake in response to air temperature, wind speed, and water clarity drivers. *Hydrology and Earth System Sciences*, 20(5~~), p.~~): 1681.

Makler-Pick, V., Gal, G., Shapiro, J. and Hipsey, M.R., 2011. Exploring the role of fish in a lake ecosystem (Lake Kinneret, Israel) by coupling an individual-based fish population model to a dynamic ecosystem model. *Canadian Journal of Fisheries and Aquatic Sciences*, *68*(7~~), pp.~~): 1265-1284.

Markfort, C.D., Perez, A.L.S., Thill, J. W., Jaster, D.A., Porté-Agel, F. and Stefan, H.G. 2010. Wind sheltering of a lake by a tree canopy or bluff topography. *Water Resources Research*, 46: 1–13.

Martynov, A., Sushama, L., Laprise, R., Winger, K. and Dugas, B., 2012. Interactive lakes in the Canadian Regional Climate Model, version 5: The role of lakes in the regional climate of North America. *Tellus, Series A Dynamic Meteorology And Oceanography*, 64: 1-22.

Matzinger, A., Schmid, M., Veljanoska-Sarafiloska, E., Patceva, S., Guseska, D., Wagner, B., Müller, B., Sturm, M. and Wüest, A., 2007. Eutrophication of ancient Lake Ohrid: global warming amplifies detrimental effects of increased nutrient inputs, *Limnology and Oceanography*, 52(1~~),~~): 338-353~~, doi:10.4319/lo.2007.52.1.0338~~.

McKay, G.A., 1968. Problems of measuring and evaluating snow cover. In: *Proceedings Workshop Seminar of Snow Hydrology.(Secretariat Canadian National Committee for the IHD*, Ottawa: p.49-62.

McCord, S.A. and Schladow, S.G., 1998. Numerical simulations of degassing scenarios for CO2-rich Lake Nyos, Cameroon. *Journal of Geophysical Research: Solid Earth*, 103(B6): 12355-12364.

Menció, A., Casamitjana, X., Mas-Pla, J., Coll, N., Compte, J., Martinoy, M., Pascual, J. and Quintana, X.D., 2017. Groundwater dependence of coastal lagoons: The case of La Pletera salt marshes (NE Catalonia). *Journal of Hydrology*, 552~~, pp.~~: 793-806.

Mueller H, Hamilton DP and Doole GJ. 2016. Evaluating services and damage costs of degradation of a major lake ecosystem. *Ecosystem Services*, 22: 370-380.

Mooij, W.M., Trolle, D., Jeppesen, E., Arhonditsis, G., Belolipetsky, P.V., Chitamwebwa, D.B.R., Degermendzhy, A.G., DeAngelis, D.L., De Senerpont Domis, L.N., Downing, A.S., Elliott, A.E., Fragoso Jr, C.R., Gaedke, U., Genova, S.N., Gulati, R.D., Håkanson, L., Hamilton, D.P., Hipsey, M.R., Hoen, J., Hülsmann, S., Los, F.J., Makler-Pick, V., Petzoldt, T.,



Prokopkin, I.G., Rinke, K., Schep, S.A., Tominaga, K., Van Dam, A.A., Van Nes, E.H., Wells, S.A. and Janse, J.H., 2010. Challenges and opportunities for integrating lake ecosystem modelling approaches. *Aquatic Ecology*, 44: 633–667.

Monin, A.S. and Obukhov, A.M., 1954. Basic laws of turbulent mixing in the atmosphere near the ground. *Jr. Akad. Nauk SSSR Geofiz. Inst.,* 24: 163-187.

National Research Council (NRC), 2013. Next generation science standards: For states, by states. Washington, DC: The National Academies Press.

O'Reilly, C. M., Sharma, S., Gray, D. K., Hampton, S. E., Read, J. S., Rowley, R. J., Schneider, P., Lenters, J. D., McIntyre, P. B., Kraemer, B. M., et al., 2015. Rapid and highly variable warming of lake surface waters around the globe. *Geophysical Research Letters*, 42(24): ~~10,773–10,781~~10773–10781.

Patterson, J.C., Hamblin, P.F. and Imberger, J., 1984. Classification and dynamics simulation of the vertical density structure of lakes. *Limnology and Oceanography*, 29: 845-861.

Patterson, J.C. and Hamblin, P.F., 1988. Thermal simulation of a lake with winter ice cover. *Limnology and Oceanography*, 33: 323-338.

Paulson, C. A., 1970. The mathematical representation of wind speed and temperature profiles in the unstable atmospheric surface layer. *Journal of Applied Meteorology*, 9: 857-861.

Peeters, F., Straile, D. Loke, A. and Livingstone, D. M., 2007. Earlier onset of the spring phytoplankton bloom in lakes of the temperate zone in a warmer climate. *Global Change Biology*. 13: 1898–1909~~, doi:10.1111/j.1365-2486.2007.01412.x~~.

Perroud, M., Goyette, S., Martynov, A., Beniston, M. and ~~Annevillee~~Anneville, O., 2009. Simulation of multiannual thermal profiles in deep Lake Geneva: A comparison of one-dimensional lake models. *Limnology and Oceanography*, *54*(5~~), pp.~~): 1574-1594.

Porter, J.H., Hanson, P.C. and Lin, C.C., 2012. Staying afloat in the sensor data deluge. *Trends ~~in~~in Ecology ~~&~~and Evolution*, 27(2): 121-129.

Read, J.S., Hamilton, D.P., Jones, I.D., Muraoka, K., Winslow, L.A., Kroiss, R., Wu, C.H. and Gaiser, E., 2011. Derivation of lake mixing and stratification indices from high-resolution lake buoy data. *Environmental Modelling ~~&~~and Software,* 26: 1325–1336.

Read, J.S., Hansen, G., Van Den Hoek, J., Hanson, P.C., Bruce, L.C. and Markfort, C.D., 2014. Simulating 2368 temperate lakes reveals weak coherence in stratification phenology. *Ecological Modelling*, 291: 142-150.

Read, J.S., Gries, C., Read, E.K., Klug, J., Hanson, P.C., Hipsey, M.R., Jennings, E., O'Reilly, C., Winslow, L., Pierson, D., McBride, C. and Hamilton, D.P., 2016. Generating community-built tools for data sharing and analysis in environmental networks. *Inland Waters*, 6(4): 637-644.



Rigosi, A., Hanson, P.C., Hamilton, D.P., Hipsey, M., Rusak, J. A., Bois, J., Sparber, K., Chorus, I., Watkinson, A.J., Qin, B., Kim, B. and Brookes, J.D., 2015. Determining the probability of cyanobacterial blooms: the application of Bayesian networks in multiple lake systems. *Ecological Applications*, 25: 186–199.

Rogers, C.K., Lawrence, G.A. and Hamblin, P.F., 1995. Observations and numerical simulation of a shallow ice-covered mid-latitude lake. *Limnology and Oceanography,* 40: 374-385.

Romarheim, A.T., Tominaga, K., Riise, G. and Andersen, T., 2015. The importance of year-to-year variation in meteorological and runoff forcing for water quality of a temperate, dimictic lake. *Hydrology and Earth System Sciences*, 19(6): 2649-2662.

Salmon, S.U., Hipsey, M.R., Wake, G.W., Ivey, G.N. and Oldham, C.E., 2017. Quantifying Lake Water Quality Evolution: Coupled Geochemistry, Hydrodynamics, and Aquatic Ecology in an Acidic Pit Lake. *Environmental Science ~~&~~and Technology*, 51(17): 9864-9875.

Saloranta, T.M. and Andersen, T., 2007. MyLake—A multi-year lake simulation model code suitable for uncertainty and sensitivity analysis simulations. *Ecological ~~modelling~~Modelling*, 207(1~~), pp.~~): 45-60.

Schwarz, C.V. and White, B.Y., 2005. Metamodeling knowledge: Developing students' understanding of scientific modeling. *Cognition and Instruction*, 23(2): 165-205.

Schwarz, C.V., Reiser, B.J., Davis, E.A., Kenyon, L., Achér, A., Fortus, D., Shwartz, Y., Hug, B. and Krajcik, J., 2009. Developing a learning progression for scientific modeling: Making scientific modeling accessible and meaningful for learners. *Journal of Research in Science Teaching*, 46(6): 632-654.

Sherman, F.S., Imberger, J. and Corcos, G.M., 1978. Turbulence and mixing in stably stratified waters. *Annual Review of Fluid Mechanics,* 10: 267-288.

Snortheim, C.A., P.C. Hanson, K.D. McMahon, J.S. Read, C.C. Carey, and H.A. Dugan. Meteorological drivers of hypolimnetic anoxia in a eutrophic, north temperate lake. *Ecological Modelling*. 343: 39-53. ~~DOI: 10.1016/j.ecolmodel.2016.10.014~~

Spigel, B., 1978. Wind mixing in ~~Lakes~~lakes. PhD thesis, University of California, Berkeley.

Spigel, R.H., Imberger, J. and Rayner, K.N., 1986. Modeling the diurnal mixed layer. *Limnology and Oceanography*, 31: 533-556.

Stepanenko, V., Mammarella, I., Ojala, A., Miettinen, H., Lykosov, V. and Vesala, T., 2016. LAKE 2.0: a model for temperature, methane, carbon dioxide and oxygen dynamics in lakes. *Geoscientific Model Development*, *9*(5~~), pp.~~): 1977-2006.

Stepanenko, V.M., Martynov, A., Jöhnk, K.D., Subin, Z.M., Perroud, M., Fang, X., Beyrich, F., Mironov, D. and Goyette, S., 2013. A one-dimensional model intercomparison study of thermal regime of a shallow, turbid midlatitude lake. *Geoscientific Model Development*, *6*(4~~), pp.~~): 1337-1352.



Stewart, J., Cartier, J.L. and Passmore, C.M., 2005. Developing understanding through model-based inquiry. In M.S. Donovan & J.D. Bransford (Eds.), How students learn ~~(pp. 515–565).~~ Washington, DC: National Research Council. pp. 515–565.

Strub, P.T. and Powell, T.M., 1987. Surface temperature and transport in Lake Tahoe: inferences from satellite (AVHRR) imagery. *Continental Shelf Research,* 7: 1001-1013.

Subratie, K., Aditya, S., Figueiredo, R., Carey, C.C. and Hanson, P.C., 2017. GRAPLEr: A distributed collaborative environment for lake ecosystem modeling that integrates overlay networks, high-throughput computing, and web services. *Concurrency and Computation: Practice and Experience*, 29(13): e4139.

Swinbank, W.C., 1963. Longwave radiation from clear skies. *Quarterly Journal of the Royal Meteorological Society*, 89: 339-348.

Tennessee Valley Authority (TVA), 1972. Heat and mass transfer between a water surface and the atmosphere. Water Resources Research Laboratory Report 14, Report No. 0-6803.

Tabata, S., 1973. A simple but accurate formula for the saturation vapour pressure over liquid water. *Journal of Applied Meteorology*, 12: 1410-1411.

Thain, D., Tannenbaum, T. and Livny, M. (2005). "Distributed Computing in Practice: the Condor Experience" ~~(PDF).~~ *Concurrency and Computation: Practice and Experience*, 17 (2–4): 323–356.

Ticehurst J.L., Newham ~~LTH,~~ L.T.H., Rissik, D~~.~~, Letcher ~~RA,~~ R.A. and Jakeman ~~AJ.,~~ A.J., 2007. A Bayesian network approach for assessing the sustainability of coastal lakes in New South Wales, Australia. *Environmental Modelling ~~&~~and Software*, 22(8):1129-1139.

Tranvik, L.J., Downing, J.A., Cotner, J.B., Loiselle, S.A., Striegl, R.G., Ballatore, T.J., Dillon, P., Finlay, K., Fortino, K., Knoll, L.B. and Kortelainen, P.L., 2009. Lakes and reservoirs as regulators of carbon cycling and climate. *Limnology and Oceanography*, 54~~(6part2):~~ 2298-2314.

Trolle, D., Hamilton, D.P., Hipsey, M.R., Bolding, K., Bruggeman, J., Mooij, W. M., Janse, J. H., Nielsen, A., Jeppesen, E., Elliott, J.E., Makler-Pick, V., Petzoldt, T., Rinke, K., Flindt, M. R., Arhonditsis, G.B., Gal, G., Bjerring, R., Tominaga, K., Hoen, J., Downing, A.S., Marques, D. M., Fragoso Jr, C.R., Søndergaard, M. and Hanson, P.C., 2012. A community-based framework for aquatic ecosystem models. *Hydrobiologia*, 683: 25-34.

~~UNESCO, 1981. Technical papers in Marine Science. No. 36.~~

Vavrus, S.J., Wynne, R.H. and Foley, J.A., 1996. Measuring the sensitivity of southern Wisconsin lake ice to climate variations and lake depth using a numerical model. *Limnology and Oceanography*, 41: 822-831.

Vickers, D., Mahrt, L. and Andreas, E.L., 2013. Estimates of the 10-m neutral sea surface drag coefficient from aircraft eddy-covariance measurements. *Journal of Physical Oceanography*, 43: 301-310.



Weathers, K.C., Groffman, P.M., Van Dolah, E., Bernhardt, E.S., Grimm, N.B., McMahon, K.D., Schimel, J., Paolisso, M., Maranger, R.J., Baer, S., Brauman, K.A. and Hinckley, E., 2016. Frontiers in Ecosystem Ecology from a Community Perspective: The Future is Boundless and Bright. *Ecosystems*, 19(5): 753-770.

Weber, M., Rinke, K., Hipsey, M.R. and Boehrer, B., 2017. Optimizing withdrawal from drinking water reservoirs to reduce downstream temperature pollution and reservoir hypoxia. *Journal of Environmental Management*, 197: 96-105.

Weinstock, J., 1981. Vertical turbulence diffusivity for weak or strong stable stratification. *Journal of Geophysical Research*, 86(C10): 9925-9928.

Williamson, C.E., Saros, J.E., Vincent, W.F. and Smol, J.P., 2009. Lakes and reservoirs as sentinels, integrators, and regulators of climate change. *Limnology and Oceanography*, 54~~(6part2),~~ 2273-2282.

Woolway, R.I., Verburg, P., Merchant, C.J., Lenters, J.D., Hamilton, D.P., Brookes, J., Kelly, S., Hook, S., Laas, A., Pierson, D. and Rimmer, A., 2017. Latitude and lake size are important predictors of over-lake atmospheric stability. *Geophysical Research Letters*, 44 (17), 8875–8883. ~~DOI:10.1002/2017GL073941~~

Winslow, L. A., Hansen, G. J. A., Read, J. S. and Notaro, M., 2017 Data Descriptor: Large-scale modeled contemporary and future water temperature estimates for 10774 Midwestern U.S. Lakes. *Scientific Data*, 4:170053.

Wu J., 1973. Wind induced entrainment across a stable density interface. *Journal of Fluid Mechanics*, 61: 275-278.

Xenopoulos, M.A. and Schindler, D.W., 2001. The environmental control of near-surface thermoclines in boreal lakes. *Ecosystems*, 4: 699-707.

Yajima, H. and Yamamoto, S., 2015. Improvements of radiation estimations for a simulation of water temperature in a reservoir. *Journal of Japan Society of Civil Engineers, Ser. B1 (Hydraulic Engineering*, 71(4): 775-780.

Yao, H., Samal, N.R., Joehnk, K.D., Fang, X., Bruce, L.C., Pierson, D.C., Rusak, J.A. and James, A., 2014. Comparing ice and temperature simulations by four dynamic lake models in Harp Lake: past performance and future predictions. *Hydrological Processes*, 28: 4587-4601.

Yeates, P.S. and Imberger, J., 2003. Pseudo two-dimensional simulations of internal and boundary fluxes In stratified lakes and reservoirs. *International Journal of River Basin Research,* 1: 1-23.

Zhang, W. and Arhonditsis G.B., 2009. A Bayesian hierarchical framework for calibrating aquatic biogeochemical models, *Ecological Modelling*, 220(18): 2142-2161.

Zohar, A. and Dori, Y.J., 2012. *Introduction*. In: Metacognition in science education ~~(pp. 1-19).~~ Springer, Netherlands. pp. 1-19.

Geosci. Model Dev. Discuss., https://doi.org/10.5194/gmd-2017-257
Manuscript under review for journal Geosci. Model Dev.
Discussion started: 20 November 2017




**Table 1. Summary of GLM ~~physical~~ parameters with recommended values and references.**

| Symbol | ~~glm.nml ID~~ | Description | Units | ~~Default~~Value | Reference | Comments |
|---|---|---|---|---|---|---|
| ~~Model Structure~~Physical constants | | | | | | |
| $h_{min}\sigma$ | | Stefan-Boltzmann constant~~min_layer_thick~~ ~~Minimum layer thickness~~ | W $m^{-2}$ $K^{-4}$ | ~~0.~~5.67x$10^{-8}$ | Constant ~~Bruce et al. (2017) Buech e et al. (2017)~~ | Not adjustable in glm.nml~~Standardised for multi-lake comparison~~ ~~Should be estimated relative to lake depth.~~ |
| $h_{max}g$ | | ~~max_layer_thick~~acceleration due to gravity ~~Maximum layer thickness~~ | m $s^{-2}$ | ~~1.5~~9.81 | | |
| ~~Lake Properties~~$c_a$ | | specific heat capacity of air | J $kg^{-1}$ °$C^{-1}$ | 1005 | | |
| $K_w$ | ~~Kw~~ | ~~Extinction coefficient for PAR radiation~~ ~~$m^{-1}$~~ ~~0.2~~ ~~Lake~~ specific heat capacity of air | ~~Should be measured, e.g. mean of simulation period.~~ J $kg^{-1}$ °$C^{-1}$ ~~Can be estimated from Secchi depth.~~ | 2050 | | |
| $A_C c_w$ | | ~~critical_area~~specific heat capacity of liquid water | ~~Critical area below which wind sheltering may occur~~J $kg^{-1}$ °$C^{-1}$ | ~~m²~~4185.5 | ~~10²~~ | Xenopoulos and Schindler (2001) |
| ~~Surface Thermodynamics~~$\lambda_v$ | | Latent heat of evaporation | J $kg^{-1}$ | 2.453x$10^6$ | | |
| $C_H\lambda$ | ~~ch~~ | Latent heat of fusion~~Bulk aerodynamic coefficient for sensible heat transfer~~ | -J $kg^{-1}$ | 3.340 x$10^5$~~0.0013~~ | Fischer et al. (1979) ~~Bruce et al. (2017) Buech e et al. (2017)~~ | ~~From Hicks' (1972) collation of ocean and lake data; many studies since use similar values. Internally calculated if atmos stability correction is on.~~ |
| $C_E\omega$ | | ~~e~~ratio of molecular weight of water to molecular weight of air | ~~Bulk aerodynamic coefficient for latent heat transfer~~ ~~-~~ | 0.~~0013~~622 | | |
| $C_M$Time variables | | ~~ed~~ | ~~Bulk aerodynamic coefficient for transfer of momentum~~ | ~~-~~ | ~~0.0013~~ | |
| $\lambda c_{se}$ | ~~-~~ | ~~Latent heat~~number of ~~evaporation~~seconds per day | ~~J kg~~s ~~day~~$^{-1}$ | ~~2.453x10⁶~~86400 | ~~Standard~~ | ~~Not adjustable in glm.nml~~ |
| $\varepsilon_a t$ | | -time | ~~Emissivity of the water surfaces~~ | - | ~~0.985~~ | Standard ~~Water only, no ice~~ |

Geosci. Model Dev. Discuss., https://doi.org/10.5194/gmd-2017-257
Manuscript under review for journal Geosci. Model Dev.
Discussion started: 20 November 2017




| Symbol | glm.nml ID | | | | | Description | Units | DefaultValue | Reference | Comments | |
|---|---|---|---|---|---|---|---|---|---|---|---|
| | | | | | | | | | | | Ice or snow |
| $\sigma t_b$ | | | | | | time when a shear event begins | Stefan-Boltzmann constant | $W\ m^{-2}\ K^{-4}$ | $5.67x10^{-8}$ | Constant | Not adjustable in glm.nml |
| Mixing Parameters $\lfloor t \rfloor$ | | | | | | floor of time | s | - | | used to compute the time within a day, iclock | |
| $C_K \Delta t$ | | | | | | coef_mix_convtime step used by the model | sMixing efficiency - convective overturn | 3600 | 0.2 | numerical time increment the model usesYeates & Imberger (2003) | Selected from a range given in Spigel et al. (1986) |
| $C_W d$ | | | | | | coef_wind_stirday of the year | Mixing efficiency - wind stirring | variable | 0.23 | Spigel et al. (1986) | From Wu (1973) |
| $C_S N$ | coef_mix_shear | Mixing efficiency - shear production | - | 0.3 | Sherman et al. (1978) | Best fitnumber of experiments reviewedtime-steps to simulate | - | configurable | | | |
| $C_T \delta t_d$ | | | | | | coef_mix_turbtime-scale of inflow parcel transport | sMixing efficiency - unsteady turbulence (acceleration) | computed | 0.51 | Bruce et al. (2017) Bueche et al. (2017) | |
| $C_{KH}$ | coef_mix_KH | Mixing efficiency - Kelvin-Helmholtz turbulent billows | - | 0.3 | Sherman et al. (1978) | "a good rule"period of thumb..."surface waves | s | computed | | Eq. 70 | |
| $C_{HYP} \delta t_{iw}$ | | | | | | coef_mix_hypperiod for internal waves | Mixing efficiency of hypolimnetic turbulences | computed | 0.5 | Weinstock (1981) | Spigel and Imberger (1980) | $\delta t_{iw} = L_{META}/2c$ |
| Inflows & Outflows $\delta t_{shear}$ | | | | | | cut-off time for internal wave induced velocity shear | s | computed | | | Eq. 40 |
| $C_D \delta t_{damp}$ | | | | | | strmbd_dragtime-scale of internal wave damping | streambed_drags | computed | | Spigel and Imberger (1980) 0.016 | Site specificEq. 43 | Set based on inflow stream type |
| GLake domain (volumes, areas, heights and depths) | | | | | | seepage_rate | Seepage rate | $m\ day^{-1}$ | 0 | | |
| Snow & Ice $N_{OUT}$ | | | | | | number of outlets configured | - | configurable | | set in &outflows | |
| $K_{wi} N_{INF}$ | | | | | | -number of inflows configured | -Waveband 1, snow ice light extinction | $m^{-1}$configurable | 48.0 | set in &inflowsRogers et al., (1995), | |

Geosci. Model Dev. Discuss., https://doi.org/10.5194/gmd-2017-257
Manuscript under review for journal Geosci. Model Dev.
Discussion started: 20 November 2017






| Symbol | glm.aml ID | Description | Units | DefaultValue | Reference | Comments | |
|---|---|---|---|---|---|---|---|
| | | | | | | Patterson and Hamblin (1988)<br><br>Ashton (1986)<br><br>Yao et al., (2014) | |
| $K_{wz}N_{LEV}$ | | number of layers, which varies over time | Waveband 2, snow ice light extinction | m variable | 20.0 | | |
| $K_{bt}N_{BSN}$ | | user provided number of basin height points | Waveband 1, blue ice light extinction | m configurable | 1.5 | set in &morphometry | |
| $K_{bz}N_{MORPH}$ | | internally computed number of vertical height increments for the hypsographic curve | Waveband 2, blue ice light extinction | m computed | 20.0 | $H_{b=N_{BSN}}\ \Delta H_m + 10$ | |
| $K_{st}V_{max}$ | | maximum volume of the lake | $m^3$ Waveband 1, snow light extinction | m computed | 6 | once exceeded, excess water is passed to overflow | |
| $K_{sz}V_b$ | | lake volume at the hypsographic data point b | $m^3$ Waveband 2, snow light extinction | m configurable | 20 | Eq 1 | |
| $D_z V_{mi}$ | | interpolated volume at internal morphometry table increment mi | Distance of heat transfer, ice water $m^3$ | m computed | 0.039 | Eq. 2 | |
| $\rho_{white}V_i$ | | volume of the lake at the top of the $i^{th}$ layer | Density, snow ice $m^3$ | kg $m^{-3}$ variable | 890 | $\sum_{j=1}^{i}\Delta V_j$ | |
| $\rho_{blue}V_s$ | | volume of the lake at the top of the surface layer ($i = N_{LEV}$) | Density, blue ice $m^3$ | kg $m^{-3}$ variable | 917 | $V[h_{i=N_{LEV}}]$ | |
| $\rho_{snow}V_S^*$ | | interim calculation of the volume of the lake at the top of the surface layer | Density, snow $m^3$ | variable kg $m^{-3}$ | Variable | used to estimate lake volume prior to overflow calculation | |
| $c_{pi}\Delta V_i$ | | volume of the $i^{th}$ layer | Heat capacity, ice $m^3$ | kJ $kg^{-1}$ $°C^{-1}$ variable | 2.1 | $V[h_i] - V[h_{i-1}]$ | |
| $c_{pw}\tilde{V}_{N^2}$ | | a fractional volume of the lake that contains 85% of $N^2$ variance | Heat capacity, ice $m^3$ | kJ $kg^{-1}$ $°C^{-1}$ variable | 4.2 | | |
| $K_e\Delta V_{epi}$ | | volume of the epilimnion | Compaction coefficient $m^3$ | variable | Variable | $\Delta V_{epi} = V_s - V_{k-1}$ | |
| $K_m\Delta V_{k-1}$ | | volume of the layer below the surface mixed layer/epilimnion | Thermal conductivity, snow ice $m^3$ | W $m^{-1}$ $°C^{-1}$ variable | 2.0 | $V[h_{i=k-1}]$ | |
| $K_m A_{max}$ | | maximum possible area of the lake | Thermal conductivity, blue ice $m^2$ | W $m^{-1}$ $°C^{-1}$ configurable | 2.3 | $A_{max} = A_{b=N_{BSN}}$ | |
| $K_m A_b$ | | lake area above datum at the hypsographic data point b | Thermal conductivity, snow $m^2$ | W $m^{-1}$ $°C^{-1}$ configurable | Variable | set in &morphometry | |
| $K_m A_{mi}$ | | lake area at internal morphometry table increment mi | Thermal conductivity, sediment $m^2$ | W $m^{-1}$ $°C^{-1}$ computed | 1.2 | | |
| $K_m A_i$ | | lake area of the $i^{th}$ layer | Thermal conductivity, water $m^2$ | W $m^{-1}$ $°C^{-1}$ variable | 0.57 | | |

Geosci. Model Dev. Discuss., https://doi.org/10.5194/gmd-2017-257
Manuscript under review for journal Geosci. Model Dev.
Discussion started: 20 November 2017




| Symbol ~~glm.aml ID~~ | Description | Units | ~~Default~~Value | Reference | Comments |
|---|---|---|---|---|---|
| ~~L~~$A[H]$ | -lake area at a given height / elevation | $m^2$ ~~Latent heat of fusion~~ | ~~kJ kg~~$^{+}$configurable | ~~0334~~ | area-height relationship |
| ~~Bottom Stress~~$A_s$ | area of the lake surface | $m^2$ | variable | | |
| ~~D~~$A_{BEN}$ | -lake bottom (benthic) area exceeding the critical light threshold $\phi_{BEN_{crit}}$ | ~~Typical particle diameter~~$m^2$ | ~~m~~variable | | |
| $A_E$ | effective area of the lake surface exposed to wind stress | $m^2$ | computed | | |
| $A_C$ | critical area below which wind sheltering may occur | $m^2$ | $10^7$ | Xenopoulos and Schindler (2001) | |
| $A_{outf}$ | area of the lake at the height of the relevant outflow | $m^2$ | computed | | |
| $A_{k-1}$ | lake area at the top of the metalimnion | $m^2$ | variable | | |
| $H$ | variable referring to height above datum | m above datum | - | | |
| $H_{max}$ | maximum height of the lake, at the lake crest | m above datum | - | | set in &morphometry |
| $H_b$ | height above datum at the hyposgraphic data point b | m above datum | configurable | | set in &morphometry |
| $H_{mi}$ | height above datum at internal morphometry table increment mi | m above datum | computed | | |
| $\Delta H_{mi}$ | height increment used for the model's internal hyspograhic curve interpolation function | m | 0.01 | | |
| $h$ | height above a datum | m above lake bottom | - | | |
| $h_i$ | height above a datum at the top of layer i | m above lake bottom | variable | | |
| $h_S$ | height of the upper surface of the top-most (surface) layer above the datum | m above lake bottom | variable | | Eq 4 |
| $h_B$ | height of the upper surface of the bottom-most layer above the datum | m above lake bottom | variable | | Eq. 68 |
| $h_{BEN}$ | height at which the $\phi_{BEN_{crit}}$ is reached | m above lake bottom | variable | | |
| $\tilde{h}_i$ | height of the middle of the $i^{th}$ layer | m above lake bottom | variable | | |
| $\widetilde{h_{sml}}$ | height of the middle of the epilimnion | m above lake bottom | variable | | |
| $h_{outf}$ | height of a configured outflow | m above lake bottom | configurable | | |
| $h_{i_{ins_I}-1}$ | height of the bottom of the layer where an inflow parcel associated with the $I^{th}$ inflow inserted | m above lake bottom | variable | | |

Geosci. Model Dev. Discuss., https://doi.org/10.5194/gmd-2017-257
Manuscript under review for journal Geosci. Model Dev.
Discussion started: 20 November 2017






| Symbol | glm.aml ID | Description | Units | DefaultValue | Reference | Comments |
|---|---|---|---|---|---|---|
| $z$ | | depth from the lake surface, or height above the lake surface | m from water surface | - | | |
| $z_{avg}$ | | average depth of the lake | m | variable | | |
| $z_{BEN}$ | | depth to the lake where critical light threshold is exceeded | m from water surface | variable | | Eq. 15 |
| $z_{sml}$ | | depth to the thermocline from the surface | m from water surface | variable | | Also, vertical thickness of the surface mixed layer (sml). |
| $z/L$ | | Monin-Obukhov stability parameter | - | computed | | Eq. A26 |
| $z_o$ | | water surface roughness length | m | computed | | Eq. A24 |
| $z_\theta$ | | water surface heat roughness length | m | computed | | |
| $z_e$ | | water surface moisture roughness length | m | computed | | |
| $z_{inf_{ins_I}}$ | | depth that an inflow parcel associated with inflow I inserts | m from water surface | variable | | Depth from the surface where an inflow reaches its level of neutral buoyancy |
| $\Delta z_i$ | | thickness of the $i^{th}$ layer | m | variable | | |
| $\Delta z_{k-1}$ | | thickness of the layer below the epilimnion | m | variable | | |
| $\Delta z_{min}$ | | minimum layer thickness | m | 0.5 | Bruce et al. (2017) Buech e et al. (2017) | Should be estimated relative to lake depth; set in &glm_setup |
| $\Delta z_{max}$ | | maximum layer thickness | m | 1.5 | | |
| $\Delta z_{ice}$ | | combined thickness of the white ice and blue ice | m | computed | | $\Delta z_{white} + \Delta z_{blue}$ |
| $\Delta z_{ice,snow}$ | | thickness of top layer of ice cover, depending on ice or snow presence | m | computed | | Eq. 29 |
| $\Delta z_{snow}$ | | thickness of snow | m | variable | | Eq. 29; Fig. 6 |
| $\Delta z_{white}$ | | thickness of white ice | m | variable | | Eq. 29 |
| $\Delta z_{blue}$ | | thickness of blue ice | m | variable | | Eq. 32 |
| $\Delta z_{inf_0}$ | | thickness of an inflow parcel before transport into the lake | m | computed | | Eq. 55 |
| $\Delta z_{inf_j}$ | | thickness of inflow parcel $j$ | m | variable | | Eq. 57 |
| $\delta z_{inf_j}$ | | vertical transport length of inflow parcel $j$ | m | variable | | $\delta z_{inf_j} = \left(h_s - z_{inf_j}\right) - h_{i_{j-1}}$ |
| $\delta z_{wave}$ | | significant wave height of surface waves | m | computed | | Eq. 73 |
| $\delta z_{soil}$ | | thickness of soil layer | m | 0.5 | | Relevant layer thickness for computing sediment heat diffusion or water seepage |

Geosci. Model Dev. Discuss., https://doi.org/10.5194/gmd-2017-257
Manuscript under review for journal Geosci. Model Dev.
Discussion started: 20 November 2017




| Symbol | ~~glm.aml ID~~ | Description | Units | ~~Default~~Value | Reference | Comments |
|---|---|---|---|---|---|---|
| Simulation variables and parameters | | | | | | |
| $a$ | | Charnock constant | - | 0.012 | | |
| $c$ | | internal wave speed | m $s^{-1}$ | computed | | Eq. 41 |
| $c_{damp}$ | | coefficient related to damping rate of internal waves | - | 104.1 | Spigel (1978) | |
| $C_i$ | | concentration of relevant scaler, including, salinity or water quality variable, in the $i^{th}$ layer | various | variable | | Eq. 51 |
| $\bar{C}$ | | mean concentration of two or more layers | various | variable | | |
| $\Delta C$ | | difference in concentration of two layers | various | variable | | |
| $C_{KH}$ | | Mixing efficiency - Kelvin-Helmholtz turbulent billows | - | 0.3 | Sherman et al. (1978) | "a good rule of thumb..." |
| $C_{HYP}$ | | mixing efficiency of hypolimnetic turbulence | - | 0.5 | Weinstock (1981) | General diffusivities in Jellison and Melack (1993) |
| $C_T$ | | Mixing efficiency - unsteady turbulence (acceleration) | - | 0.51 | Sherman et al. (1978) Spigel et al. (1986) Yeates & Imberger (2003) | |
| $C_S$ | | Mixing efficiency - shear production | - | 0.3 | | Best fit of experiments reviewed |
| $C_W$ | | Mixing efficiency - wind stirring | - | 0.23 | | From Wu (1973) |
| $C_K$ | | Mixing efficiency - convective overturn | - | 0.2 | | Selected from a range given in Spigel et al. (1986) |
| $C_{D_{inf}}$ | | stream-bed drag of inflowing rivers | - | 0.016 | | set based on inflow bed roughness |
| $C_{D_{weir}}$ | | drag associated with weir crest | - | 0.62 | | |
| $C_D$ | | bulk aerodynamic coefficient for momentum | - | 0.0013 | Fischer et al. (1979) Bruce et al. (2017) Buechee et al. (2017) | see also Appendix B; Eq A23 |
| $C_E$ | | bulk aerodynamic coefficient for latent heat transfer | - | 0.0013 | | From Hicks' (1972) collation of ocean and lake data; many studies since use similar values. Internally calculated if atmos stability correction is on. |
| $C_H$ | | bulk aerodynamic coefficient for sensible heat transfer | - | 0.0013 | | |
| $C_{XN}$ | | generic notation for neutral value of bulk transfer coefficient | - | - | | X = H or E |
| $C_{DN-10}$ | | value of bulk transfer coefficient for momentum under neutral atmospheric conditions, referenced to 10m height. | - | computed | | see also Appendix B |

Geosci. Model Dev. Discuss., https://doi.org/10.5194/gmd-2017-257
Manuscript under review for journal Geosci. Model Dev.
Discussion started: 20 November 2017




| Symbol | glm.aml ID | Description | Units | DefaultValue | Reference | Comments |
|---|---|---|---|---|---|---|
| $C_{HWN-10}$ | | value of bulk transfer coefficient for heat/moisture under neutral atmospheric conditions, referenced to 10m height. | - | 0.0013 | | |
| $C_x$ | | cloud cover fraction | - | time-series input | | |
| $D_Z$ | | effective vertical diffusivity of scalars in water | $m^2 s^{-1}$ | computed | | |
| $D_\varepsilon$ | | diffusivity of scalars in water due to turbulent mixing | $m^2 s^{-1}$ | computed | | |
| $D_m$ | | molecular diffusivity for scalars in water | $m^2 s^{-1}$ | $1.25x10^{-9}$ | | |
| $D_a$ | | molecular heat diffusivity of air | $m^2 s^{-1}$ | $2.14x10^{-5}$ | TVA (1972) | Reported as 0.077 $m^2 hr^{-1}$ |
| $D_{outf}$ | | average vertical diffusivity of scalars in layers spanning the withdrawal thickness | $m^2 s^{-1}$ | computed | Imberger and Patterson (1981) | |
| $e_s$ | | saturation vapour pressure | hPa | computed | various | Eq. 22 |
| $e_a$ | | atmospheric vapour pressure | hPa | computed | | Eq. 23 |
| $e_*$ | | | | - | | |
| $E_{TKE}$ | | turbulent kinetic energy available for mixing, per mass per wavenumber | $m^3 s^{-2}$ | - | Imberger and Patterson (1981) | Eq. 34 |
| $E_{PE}$ | | potential energy within the stratified water column | $m^2 s^{-2}$ | - | Imberger and Patterson (1981); Hamilton and Schladow (1997) | Eq. 35 |
| $E$ | | evaporation mass flux | $m\ s^{-1}$ | variable | | |
| $E_{inf}$ | | inflow entrainment | - | computed | | Eq. 53 |
| $F$ | | fetch | m | computed | | estimated as the square root of the lake area, Eq. 69 |
| $Fr$ | | internal Froude number of the lake subject to a water withdrawal | - | computed | | Eq. 61 |
| $f_R, f_S$ | | rainfall scaling factor | - | 1 | | used to adjust/calibrate model to meteorological data |
| $f_{SW}$ | | solar radiation scaling factor | - | 1 | | |
| $f_U$ | | wind-speed scaling factor | - | 1 | | |
| $f_{AT}$ | | air temperature scaling factor | - | 1 | | |
| $f_{RH}$ | | relative humidity scaling factor | - | 1 | | |
| $f_{inf}$ | | inflow rate scaling factor | - | 1 | | |

Geosci. Model Dev. Discuss., https://doi.org/10.5194/gmd-2017-257
Manuscript under review for journal Geosci. Model Dev.
Discussion started: 20 November 2017




| Symbol | glm.nml ID | Description | Units | DefaultValue | Reference | Comments |
|---|---|---|---|---|---|---|
| $f_{outf}$ | | outflow rate scaling factor | - | 1 | | |
| $f_{SWE}$ | | snow water equivalent fraction | m rain/m snow | 0.1 | | |
| $f_{WS}$ | | wind-sheltering scaling factor | - | 1 | | function used to scale the wind-sheltering length scale or lake surface area, based on the direction of the wind |
| $f_{ro}$ | | runoff coefficient | m runoff/m rain | 0.2 | | depends on land slope and soil type |
| $f_{PAR}$ | | fraction of global incoming radiation flux which is photosynthetically active | - | 0.45 | Jellison and Melack (1993) | |
| $f_{VIS}$ | | visible bandwidth fraction | - | 0.3 | Rogers et al. (1995) | |
| $f_{BEN_{crit}}$ | | fraction of surface irradiance at the benthos, which is considered critical for productivity | - | 0.2 | | set in &glm_setup |
| $f_w$ | | friction factor used for current stress calculation | - | computed | Kleinhans and Grasmeijer (2006) | Eq. 78 |
| $f_c$ | | friction factor used for wave stress calculation | - | computed | | |
| $f_0$ | | roughness correction coefficient for the lake surface | - | 0.5 | TVA (1972) | |
| $f_{dif}$ | | smoothing factor used for diffusion | - | computed | | Eq. 52 |
| $g'_k$ | | reduced gravity between the mixed layer and the $k-1$ layer | m $s^{-2}$ | computed | | |
| $g'_{EH}$ | | reduced gravity between the epilimnion and the hypolimnion | m $s^{-2}$ | computed | | |
| $g'_{inf}$ | | reduced gravity between the inflowing water and adjacent lake water | m $s^{-2}$ | computed | | |
| $G$ | | seepage rate | m $day^{-1}$ | 0 | | |
| $Gr$ | | Grashof number related to an outflow extraction | - | computed | Imberger and Patterson (1981) | Eq. 62 |
| $k_{TKE}$ | | turbulence wavenumber | $m^{-1}$ | computed | | Eq. 46 |
| $K_w$ | | light extinction coefficient | $m^{-1}$ | 0.5 | | set in &glm_setup, or form the linked water quality model Can be estimated from Secchi depth. |
| $K_{w1}$ | | Waveband 1, snow ice light extinction | $m^{-1}$ | 48.0 | | |

Geosci. Model Dev. Discuss., https://doi.org/10.5194/gmd-2017-257
Manuscript under review for journal Geosci. Model Dev.
Discussion started: 20 November 2017




| Symbol | glm.aml ID | Description | Units | DefaultValue | Reference | Comments |
|---|---|---|---|---|---|---|
| $K_{w2}$ | | Waveband 2, snow ice light extinction | $m^{-1}$ | 20.0 | Rogers et al., (1995), Patterson and Hamblin (1988), Ashton (1986), Yao et al., (2014) | |
| $K_{b1}$ | | Waveband 1, blue ice light extinction | $m^{-1}$ | 1.5 | | |
| $K_{b2}$ | | Waveband 2, blue ice light extinction | $m^{-1}$ | 20.0 | | |
| $K_{s1}$ | | Waveband 1, snow light extinction | $m^{-1}$ | 6 | | |
| $K_{s2}$ | | Waveband 2, snow light extinction | $m^{-1}$ | 20 | | |
| $K_{snow}$ | | molecular heat conductivity of snow | J $m^{-1}$ $s^{-1}$ °$C^{-1}$ | computed | | Fig. 6 |
| $K_{ice_{white}}$ | | molecular heat conductivity of white ice | J $m^{-1}$ $s^{-1}$ °$C^{-1}$ | 2.3 | | |
| $K_{ice_{blue}}$ | | molecular heat conductivity of blue ice | J $m^{-1}$ $s^{-1}$ °$C^{-1}$ | 2.0 | | |
| $K_{water}$ | | molecular heat conductivity of water | J $m^{-1}$ $s^{-1}$ °$C^{-1}$ | 0.57 | | |
| $K_{air}$ | | molecular heat conductivity of air | J $m^{-1}$ $s^{-1}$ °$C^{-1}$ | $2.8 \times 10^{-3}$ | TVA (1972) | Reported as 0.1 kJ $m^{-1}$ $hr^{-1}$ $K^{-1}$ |
| $L_D$ | | equivalent circular diameter of the lake | m | computed | | |
| $L_{META}$ | | length of the lake at the depth of the thermocline region (metalimnion) | m | computed | | |
| $L_{outf}$ | | length of the lake at the height of the relevant outflow | m | computed | | |
| $L_{crest}$ | | length of the lake at the upper most height of the domain | m | configurable | | |
| $m$ | | constant used to compute the rate at which work from the wind is converted | - | $4.6 \times 10^{-7}$ | | |
| $N^2$ | | the buoyancy frequency, a measure of water column stratification | $s^{-2}$ | computed | | |
| $N^2_{outf}$ | | the buoyancy frequency, a measure of water column stratification, about the layers impacted by the water outflow | $s^{-2}$ | computed | | |
| $p$ | | air pressure | hPa | 1013 | - | assumed constant |
| $Q_{inf_x}$ | | rate of water inflow provided by the user as input to the model | $m^3$ $day^{-1}$ | time-series input | | |
| $Q_{inf_0}$ | | rate of water inflow prior to the inflow entering the lake | $m^3$ $s^{-1}$ | computed | | $Q_{inf_0} = f_{inf}\ Q_{inf_x}/c_{secday}$ |
| $Q_{inf_j}$ | | flow rate of inflow water parcel during transit, at the $j^{th}$ increment | $m^3$ $s^{-1}$ | variable | | Eq. 60 used to increment between j steps |
| $Q_{inf_{ins_I}}$ | | flow rate of inflowing water at the point of insertion, for inflow, $I$ | $m^3$ $s^{-1}$ | variable | | |
| $Q_{outf_x}$ | | rate of water outflow provided by the user as input to the model | $m^3$ $day^{-1}$ | time-series input | | |
| $Q_{outf_i}$ | | flow rate of water being extracted from the $i^{th}$ layer | $m^3$ $s^{-1}$ | computed | | |

Geosci. Model Dev. Discuss., https://doi.org/10.5194/gmd-2017-257
Manuscript under review for journal Geosci. Model Dev.
Discussion started: 20 November 2017




| Symbol | glm.aml ID | Description | Units | DefaultValue | Reference | Comments |
|---|---|---|---|---|---|---|
| $Q_{ovfl}$ | | rate of over flowing water leaving the lake | $m^3 s^{-1}$ | computed | | Eq. 73 |
| $Q_{weir}$ | | flow rate of water discharging over the crest, before flooding | $m^3 s^{-1}$ | computed | | Eq. 72 |
| $Q_R$ | | boundary run-off into the lake surface layer | $m^3 s^{-1}$ | computed | | |
| $R$ | | dimensionless parameter describing a water withdrawal flow regime | - | computed | | |
| $R_L$ | | rainfall intensity threshold before run-in occurs | $m\ day^{-1}$ | 0.04 | | depends on land slope and soil type |
| $RH_x$ | | relative humidity | - | time-series input | | user supplied relative humidity between 0 and 1 |
| $R_F$ | | rainfall rate | $m\ s^{-1}$ | computed | | Eq 5 |
| $R_x$ | | rainfall rate supplied in the input file | $m\ day^{-1}$ | time-series input | | user supplied rainfall rate |
| $r$ | | mixing ratio | - | computed | | ratio of water mass to total air mass |
| $Ri_{inf}$ | | Richardson number of the inflow water | - | computed | | Eq. 54 |
| $Ri_B$ | | bulk Richardson number of the atmosphere over the lake | - | computed | | A34 |
| $S_x$ | | snowfall rate supplied in the input file | $m\ day^{-1}$ | time-series input | | user supplied snowfall rate |
| $S_F$ | | snowfall rate | $m\ s^{-1}$ | computed | | Eq 6. |
| $S_i$ | | salinity of the $i^{th}$ layer | ppt | variable | | |
| $S_{inf_x}$ | | salinity of water entering in an inflow | $g\ m^{-3}$ | time-series input | | |
| $T_s$ | | temperature of the surface layer | °C | variable | | Eq. 8 |
| $T_x$ | | air temperature supplied by the user | °C | time-series input | | user supplied air temperature |
| $T_a$ | | air temperature | °C | computed | | $T_a = f_{AT} T_x$ |
| $T_i$ | | temperature of the $i^{th}$ layer | °C | variable | | |
| $T_m$ | | melt-water temperature | °C | 0 | | |
| $T_0$ | | temperature at the solid surface | °C | variable | | |
| $T_{inf_x}$ | | temperature of water entering in an inflow | °C | time-series input | | |
| $\theta_V$ | | virtual temperature of the atmospheric boundary layer above the lake | °K | computed | | |
| $\theta_a$ | | temperature of the atmospheric boundary layer above the lake | °K | computed | | $\theta_a = f_{AT} T_x + 273.15$ |
| $\theta_s$ | | temperature of the atmospheric at the lake surface | °K | variable | | $\theta_a = T_s + 273.15$ |
| $\theta_*$ | | | | | | |
| $U_{10}$ | | wind speed above the lake referenced to 10m height | $m\ s^{-1}$ | - | | wind speed corrected to reference height |

Geosci. Model Dev. Discuss., https://doi.org/10.5194/gmd-2017-257
Manuscript under review for journal Geosci. Model Dev.
Discussion started: 20 November 2017






| Symbol | glm.aml ID | Description | Units | DefaultValue | Reference | Comments |
|---|---|---|---|---|---|---|
| $U_x$ | | wind speed above the lake surface provided by the user | m s$^{-1}$ | time-series input | | user supplied snowfall rate |
| $U_{orb_i}$ | | orbital wave velocity experienced at the bottom of the $i^{th}$ layer | m s$^{-1}$ | variable | | Eq. 75 |
| $U_{m_i}$ | | mean layer velocity of the $i^{th}$ layer | m s$^{-1}$ | variable | | Eq. 77 |
| $u_{inf_j}$ | | average velocity of an inflow parcel being tracked, prior to insertion | m s$^{-1}$ | variable | | Eq. 59 |
| $u_*$ | | friction velocity | m$^3$ s$^{-3}$ | computed | | Eq. 37 |
| $u_b$ | | velocity shear at the base of the thermocline | m s$^{-1}$ | variable | | Eq. 39 |
| $u_{b_{old}}$ | | velocity shear at the thermocline at the previous time-step | m s$^{-1}$ | variable | | reset between shear events |
| $W_{crest}$ | | width of the lake at the upper most point | m | configured | | |
| $W_{outf}$ | | width of the lake at the height of an outflow | m | computed | | Eq. 65 |
| $w_*^3$ | | turbulent velocity scale within the surfaced mixed layer, due to convective cooling | m s$^{-1}$ | computed | Imberger and Patterson (1981) | Eq 36 |
| $x_{WS}$ | | default sheltering distance defined as the distance from the shoreline at which wind stress is no longer affected by sheltering | m | configurable | Markfort et al (2009) | Approximated as 50x the vertical height of the sheltering obstacle/landform |
| ${x_{WS}}^{\Phi}$ | | sheltering distance adjusted for changes in wind direction | m | computed | | ${x_{WS}}^{\Phi} = x_{WS}\,(1 - min(f_{WS}[\Phi_{wind}], 1))$ |
| $\delta x_{wave}$ | | wave length of surface waves | m | computed | | Eq. 72 |
| $\Delta x_{inf_j}$ | | lateral distance travelled by an inflow parcel per $j$ increment, prior to insertion | m | computed | | Eq. 58 |
| $\alpha_{inf}$ | | half-angle of inflow river channel | deg | configurable | | user supplied based on width and depth of the relevant river |
| $\alpha_h$ | | coefficient for sensible heat flux into still air | J m$^{-2}$ s$^{-1}$ °C$^{-1}$ | computed | TVA (1972) | Eq. 27b |
| $\alpha_e$ | | coefficient for evaporative flux into still air | m s$^{-1}$ | computed | TVA (1972) | Eq. 27a |
| $\alpha_{LW}$ | | longwave albedo | - | 0.03 | | |
| $\alpha_{SW}$ | | albedo of shortwave radiation at the water surface | - | 0.08 | | Eq. 12 |
| $\alpha_{SKY}$ | | scattered radiation within the sky | - | computed | Bird (1984) | $\alpha_{SKY} = 0.0685 + (1 - 0.84)\,(1 - T_{as})$ |
| $\alpha_b$ | | interpolation coefficient for volume | - | computed | | Eq. 3 |
| $\beta_b$ | | interpolation coefficient for area | - | computed | | Eq. 3 |

Geosci. Model Dev. Discuss., https://doi.org/10.5194/gmd-2017-257
Manuscript under review for journal Geosci. Model Dev.
Discussion started: 20 November 2017




| Symbol | ~~glm.aml ID~~ | Description | Units | ~~Default~~Value | Reference | Comments |
|---|---|---|---|---|---|---|
| $\delta_{wi}$ | | length-scale associated with conduction of heat at the ice-water interface | m | 0.039 | Rogers *et al.* (1995) | |
| $\delta_{KH}$ | | length-scale associated with formation of Kelvin-Helmholtz billows at the interface of two-layer stratification | m | computed | Imberger and Patterson (1981) | |
| $\delta_{outf}$ | | length-scale associated with the vertical thickness of the zone of influence of a withdrawal | m | computed | Imberger and Patterson (1981) | Eq. 66 |
| $\delta_{outf_{top}}$ | | thickness of withdrawal layer above the withdrawal height | m | computed | | |
| $\delta_{outf_{bot}}$ | | thickness of withdrawal layer below the withdrawal height | m | computed | | |
| $\delta_{ss}$ | | particle diameter of bottom sediment | m | $80x10^{-6}$ | | |
| $\varepsilon_{TKE}$ | | TKE dissipation flux per unit mass | $m^2\ s^{-3}$ | - | | Eq. 48 |
| $\overline{\varepsilon_{TKE}}$ | | steady-state/equilibrium TKE dissipation flux per unit mass | $m^2\ s^{-3}$ | computed | | Eq. 49 |
| $\varepsilon_{WIND}$ | | TKE dissipation flux created by power introduced by the wind | $m^2\ s^{-3}$ | computed | | Eq. 49 |
| $\varepsilon_{INFLOW}$ | | TKE dissipation flux caused by inflow plunging creating seiching | $m^2\ s^{-3}$ | computed | | Eq. 49 |
| $\varepsilon_w$ | | emissivity of the water surface | - | 0.985 | | |
| $\varepsilon_a$ | | emissivity of the atmosphere under cloud-free conditions | - | | | |
| $\varepsilon_a^*$ | | emissivity of the atmosphere including cloud reflection | - | computed | Henderson-Sellers (1986) | Eq. 19 |
| $\phi_{SW_x}$ | | shortwave radiation flux provided in the input file | $W\ m^{-2}$ | time-series input | - | user supplied solar radiation data |
| $\phi_{SW_s}$ | | shortwave radiation flux crossing the water surface | $W\ m^{-2}$ | computed | - | Eq. 9. |
| $\hat{\phi}_{SW}$ | | total incident shortwave radiation flux computed from the BCSM assuming clear-sky conditions | $W\ m^{-2}$ | computed | Bird (1984) | Eq. 10 and Appendix A |
| $\hat{\phi}_{DB}$ | | direct beam radiation on a horizontal surface at ground level on a clear day | $W\ m^{-2}$ | computed | Bird (1984) | Eq. A19 |
| $\hat{\phi}_{AS}$ | | radiation from atmospheric scattering hitting ground level on a clear day | $W\ m^{-2}$ | computed | Bird (1984) | Eq. A20 |
| $\phi_{PAR}$ | | downwelling PA radiation intensity within the water column | $W\ m^{-2}$ | computed | Kirk (1994) | Eq. 13 |

Geosci. Model Dev. Discuss., https://doi.org/10.5194/gmd-2017-257
Manuscript under review for journal Geosci. Model Dev.
Discussion started: 20 November 2017




| Symbol | glm.aml ID | Description | Units | DefaultValue | Reference | Comments |
|---|---|---|---|---|---|---|
| $\phi_{PAR_{BEN}}$ | | light incident on the bottom of a layer, corresponding to the benthic area | W m$^{-2}$ | variable | - | |
| $\phi_{LWin}$ | | longwave radiation incident heat flux at the water surface | W m$^{-2}$ | variable | | Eq. 18 |
| $\phi_{LWout}$ | | longwave radiation outgoing heat flux from the water surface | W m$^{-2}$ | variable | | Eq. 17 |
| $\phi_{LW_{net}}$ | | net longwave radiation flux across the lake surface | W m$^{-2}$ | computed | | Eq. 16 |
| $\phi_H$ | | sensible heat flux across the water surface | W m$^{-2}$ | computed | | Eq. 20 |
| $\phi_E$ | | latent heat flux | W m$^{-2}$ | computed | | Eq. 21 |
| $\phi_{E_0}$ | | latent heat flux under zero-wind conditions | W m$^{-2}$ | computed | | Eq. 26a |
| $\phi_{H_0}$ | | sensible heat flux under zero-wind conditions | W m$^{-2}$ | computed | | Eq. 26b |
| $\phi_X$ | | generic identifier for either of $\phi_E$ or $\phi_H$ | W m$^{-2}$ | computed | | |
| $\phi_{X_0}$ | | generic identifier for either of $\phi_{E_0}$ or $\phi_{H_0}$ | W m$^{-2}$ | computed | | |
| $\phi_X^*$ | | maximum value of either $\phi_{X_0}$ or $\phi_X$ | W m$^{-2}$ | selected | | Eq. 21 |
| $\phi_0$ | | upward conductive heat flux through the ice and snow cover to the atmosphere | W m$^{-2}$ | computed | | |
| $\phi_{net}$ | | net incoming heat flux at the ice-atmosphere interface | W m$^{-2}$ | computed | Rogers et al. (1995) | Eq. 29 |
| $\phi_R$ | | heat flux due to rainfall | W m$^{-2}$ | computed | Rogers et al. (1995) | |
| $\phi_f$ | | heat flux at the ice-water interface into the blue ice | W m$^{-2}$ | computed | | Eq. 31 |
| $\phi_w$ | | heat flux from the water to the blue ice | W m$^{-2}$ | computed | | Eq. 33 |
| $\phi^*_{white}$ | | Heat flux per unit volume due to formation of white ice by flooding | W m$^{-2}$ | computed | Rogers et al. (1995) | |
| $\Phi_{wind}$ | | wind direction | degrees | time-series input | | optionally provided as a boundary condition |
| $\Phi_{inf}$ | | slope of inflow coming into the lake | degrees | | | user provided in &inflow |
| $\Phi_{zen}$ | | solar zenith angle | radians | variable | | |
| SZA | | solar zenith angle | degrees | variable | | SZA = $\Phi_{zen} 180/\pi$ |
| $\rho_a$ | | air density | kg m$^{-3}$ | computed | TVA (1972) | computed as a function of air temperature, humidity and pressure in atm_density |
| $\rho_o$ | | density of saturated air at the water surface temperature | kg m$^{-3}$ | computed | TVA (1972) | |

Geosci. Model Dev. Discuss., https://doi.org/10.5194/gmd-2017-257
Manuscript under review for journal Geosci. Model Dev.
Discussion started: 20 November 2017




| Symbol | glm.aml ID | Description | Units | DefaultValue | Reference | Comments |
|---|---|---|---|---|---|---|
| $\rho_i$ | | density of the i$^{th}$ layer | kg m$^{-3}$ | variable | UNESCO (1981) | compute for each layer based on temperature and salinity |
| $\rho_s$ | | density of the surface water layer (i=$N_{LEV}$) | kg m$^{-3}$ | variable | | |
| $\rho_{sml}$ | | mean density of the mixed layer | kg m$^{-3}$ | variable | | |
| $\rho_{ref}$ | | average of layer densities over which reduced gravity is being computed | kg m$^{-3}$ | computed | | |
| $\rho_{ice,snow}$ | | density of the snow or ice | kg m$^{-3}$ | selected | | |
| $\rho_{white}$ | | density of snow ice | kg m$^{-3}$ | 890 | | |
| $\rho_{blue}$ | | density of blue ice | kg m$^{-3}$ | 917 | | |
| $\rho_{snow}$ | | density of snow | kg m$^{-3}$ | variable | | |
| $\rho_{s,min}$ | | assigned minimum snow density | kg m$^{-3}$ | 50 | | |
| $\rho_{s,max}$ | | assigned maximum snow density | kg m$^{-3}$ | 300 | | |
| $\rho_{snow*}$ | | intermediate snow density estimate | kg m$^{-3}$ | computed | | see Figure 6 |
| $\rho_{outf}$ | | density of the lake layer corresponding to the height of withdrawal, $i_{outf}$ | kg m$^{-3}$ | computed | | |
| $\rho_{i_j}$ | | density of the lake layer, $i$, which is at an equivalent depth to inflow parcel $j$ | kg m$^{-3}$ | computed | | |
| $\rho_{inf}$ | | density of inflowing water | kg m$^{-3}$ | computed | | |
| $\rho_{ins_I}$ | | density of the inflow parcel associated with inflow $I$ when it inserted | kg m$^{-3}$ | computed | | |
| $\rho_{i_{ins_I}}$ | | density of the lake layer, $i$, where the inflow $I$ inserted | kg m$^{-3}$ | computed | | |
| $\kappa$ | | von Karman's constant | - | 0.41 | | |
| $\vartheta_s$ | | dimensionless moisture content of air at water's surface | - | computed | TVA (1972) | $\vartheta_s = \kappa\, e_s/p$ |
| $\vartheta_a$ | | dimensionless moisture content of the air above the lake | - | computed | TVA (1972) | $\vartheta_a = \kappa\, e_a/p$ |
| $\nu_a$ | | kinematic viscosity of air | m$^2$ s$^{-1}$ | 1.52×10$^{-5}$ | TVA (1972) | Reported as 0.0548 m$^2$ hr$^{-1}$ |
| $\nu_w$ | | kinematic viscosity of water | m$^2$ s$^{-1}$ | 1.14×10$^{-6}$ | | |
| $\tau_i$ | | total shear stress experienced at the lake bed portion of layer $i$ | N m$^{-2}$ | computed | | Eq. 76 |
| $\psi_M$ | | similarity function for momentum in the air above the lake | - | computed | | Eq. A30 |
| $\psi_E$ | | similarity function for moisture in the air above the lake | - | computed | | Eq. A30 |

Geosci. Model Dev. Discuss., https://doi.org/10.5194/gmd-2017-257
Manuscript under review for journal Geosci. Model Dev.
Discussion started: 20 November 2017




| Symbol | glm.aml ID | Description | Units | DefaultValue | Reference | Comments |
|---|---|---|---|---|---|---|
| $\psi_H$ | | similarity function for heat in the air above the lake | - | computed | | Eq. A30 |
| $\xi$ | | dimensionless parameter used for wave period calculation | - | computed | | Eq. 71 |
| $\zeta$ | | dimensionless parameter used for wave period calculation | - | computed | | Eq. 74 |
| $\varsigma$ | | constant related to atmospheric diffuse radiation | - | 6 | Yajima and Yamamoto (2015) | |
| Indices | | | | | | |
| $b$ | | hyposgraphic data point index | - | index | | |
| $mi$ | | internal hyposgraphic curve increment | - | index | | |
| $i$ | | index of computational layer | - | index | | |
| $i_j$ | | index of the lake layer at an equivalent depth to inflow parcel $j$ | - | index | | |
| $i_{bot}$ | | index of lower most layer impacted by a given withdrawal/outflow | - | index | | |
| $i_{top}$ | | index of the upper-most layer impacted by a given withdrawal/outflow | - | index | | |
| $i_{outf}$ | | index of the lake layer aligning with a withdrawal/outflow extraction point | - | index | | |
| $s$ | | layer index of the layer at the surface of the lake | - | index | | |
| $k$ | | layer index of the layer at the bottom of the surface mixed layer (sml; epilimnion) | - | index | | |
| $j$ | | index of inflow parcel transport, prior to insertion | - | index | | |
| $I$ | | inflow index | - | index | | |
| $O$ | | outflow index | - | index | | |

Geosci. Model Dev. Discuss., https://doi.org/10.5194/gmd-2017-257
Manuscript under review for journal Geosci. Model Dev.
Discussion started: 20 November 2017


Geoscientific Model Development Discussions

Revision 8 Mar 2018

**Appendix A: Bird solar radiation model**

The Bird Clear Sky Model (BCSM) was developed by (Bird, 1984) to predict clear-sky direct beam, hemispherical diffuse, and total hemispherical broadband solar radiation on a horizontal surface. Average solar radiation is computed at the model time-step (e.g., hourly) based on ten user-specified input parameters (Table A1).

**Table A1: Parameters required for the BCSM model.**

| Variable | Description | Example values (e.g., Luo et al., 2010) |
|---|---|---|
| Lat | Latitude (degrees, + for N) | -31.77 |
| Long | Longitude (degrees + for E) | 116.03 |
| TZ | Time Zone indicated by number of hours from GMT | +7.5 |
| *AP* | Atmospheric Pressure (millibars) | 1013 |
| *Oz* | Ozone Conc. (atm-cm) | 0.279 - 0.324 |
| *W* | Total Precipitable Water Vapour (atm-cm) | 1.1 - 2.2 |
| $AOD_{500}$ | Aerosol Optical Depth at 500 nm | 0.033 – 0.1 |
| $AOD_{380}$ | Aerosol Optical Depth at 380 nm | 0.038 – 0.15 |
| $\alpha_{SW}$ | Surface albedo | 0.2 |

The solar constant in the model is taken as 1367 W~~/m~~$^{-2}$ m$^{-2}$. This is corrected due to the elliptical nature of the earth's orbit and consequent change in distance to the sun. This calculation gives us the Extra-Terrestrial Radiation ($\hat{\phi}_{ETR}$), at the top of the atmosphere:

$$\hat{\phi}_{ETR} = 1367\left(1.00011 + 0.034221\cos(\Phi_{day}) + 0.00128\sin(\Phi_{day}) + 0.000719\cos(\Phi_{day})\right) \quad (A1)$$

where the day angle, $\Phi_{day}$, is computed using, *d,* the day number:

$$\Phi_{day} = 2\pi\left(\frac{d-1}{365}\right) \quad (A2)$$

The solar declination, $\Phi_{dec}$ (radians), is computed from:

$$\Phi_{dec} = \begin{bmatrix} 0.006918 - 0.399912\,cos(\Phi_{day}) + 0.070257\,sin(\Phi_{day}) - 0.006758\,cos\left(2(\Phi_{day})\right) + \\ 0.000907\,sin(2\Phi_{day}) - 0.002697\,cos\left(3(\Phi_{day})\right) + 0.00148\,sin\left(3(\Phi_{day})\right) \end{bmatrix} \quad (A3)$$

We then solve the equation of time:

Geosci. Model Dev. Discuss., https://doi.org/10.5194/gmd-2017-257
Manuscript under review for journal Geosci. Model Dev.
Discussion started: 20 November 2017


Geoscientific Model Development Discussions
Open Access
EGU



$$EQT = \begin{bmatrix} 0.0000075 + 0.001868\ cos(\Phi_{day}) - 0.032077\ sin(\Phi_{day}) \\ -0.014615\ cos\left(2(\Phi_{day})\right) - 0.040849\ sin\left(2(\Phi_{day})\right) \end{bmatrix} \times 229.18 \quad \text{(A4)}$$

in order to compute the hour angle, $\Phi_{hr}$, calculated with noon zero and morning positive as:

$$\Phi_{hr} = 15(hr - 12.5) + Long - 15\ TZ\ + \left(\frac{EQT}{4}\right) \quad \text{(A5)}$$

where TZ is the time-zone shift from GMT. The zenith angle, $\Phi_{zen}$ (radians), is calculated from:

$$\cos(\Phi_{zen}) = \cos(\Phi_{dec})\cos(\Phi_{hr})\cos(Lat) + \sin(\Phi_{dec})\sin(Lat) \quad \text{(A6)}$$

When $\Phi_{zen}$ is less than 90°, the air mass factor is calculated as:

$$\mathrm{AM} = \left[cos(\Phi_{zen}) + \frac{0.15}{(93.885 - \Phi_{zen})^{1.25}}\right]^{-1} \quad \text{(A7)}$$

which is corrected for atmospheric pressure, $p$ (hPa),

$$AM_p = \frac{AM\ p}{1013} \quad \text{(A8)}$$

$AM_P$ is then used to calculate the Rayleigh Scattering as:

$$T_{rayleigh} = e^{[(-0.0903\ AM_p{}^{0.84}) + (1 + AM_p - AM_p{}^{1.01})]} \quad \text{(A9)}$$

The effect of ozone scattering is calculated by computing ozone mass, which for positive air mass is:

$$T_{ozone} = \left[1 - \left(0.1611\ (Oz\ AM)\ \left(1 + 139.48\ (Oz\ AM)\right)^{-0.3035}\right) - \frac{0.002715\ (Oz\ AM)}{1 + 0.044\ (Oz\ AM) + 0.0003\ (Oz\ AM)^2}\right] \quad \text{(A10)}$$

The scattering due to mixed gases for positive air mass is calculated as:

$$T_{mix} = e^{[-0.0127\ AMp^{0.26}]} \quad \text{(A11)}$$

Then the water scattering is calculated by getting the water mass:

$$Wm = WAM_p \quad \text{(A12)}$$

where W is the precipitable water vapour. This can be approximated from dew point temperature, eg.:

$$\ln W = a\ T_d + b \quad \text{(A13)}$$

where a and b are regression coefficients which have been taken as 0.09, 0.07, 0.07 and 0.08 for values of a, while b is 1.88, 2.11, 2.12 and 2.01 in spring, summer, autumn and winter (Luo et al., 2010).

Then the water scattering effect is calculated as:

$$T_{water} = \left[1 - \frac{(2.4959\ Wm)}{1 + (79.034\ Wm)^{0.6828} + 6.385\ Wm}\right] \quad \text{(A14)}$$

The scattering due to aerosols requires the Aerosol Optical Depth at 380 nm and 500 nm:

$$TauA = 0.2758\ AOD_{380} + 0.35\ AOD_{500} \quad \text{(A15)}$$

and the scattering due to aerosols is then calculated as:

Geosci. Model Dev. Discuss., https://doi.org/10.5194/gmd-2017-257
Manuscript under review for journal Geosci. Model Dev.
Discussion started: 20 November 2017




$$T_{aerosol} = e^{(-TauA)^{0.873}\,(1+TauA-TauA^{0.7088})\,AM^{0.9108}} \quad \text{(A16)}$$

We also define:

$$T_{aa} = 1 - [0.1\,(1 - AM + AM^{1.06})\,(1 - T_{aerosol})] \quad \text{(A17)}$$

and:

$$\frac{0.5(1 - T_{rayleigh}) + 0.84(1 - T_{as})}{1 - AM + AM^{1.02}} \quad \text{(A18)}$$

where the 0.84 value used is actually the proportion of scattered radiation reflected in the same direction as incoming radiation.

The direct beam radiation on a horizontal surface at ground level on a clear day is given by,

$$\hat{\phi}_{DB} = 0.9662\,\hat{\phi}_{ETR}\,T_{rayleigh}\,T_{ozone}\,T_{mix}\,T_{watvap}\,T_{aerosol}\;cos(\Phi_{zen}) \quad \text{(A19)}$$

$$\hat{\phi}_{AS} = 0.79\,\hat{\phi}_{ETR}\;T_{ozone}T_{mix}\,T_{watvap}\,T_{aa}\;cos(\Phi_{zen}) \quad \text{(A20)}$$

The total irradiance hitting the surface is therefore (W m$^{-2}$):

$$\hat{\phi}_{SW} = \frac{\hat{\phi}_{DB} + \hat{\phi}_{AS}}{1 - (\alpha_{SW}\,\alpha_{SKY})} \quad \text{(A21)}$$

The albedo is computed for the sky as:

$$\alpha_{SKY} = 0.068 + (1 - 0.84)\left(1 - \frac{T_{aerosol}}{T_{aa}}\right) \quad \text{(A22)}$$

Geosci. Model Dev. Discuss., https://doi.org/10.5194/gmd-2017-257
Manuscript under review for journal Geosci. Model Dev.
Discussion started: 20 November 2017


Geoscientific Model Development Discussions



**Appendix B: Non-neutral bulk transfer coefficients**

The iterative procedure used in this analysis to update correct the bulk-transfer coefficients based on atmospheric conditions is conceptually similar to the methodology discussed in detail in Launiainen and Vihma (1990). The first estimate for the neutral drag coefficient, $C_{DN}$, is specified as a function of ~~windspeed~~wind speed as it is ~~has been~~ commonly observed ~~that $C_{DN}$ increases~~to increase with ~~$U_{10}$ (Figure A1).~~$U_{10}$. This is modelled by first ~~by~~ estimating the value referenced to 10m height above the water from:

$$C_{DN-10} = \begin{cases} 0.001 & U_{10} \le 5 \\ 0.001\,(1 + 0.07[U_{10} - 5]) & U_{10} > 5 \end{cases} \quad \text{Option 1 : Francey and Garratt (1978), Hicks (1972)} \qquad (A23)$$

$$C_{DN-10} = 1.92\times10^{-7} U_{10}^3 + 0.00096 \quad \text{Option 2 : Babanin and Makin (2008)}$$

and then computing the Charnock formula with the smooth flow transition (e.g., Vickers et al., 2013):

$$z_o = \frac{\alpha u_*^2}{g} \frac{a u_*^2}{g} + 0.11 \frac{\nu}{u_*} \frac{\nu_a}{u_*} \qquad (A24)$$

where ~~$\alpha$~~$a$ is the Charnock constant (0.012), ~~$u_*$~~$u_*$ is the approximated friction velocity ($\sqrt{C_{DN-10}\, U_{10}^2}$) using Eq A23~~, and the final~~. The drag is re-computed using:

$$C_{DN-10} = \left[\frac{k}{\ln\left(\frac{10}{z_o}\right)}\right]^2 \left[\frac{\kappa}{\ln\left(\frac{10}{z_o}\right)}\right]^2 \qquad (A25)$$

where ~~$k$~~$\kappa$ is the von Karman constant~~.~~ (Figure A1). Note the neutral humidity/temperature coefficient, $C_{HWN-10}$, is held constant at the user defined $C_H$ value and ~~doesn't scale~~is assumed not to vary with wind speed.

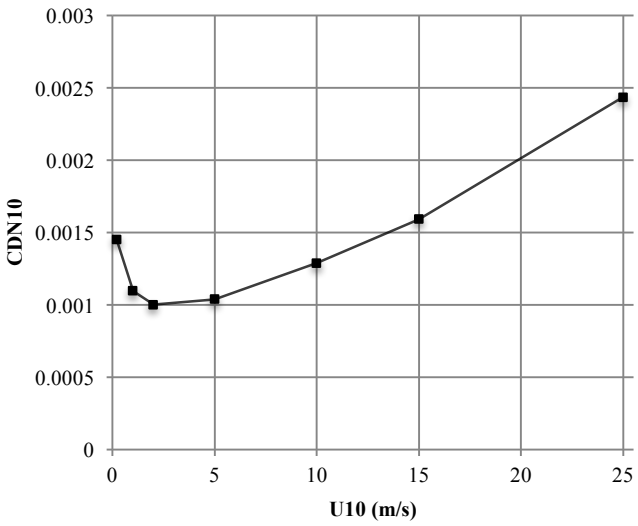

Geosci. Model Dev. Discuss., https://doi.org/10.5194/gmd-2017-257
Manuscript under review for journal Geosci. Model Dev.
Discussion started: 20 November 2017






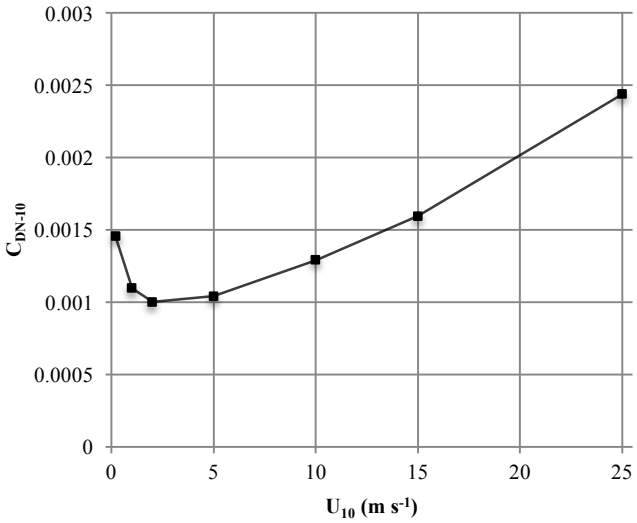


**Figure A1: Scaling of the ~~10m~~10-m neutral drag coefficient with wind speed, $U_{10}$ (Eqns A23-25)**

Under non-neutral conditions in the atmospheric boundary layer, the transfer coefficients vary due to stratification ~~seen~~ in the air column, as was parameterised by Monin and Obukhov (1954) using the now well-known stability parameter, $z/L$, where $L$ is the Obukhov length defined as:

$$~~L = \frac{-\rho_a u_*^3 \theta_V}{kg\left(\frac{H}{c_p} + 0.61\frac{\theta E}{\lambda}\right)}~~ L = \frac{-\rho_a u_*^3 \theta_V}{\kappa\, g\left(\frac{\phi_H}{c_a} + 0.61\frac{\theta_a \phi_E}{\lambda_v}\right)} \quad (~~A26~~)$$

where $\theta_V = ~~\theta(1+0.61q)~~\theta_a(1+0.61e_a)$ is the virtual air temperature and ~~H~~$\phi_H$ and ~~E~~$\phi_E$ are the bulk fluxes. Paulson (1970) presented a solution for the vertical profiles of wind speed, temperature and moisture in the developing boundary layer as a function of the Monin-Obukhov stability parameter; the so-called flux-profile relationships:

$$U_z = ~~\frac{u_*}{k}~~\frac{u_*}{\kappa}\left[\ln\left(\frac{z}{z_o}\right) - \psi_M\left(\frac{z}{L}\right)\right] \quad (~~A27a~~-c)$$

$$~~\theta_z\theta_a - \theta_s = \frac{\theta_*}{k}\left[\ln\left(\frac{z}{z_\theta}\right) - \psi_H\left(\frac{z}{L}\right)\right]~~ \frac{\theta_*}{\kappa}\left[\ln\left(\frac{z}{z_\theta}\right) - \psi_H\left(\frac{z}{L}\right)\right] \quad (~~A27b~~)$$

$$~~q_z - q_s = \frac{q_*}{k}\left[\ln\left(\frac{z}{z_q}\right) - \psi_E\left(\frac{z}{L}\right)\right]~~ e_a - e_s = \frac{e_*}{\kappa}\left[\ln\left(\frac{z}{z_e}\right) - \psi_E\left(\frac{z}{L}\right)\right] \quad (~~A27c~~)$$

where $\psi_M$, $\psi_H$ and $\psi_E$ are the similarity functions for momentum, heat and moisture respectively, and $z_o$, $z_\theta$ and ~~$z_q$~~$z_e$ are their respective roughness lengths. For unstable conditions ($L<0$), the stability functions are defined as (Paulson 1970; Businger et al., 1971; Dyer, 1974):

$$\psi_M = 2\ln\left(\frac{1+x}{2}\right) + \ln\left(\frac{1+x^2}{2}\right) - 2\tan^{-1}x + \frac{\pi}{2} \quad (~~A28a~~)$$

Geosci. Model Dev. Discuss., https://doi.org/10.5194/gmd-2017-257
Manuscript under review for journal Geosci. Model Dev.
Discussion started: 20 November 2017






$$\psi_E = \psi_H = 2\ln\left(\frac{1+x^2}{2}\right) \quad \text{(A28b)}$$

where

$$x = \left[1 - 16\left(\frac{z}{L}\right)^{1/4}\right] \quad \text{(A29)}$$

During stable stratification ($L>0$) they take the form:

$$\psi_M = \psi_E = \psi_H = \begin{cases} -5\left(\frac{z}{L}\right) & 0 < \frac{z}{L} < 0.5 \\ 0.5\left(\frac{z}{L}\right)^{-2} - 4.25\left(\frac{z}{L}\right)^{-1} - 7\left(\frac{z}{L}\right) - 0.852 & 0.5 < \frac{z}{L} < 10 \\ \ln\left(\frac{z}{L}\right) - 0.76\left(\frac{z}{L}\right) - 12.093 & \frac{z}{L} > 10 \end{cases} \quad \text{(A30)}$$

Substituting ~~equations (17) (18)~~Eqns. 20-21 into (A27) and ignoring the similarity functions leaves us with neutral transfer coefficients as a function of the roughness lengths:

$$C_{XN} = ~~k^2~~\kappa^2\left[\ln\left(\frac{z}{z_o}\right)\right]^{-1}\left[\ln\left(\frac{z}{z_X}\right)\right]^{-1} \quad \text{(A31)}$$

where the $N$ sub-script denotes the neutral value and $X$ signifies either $D$, $H$ or $E$ for the transfer coefficient and $o$, $\theta$ or ~~$q$~~$e$ for the roughness length scale. Inclusion of the stability functions into the substitution and some manipulation (Imberger and Patterson, 1990; Launianen and Vihma, 1990) yields the transfer coefficients relative to these neutral values:

$$\frac{C_X}{C_{XN}} = ~~\left[1 + \frac{C_{XN}}{k^2}\left(\psi_M\psi_x - \frac{k\psi_x}{\sqrt{C_{DN}}} - \frac{k\psi_M\sqrt{C_{DN}}}{C_{XN}}\right)\right]~~\left[1 + \frac{C_{XN}}{\kappa^2}\left(\psi_M\psi_X - \frac{\kappa\psi_X}{\sqrt{C_{DN}}} - \frac{\kappa\psi_M\sqrt{C_{DN}}}{C_{XN}}\right)\right] \quad \text{(A32)}$$

Hicks (1975) and Launianen and Vihma (1990) suggested an iterative procedure to solve for the stability corrected transfer coefficient using (A32) based on some initial estimate of the neutral ~~value.~~values (as input by the user). The surface flux is subsequently estimated according to ~~(17 18)~~Eqns. 20-21 and used to provide an initial estimate for $L$ (~~equation~~Eq. A26). The partially corrected transfer coefficient is then recalculated and so the cycle goes. Strub and Powell (1987) and Launiainen (1995), presented an alternative based on estimation of the bulk Richardson number, $Ri_B$, defined as:

$$Ri_B = \frac{gz}{\theta_V}~~\left(\frac{\Delta\theta + 0.61\,\theta_V\Delta q}{U_z^2}\right)~~\left(\frac{\Delta\theta + 0.61\,\theta_V\Delta e}{U_z^2}\right) \quad \text{(A33)}$$

and related as a function of the stability parameter, $z/L$, according to:

$$~~Ri_B = \frac{z}{L}\left(\frac{k\sqrt{C_{DN}}/C_{HWN} - \psi_{HW}}{\left[k/\sqrt{C_{DN}} - \psi_M\right]^2}\right)~~Ri_B = \frac{z}{L}\left(\frac{\kappa\sqrt{C_{DN}}/C_{HWN} - \psi_{HW}}{\left[\kappa/\sqrt{C_{DN}} - \psi_M\right]^2}\right) \quad \text{(A34)}$$

where it is specified that $C_{HN} = C_{WN} = C_{HWN}$. Figure A2 illustrates the relationship between the degree of atmospheric stratification (as described by both the bulk Richardson number and the Monin-Obukhov stability parameter) and the transfer coefficients scaled by their neutral value.

Geosci. Model Dev. Discuss., https://doi.org/10.5194/gmd-2017-257
Manuscript under review for journal Geosci. Model Dev.
Discussion started: 20 November 2017


Geoscientific Model Development Discussions

Revision 8 Mar 2018

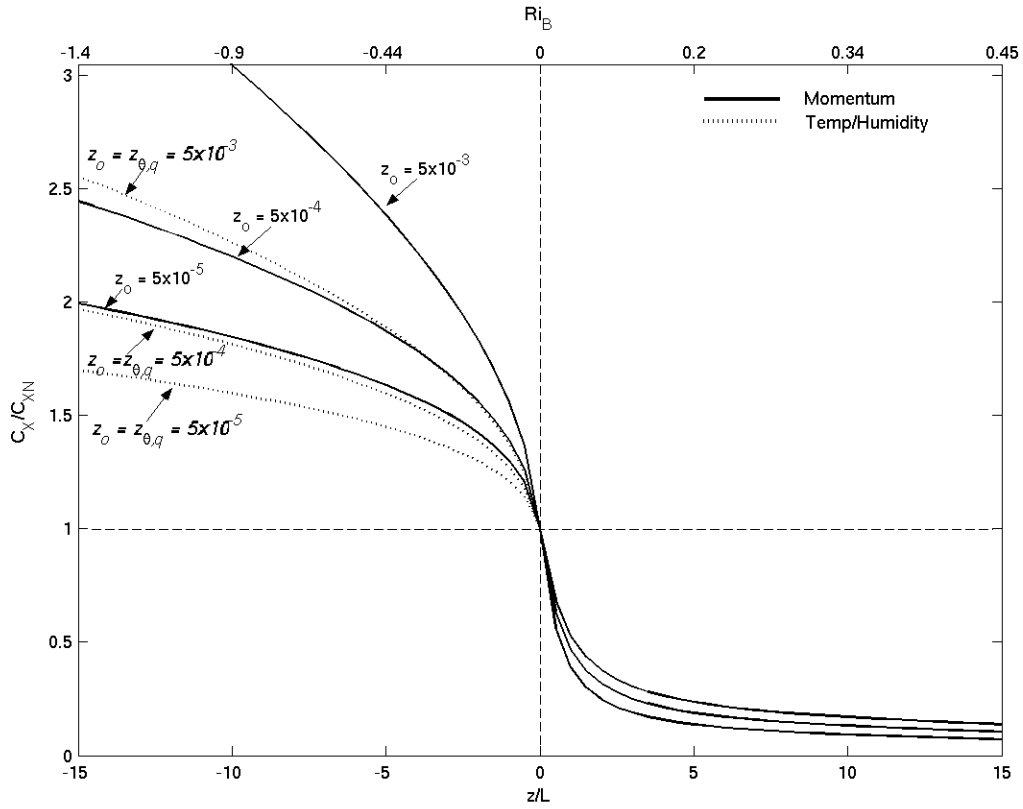


**Figure A2: Relationship between atmospheric stability (bottom axis – $z/L$, top axis – $Ri_B$) and the bulk-transfer coefficients relative to their neutral value ($C_X/C_{XN}$ where $X$ represents $D$, $H$ or $W$) for several roughness values (computed from Eq. A32). The solid line indicates the momentum coefficient variation ($C_D/C_{DN}$) and the broken line indicates humidity and temperature coefficient ($C_{HW}/C_{HWN}$) variation.**